

INFORMATION TO USERS

This manuscript has been reproduced from the microfilm master. UMI films the text directly from the original or copy submitted. Thus, some thesis and dissertation copies are in typewriter face, while others may be from any type of computer printer.

The quality of this reproduction is dependent upon the quality of the copy submitted. Broken or indistinct print, colored or poor quality illustrations and photographs, print bleedthrough, substandard margins, and improper alignment can adversely affect reproduction.

In the unlikely event that the author did not send UMI a complete manuscript and there are missing pages, these will be noted. Also, if unauthorized copyright material had to be removed, a note will indicate the deletion.

Oversize materials (e.g., maps, drawings, charts) are reproduced by sectioning the original, beginning at the upper left-hand corner and continuing from left to right in equal sections with small overlaps.

Photographs included in the original manuscript have been reproduced xerographically in this copy. Higher quality 6" x 9" black and white photographic prints are available for any photographs or illustrations appearing in this copy for an additional charge. Contact UMI directly to order.

ProQuest Information and Learning
300 North Zeeb Road, Ann Arbor, MI 48106-1346 USA
800-521-0600

UMI[®]

**MECHANISM OF INWARD RECTIFICATION OF
NEURONAL NICOTINIC ACETYLCHOLINE
RECEPTORS**

by

Ali Pejmun Haghghi

Department of Physiology
Faculty of Medicine
McGill University
Montreal, Quebec, Canada

September 1999

A thesis submitted to the
Faculty of Graduate Studies and Research
in partial fulfillment
of the requirements for the degree of
Doctor of Philosophy

© Ali Pejmun Haghghi, August, 31st 1999



**National Library
of Canada**

**Acquisitions and
Bibliographic Services**

**395 Wellington Street
Ottawa ON K1A 0N4
Canada**

**Bibliothèque nationale
du Canada**

**Acquisitions et
services bibliographiques**

**395, rue Wellington
Ottawa ON K1A 0N4
Canada**

Your file Votre référence

Our file Notre référence

The author has granted a non-exclusive licence allowing the National Library of Canada to reproduce, loan, distribute or sell copies of this thesis in microform, paper or electronic formats.

The author retains ownership of the copyright in this thesis. Neither the thesis nor substantial extracts from it may be printed or otherwise reproduced without the author's permission.

L'auteur a accordé une licence non exclusive permettant à la Bibliothèque nationale du Canada de reproduire, prêter, distribuer ou vendre des copies de cette thèse sous la forme de microfiche/film, de reproduction sur papier ou sur format électronique.

L'auteur conserve la propriété du droit d'auteur qui protège cette thèse. Ni la thèse ni des extraits substantiels de celle-ci ne doivent être imprimés ou autrement reproduits sans son autorisation.

0-612-64568-1

Canada

*To my parents,
Mehry and Mahmoud*

ABSTRACT

Neuronal nicotinic acetylcholine receptors (nAChRs) are wide spread in the nervous system. Ample evidence indicates that many central nAChRs are located at the nerve terminals, where they act to facilitate neurotransmitter release; however, little is known about how these receptors carry out their function. The focus of my study is to understand the mechanism(s) that underlie the function of neuronal nAChRs. Neuronal nAChRs conduct inward current at negative membrane potentials, but conduct little or no outward current at positive membrane potentials, a process known as inward rectification. Inward rectification prevents the ACh-evoked conductance increase from short-circuiting the action potential at the nerve terminal, thereby ensuring optimal depolarization of the terminal and effective neurotransmitter release. Using the outside-out single channel patch-clamp technique, I demonstrate that intracellular polyamines block neuronal nAChRs with high affinity and in a voltage dependent manner; this is true for native nAChRs expressed by sympathetic neurons as well as recombinant $\alpha 3\beta 4$, $\alpha 4\beta 2$ nAChRs expressed in *Xenopus* oocytes. Given the physiological concentrations of polyamines inside cells, this block can fully account for the strong macroscopic inward rectification. Furthermore, using a combined approach of site-directed mutagenesis and electrophysiology, I show that the negatively charged residues at the cytoplasmic mouth of the pore (known as the intermediate ring) mediate the interaction of intracellular polyamines with the receptor; partial removal of these residues abolishes the strong inward rectification. Interestingly, I show that the intermediate ring influences the permeation of calcium through the receptor, indicating that a molecular link exists between calcium

permeability and inward rectification of neuronal nAChRs. My experiments also show that extracellular polyamines and a polyamine-related toxin, Joro spider toxin, block neuronal nAChRs. Unlike the block by intracellular polyamines, extracellular polyamines and Joro toxin do not interact with the intermediate ring. I show that a single phenylalanine residue in the pore region of the receptor is in part responsible for the high sensitivity of $\alpha 3\beta 4$ neuronal nAChR to Joro toxin; by increasing the open channel burst duration, this residue allows the toxin to interact with the receptor more readily.

RESUME

Les récepteurs nicotiniques de l'acétylcholine (nAChR) sont largement distribués dans le système nerveux. Tout indique que la majorité des nAChR centraux est localisée aux terminaisons nerveuses, où ils facilitent la libération de neurotransmetteurs; toutefois la manière dont ces récepteurs fonctionnent demeure méconnue. Le but de mon étude est de comprendre les mécanismes qui soutendent leur fonction. Les nAChR neuronaux sont des canaux qui conduisent un courant entrant pour des potentiels membranaires négatifs, mais ne conduisent que peu ou pas de courant sortant pour des potentiels membranaires positifs, un processus appelé rectification entrante. Ce phénomène empêche l'augmentation de la conductance évoquée par l'acétylcholine de court-circuiter le potentiel d'action à la terminaison nerveuse et assure ainsi une dépolarisation optimale de la terminaison et une libération efficace de neurotransmetteur. Par la technique d'enregistrement de type patch-clamp de canaux unitaires en conformation "outside-out", je démontre que les polyamines intracellulaires bloquent les nAChR avec une haute affinité et de façon voltage-dépendante. Cela est vrai tant pour les récepteurs natifs nAChR des neurones du système nerveux sympathique que pour les nAChR recombinants $\alpha 3\beta 4$ et $\alpha 4\beta 2$ exprimés dans des ovocytes de *Xenopus*. Etant données les concentrations physiologiques élevées des polyamines dans les cellules, ce blocage peut parfaitement expliquer la forte rectification entrante des nAChR observée au niveau macroscopique. De plus, en utilisant une approche combinée de mutagenèse dirigée et d'électrophysiologie, je montre que les résidus chargés négativement situés sur le bord cytoplasmique du pore (l'anneau intermédiaire) médient l'interaction des polyamines intracellulaires avec les récepteurs. En effet, le retrait partiel de ces résidus entraîne une perte de la forte rectification. J'ai identifié l'anneau intermédiaire servant de filtre ionique pour la perméation du calcium à travers le récepteur, indiquant un lien moléculaire entre la perméabilité au calcium et la rectification entrante des nAChR neuronaux. Mes expériences montrent aussi que des polyamines et une toxine apparentée, celle de l'araignée *Joro*, appliquées de manière extracellulaire, bloquent le récepteur neuronal nAChR. Contrairement au blocage par

des polyamines intracellulaires, les polyamines extracellulaires et la toxine n'interagissent pas avec l'anneau intermédiaire. Un seul résidu phénylalanine dans la région du pore du récepteur est en partie responsable de la forte sensibilité du récepteur neuronal nAChR $\alpha 3\beta 4$ à la toxine de l'araignée Joro: en augmentant la durée d'ouverture du canal, ce résidu permet à la toxine d'interagir plus étroitement avec le récepteur.

AKNOWLEDGEMENTS

This acknowledgement will be short because I am in a big rush to make the 5pm, Aug.31.1999 deadline for submission; otherwise they are going to charge me tuition for one whole semester. So if I forget any names, please forgive me; I love you all and thank you all. I guess I should start with Ellis; Ellis, I wouldn't have been able to accomplish this work without your guidance and support. I really think you are an amazing teacher and a great scientist. I learned a lot here; I should say I learned everything about science and research here. Thank you; and I hope we stay friends for years to come. Five years and eight months ago I started my Ph.D. and in less than two hours I am going to hand in my thesis; I tell you it is exciting. Kevin, I am telling you; it does feel good! It's almost like I am about to see the *Hip* at the spectrum again; may be not that exciting. Dear Kevin, my time here wouldn't have been the same without your friendship. Thank you for all the good times and the breaks; this is just the beginning and many better days are yet to come if Damian stops bit...ing about the music of course. Damian, thank you for letting me stay at your apartment, man. You knew from day one that I wasn't going anywhere in September! Tom, thank you for those DMC's (deep meaningful conversations); I guess you're coming to California soon! I would like to thank you all one by one, but I really don't have much time, so I'll just say: many thanks to the present and past members of the Cooper lab: Paul, Misha, Brigitte, Damian, Isabelle, Tom, Vincent, David and of course Ellis himself. I specially thank Vincent, Isabelle and David for their help with my thesis. I would also like to thank many members of our department for their help and support throughout my Ph.D., thank you Linda, John(W), Alvin, John(H), Armin, Tiger, Rubin and many more that I can't think of right now. I guess I have to acknowledge the fact that all of the experiments in this thesis were done by myself, but I have to thank Tom for his the art work in figure 5.2 of my thesis.

So now that I am over with the department, I would like to thank many important people in my life for many things. That is not to say that my friends who I mentioned already aren't important, ok! Dear Erica, I would like to thank you for all the great things that we shared together, thanks for all the good times and thanks for your love, friendship and support. And the food you brought me last night was delicious! Thanks for being so patient with me these past few weeks and thanks for your help with my thesis and also thanks for packing my stuff for me. So I really have to go now, but before I finish: my dear little sister Pantea, thank you for your love and support and also packing and helping with my thesis, gonna love you forever. Big Brother Peimun, thanks for being a cool brother. Finally, I would like to thank my parents Mahmoud and Mehry for their love and support all throughout my life; I would like to dedicate this work to them. I hope I haven't missed any one, oh, Kim dear buddy, are you gonna come back here and finish your thesis? Anyway, thanks everyone in Montreal and Vancouver and Tehran and Germany and so on. I love you all and will try my best to be a good scientist. Pejmun 5pm, Aug.31.1999.

CONTRIBUTION TO PUBLICATIONS

Chapters 2, 3, and 4 of my thesis are duplicates of the following three manuscripts:

1. **Haghighi, A. P.** and Cooper, E. A phenylalanine in the M2 of $\beta 4$ neuronal nAChR subunit governs gating kinetics and influences the block by extracellular polyamine-related Joro spider toxin (in preparation for publication).

For this study, I performed all of the experiments (electrophysiology and mutagenesis), carried out all of the analysis and generated all figures. The initiation of this work and the writing of the manuscript were in collaboration with Dr. Ellis Cooper, my Ph.D. supervisor.

2. **Haghighi, A. P.** and Cooper, E. A molecular link between inward rectification and calcium permeability of neuronal nicotinic $\alpha 3\beta 4$ and $\alpha 4\beta 2$ receptors (in press).

I initiated this project in collaboration with Dr. Ellis Cooper. I performed all mutagenesis and electrophysiological experiments, performed all of the analysis and generated all figures. The writing of the manuscript was done in collaboration with Dr. Ellis Cooper, my Ph.D. supervisor.

3. **Haghighi, A. P.** and Cooper, E., (1998). Neuronal nicotinic acetylcholine receptors are blocked by intracellular spermine in a voltage-dependent manner. *J. Neurosci.*, 18, 4050-4062.

For this study, I performed all of the experiments, carried out all of the analysis and generated all 9 figures. The initiation of this work and the writing of the manuscript were in collaboration with Dr. Ellis Cooper, my Ph.D. supervisor.

I have not included the following three publications in the body of my thesis because they are not directly related to the main focus of my thesis.

1. Séguéla, P., **Haghighi, A.**, Soghomonian, J. J. and Cooper, E., (1996). A novel neuronal P2x ATP receptor ion channel with widespread distribution in the brain. *J. Neurosci.*, 16, 448-455.

In this study, I carried out a comprehensive electrophysiological and pharmacological analysis of P2x4 ATP-gated receptor. I designed the experiments in collaboration with Dr. Ellis Cooper and generated three of the six figures in the manuscript and contributed to writing and organization of the manuscript. I performed all of electrophysiological analysis.

2. Slack, R. S., Belliveau, D., Rosenberg, M., Atwal, J., Lochmuller, H., Aloyz R., **Haghighi, A.**, Lach B., Seth, P., Cooper, E. and Miller, F. D., (1996). Adenovirus-mediated gene transfer of the tumor suppressor, p53, induces apoptosis in postmitotic neurons. *J. Cell Biol.*, 135, 1085-1096.

In this study, I tested the properties of voltage-gated K⁺ currents in sympathetic neurons transfected using adenovirus-mediated gene transfer to show that this process does not interfere with the overall excitability and health of these neurons. I generated 1 of 9 figures and the related text in the results and methods.

3. Mukerji, J., **Haghighi, A.** and Séguéla, P., (1996). Immunological characterization and transmembrane topology of 5-HT₃ receptors by functional epitope tagging. *J. Neurochem.*, 66, 1027-1032.

In this study, I have contributed to characterization of transmembrane topology of 5HT-3 receptors by comparing the functional properties of wild type and mutant 5HT-3 receptors. I generated one of six result figures and contributed to the writing of the manuscript.

CONTRIBUTION TO ORIGINAL SCIENCE

My findings reveal novel mechanisms that underlie the functional properties of neuronal nAChRs. In chapter 2, I demonstrate, for the first time, that intracellular polyamines act as gating molecules to block neuronal nAChRs in a voltage dependent manner. Given the high concentrations of intracellular polyamines in neurons, this block can fully account for the strong inward rectification of neuronal nAChRs. All the experiments in this chapter were performed by myself.

In chapter 3, I identify the structural determinant of the block by intracellular polyamines; my findings indicate that substitution of only two negatively charged residues with neutral amino acids at the intermediate ring of $\alpha 3\beta 4$ and $\alpha 4\beta 2$ nAChRs is sufficient to diminish the blocking effect of intracellular polyamines. These mutations also drastically reduce calcium permeability of $\alpha 3\beta 4$ and $\alpha 4\beta 2$ receptors. These results reveal a molecular link between calcium permeability and inward rectification of neuronal nAChRs. All the experiments in this chapter were performed by myself.

In chapter 4, I demonstrate, for the first time, that Joro spider toxin, a polyamine-related toxin, blocks recombinant $\alpha 3\beta 4$ and $\alpha 4\beta 2$ receptors with high affinity and in a use dependent manner. I also identify an amino acid in the pore region of the $\beta 4$ subunit that underlies single channel gating of $\alpha 3\beta 4$ receptor. This residue also affects the sensitivity of the receptor for block by Joro toxin. All the experiments in this chapter were performed by myself.

Furthermore, I have contributed to three publications that have not been included in the body of my thesis. In the first study, entitled, "A novel neuronal P2X

ATP receptor ion channel with widespread distribution in the brain" (Séguéla et al., 1996), I carry out a comprehensive functional characterization of a novel P2X ATP-gated receptor, P2X4. I demonstrate that, when expressed in *Xenopus* oocytes, P2x4 subunits form homomeric ion channels that give rise to cationic currents in response to μM concentrations of external ATP. P2x4 receptors exhibit a slow desensitization in the continuous presence of agonist, have no selectivity for potassium over sodium and are calcium permeable. I further demonstrated that, in contrast to neuronal nAChRs, these receptors do not exhibit strong inward rectification.

Also, in a study using adenovirus-mediated gene transfer in sympathetic neurons, I test the properties of voltage-gated K^+ currents in transfected and control neurons to show that this process does not interfere with the overall excitability and health of these neurons (Slack et al., 1996).

Finally, in a study on characterization of transmembrane topology of 5HT-3 receptors, I show that the functional properties of recombinant *c-myc*-tagged and *Flag*-tagged 5HT-3 receptors are similar to those of wild type receptors expressed in *Xenopus* oocytes using the two-electrode voltage clamp technique (Mukerji et al., 1996).

TABLE OF CONTENTS

ABSTRACT	I
RESUME	III
ACKNOWLEDGMENTS	V
CONTRIBUTION TO PUBLICATIONS	VI
CONTRIBUTION TO ORIGINAL SCIENCE	VIII
TABLE OF CONTENTS	X
CHAPTER 1	1
INTRODUCTION	
Muscle nAChRs	2
<i>Ionic selectivity of muscle nAChRs</i>	3
<i>Ca⁺⁺ permeability of muscle nAChRs</i>	5
<i>Muscle nAChR subunit genes and the overall membrane</i>	6
<i>Topology</i>	
<i>The M2 membrane spanning segment lines the ion channel pore</i>	7
<i>Site-directed mutagenesis experiments</i>	7
<i>Interaction of open channel blockers with the pore</i>	9
<i>Substituted cysteine accessibility experiments</i>	12
<i>Location of the gate of the receptor</i>	13
<i>Basic science solves clinical problems</i>	15
<i>Congenital myasthenic syndromes and Muscle nAChR malfunction</i>	15
Neuronal nAChRs	18
<i>Neuronal nAChR subunit genes and overall membrane topology</i>	18
<i>Ionic selectivity of neuronal nAChRs</i>	19
<i>Neuronal nAChRs are highly calcium permeable</i>	20
<i>Molecular mechanisms underlying Ca⁺⁺ permeability of neuronal nAChR</i>	20
<i>Neuronal nAChRs are modulated by extracellular calcium</i>	21
<i>M2 segment lines the pore of neuronal nAChRs</i>	23
<i>Neuronal nAChRs and diseases of the nervous system</i>	26
<i>ADNFLE is caused by mutations in the M2 region of the $\alpha 4$ subunit</i>	27
Inward rectification of neuronal nicotinic receptors	29
<i>Polyamines and inward rectification</i>	31
<i>Polyamines cause the inward rectification of inward rectifier K channels</i>	32
<i>Polyamines cause the inward rectification of AMPA/kainate receptors</i>	34
Hypothesis and outline of the proposed experiments	37
<i>Mechanism of inward rectification of neuronal nAChRs</i>	37
<i>Hypothesis</i>	37

<i>Rationale</i>	37
<i>Experimental outline</i>	37
Characterization of the site of interaction of polyamines	38
<i>Hypothesis</i>	38
<i>Rationale</i>	38
<i>Experimental outline</i>	38
Block of neuronal nAChRs by polyamine-related spider Jorotoxin	39
<i>Hypothesis</i>	39
<i>Rationale</i>	39
<i>Experimental outline</i>	39
CHAPTER 2	40
<i>Neuronal nicotinic acetylcholine receptors are blocked by intracellular spermine in a voltage-dependent manner</i>	
Abstract	41
Introduction	42
Methods and materials	44
<i>Preparation of SCG neurons</i>	44
<i>Preparation and nuclear injection of oocytes</i>	44
<i>Electrophysiology</i>	45
<i>Analysis</i>	47
Results	49
<i>Inward rectification of macroscopic Ach currents</i>	49
<i>Lack of inward rectification in single nAChRs measured from outside-out patches of Xenopus oocytes</i>	50
<i>Intracellular spermine blocks neuronal nAChRs expressed in Xenopus oocytes</i>	52
<i>Spermine blocks native neuronal nAChRs on sympathetic neurons</i>	55
<i>Extracellular spermine blocks neuronal nAChRs</i>	57
Discussion	59
CHAPTER 3	64
<i>A molecular link between inward rectification and calcium permeability of neuronal nicotinic acetylcholine $\alpha 3\beta 4$ and $\alpha 4\beta 2$ receptors</i>	
Abstract	65

Introduction	66
Methods and materials	68
<i>Site-directed mutagenesis</i>	68
<i>Expression of nAChR subunit cDNAs in oocytes</i>	68
<i>Injection of BAPTA and spermine into the oocytes</i>	69
<i>Neuronal and myotube cultures</i>	69
<i>Electrophysiology</i>	70
<i>Analysis</i>	73
Results	76
<i>Cytoplasmic ring mutations have little effect on inward rectification</i>	77
<i>Intermediate ring mutations abolish inward rectification</i>	78
<i>Elevated intracellular spermine increased inward rectification of $\alpha 3\beta 4$ and $\alpha 4\beta 2$ receptors, but had no effect on non-rectifying mutant receptors</i>	80
<i>Extracellular spermine blocks non-rectifying mutant receptors</i>	82
<i>Relative calcium permeability</i>	83
Discussion	86
<i>Interaction between polyamines and neuronal nAChRs</i>	86
<i>Comparison to AMPA/kainate receptors</i>	88
<i>A common site affects both inward rectification and calcium permeability</i>	89
<i>Physiological implications</i>	90
CHAPTER 4	92
<i>A phenylalanine in the M2 of $\beta 4$ neuronal nAChR subunits governs gating kinetics and influences the block by extracellular polyamine related Joro spider toxin</i>	
Abstract	93
Introduction	94
Methods and materials	96
<i>Site directed mutagenesis</i>	96
<i>Expression of nAChR subunit cDNAs in oocytes</i>	96
<i>Electrophysiology</i>	97
<i>Analysis</i>	99
Results	101
<i>Differential permeability of divalent organic cations through $\alpha 3\beta 4$ and $\alpha 4\beta 2$ receptors</i>	105
<i>Extracellular polyamines block $\alpha 3\beta 4$ and $\alpha 4\beta 2$ receptors</i>	106
<i>Joro spider toxin blocks $\alpha 3\beta 4$ and $\alpha 4\beta 2$ receptors in a use-dependent manner</i>	106
<i>Phenylalanine at 253 in $\beta 4$ affects single-channel burst duration of $\alpha 3\beta 4$ receptors</i>	108
Discussion	110

<i>Both the M2 and the intermediate ring influence permeability through neuronal nAChRs</i>	111
CHAPTER 5	113
<i>General discussion and conclusion</i>	
Discussion	114
<i>Physiological role of neuronal nAChRs</i>	114
<i>Central nAChRs are mainly presynaptic and influence neurotransmitter release</i>	116
<i>Presynaptic nAChRs can modulate synaptic transmission</i>	117
<i>Physiological significance of the interaction of polyamines with neuronal nAChRs</i>	118
<i>Removal of spermine removes rectification in intact neurons: the use of an animal model</i>	119
Conclusion	121
BIBLIOGRAPHY	123

CHAPTER 1

Introduction

INTRODUCTION

My main interest has been to study the functional properties of ligand-gated receptors; in particular, I have been investigating the mechanisms underlying ionic conductance and selectivity of neuronal nicotinic acetylcholine receptors (nAChRs) using a combined molecular biological and electrophysiological approach. A large body of evidence implicates neuronal nAChRs in a variety of physiological and pathophysiological conditions including learning and memory, nicotine addiction, epilepsy and Alzheimer's disease. However, there is little known about the structure-function relationship of these receptors and the mechanisms underlying their functional properties.

One common feature of all neuronal nAChRs is that their current-voltage relationship (I-V curve) exhibits strong inward rectification; that is, they conduct inward currents at negative membrane potentials, but conduct no outward current at positive membrane potentials. This property is particularly important for the function of central nAChRs expressed at nerve terminals. The focus of my thesis is to elucidate the mechanism(s) underlying inward rectification of neuronal nAChRs. Based on previous data, I hypothesize that this inward rectification is not an intrinsic property of the receptor and can be regulated.

I will first describe the existing model of the conducting pathway of nAChRs primarily based on our knowledge of the muscle nAChRs and then discuss how existing data on neuronal nAChRs and other inwardly rectifying ion channels led me to formulate my hypothesis.

Muscle nAChRs

Since the initial description of nicotinic transmission at the vertebrate neuromuscular junction (Dale et al., 1936; Fatt and Katz, 1951), this synapse has become the best

studied of all synapses and has served as a model for chemical synapses in both the peripheral and the central nervous system (Sanes and Lichtman, 1999). Our understanding of synaptic transmission at the neuromuscular junction has benefited from many biochemical, molecular biological and electrophysiological studies that have focussed on elucidating the structure-function relationship of the muscle (or *Torpedo*) nAChRs, rendering the muscle nAChR one of the best characterized of all ligand-gated ion channels (for reviews see: Dani, 1989; Karlin, 1991; Duclert and Changeux, 1995; Karlin and Akabas, 1995). Although much less direct data is available for neuronal nAChRs, our present knowledge of the neuronal nAChRs points to a similar structure-function relationship (Sargent, 1993; Galzi and Changeux, 1995; McGehee and Role, 1995).

Ionic selectivity of muscle nAChRs

Since the early studies by Takeuchi and Takeuchi (1960) that demonstrated low selectivity of endplate nAChRs to monovalent cations, a number of studies have established the permeability of muscle and *Torpedo* nAChRs to cations and the lack of permeability to anions (Jenkinson and Nicolls, 1960; Katz and Miledi, 1969; Huang et al., 1978; Lewis, 1979; Adams et al., 1980; Dani and Eisenman, 1987).

The current carried by an ionic species through an ion channel can be described by the Goldman-Hodgkin-Katz constant field equation (Goldman, 1943; Hodgkin and Katz, 1949; Lewis, 1977):

$$I_x = F^2 Z_x^2 x P_x V / RT \left\{ ([X]_o - [X]_i) e^{Z_x F V / RT} / (1 - e^{Z_x F V / RT}) \right\},$$

where P_x is the permeability coefficient, Z_x is the valence, and $[X]_o$ and $[X]_i$ are the outside and inside concentrations, respectively, and F , R and T have their usual meanings. When there are several ionic species in the solution this equation can be

solved for the equilibrium potential or the reversal potential (E_{rev} , the potential at which the total current is zero) of the total current. For example when Na^+ , K^+ and Ca^{++} are the conducting ions one can solve this equation for the reversal potential according to the constant field voltage equation:

$$E_{rev(Ca)} - E_{rev(Na)} = RT/F \ln \left\{ \frac{([Na]_o + P_K/P_{Na} [K]_o + 4P'_{Ca}/P_{Na} [Ca]_o)}{([Na]_i + P_K/P_{Na} [K]_i + 4P'_{Ca}/P_{Na} [Ca]_i)} \right\}$$

where

$$P'_{Ca} = P_{Ca} / (1 + \exp(E_{rev(Ca)} F/RT))$$

and P_X is the permeability coefficient of ion X , $[X]_o$ is the extracellular concentration of ionic specie X , and R , T and F have their usual meanings.

Experimentally measured E_{rev} corresponding to different concentrations of conducting ions can be used in the constant field voltage equation to calculate the relative permeability of these ions (Lewis, 1979).

Hille and colleagues carried out a thorough examination of the permeability of endplate channels to monovalent and divalent cations using intracellular electrophysiological techniques (Adams et al., 1980; Dwyer et al., 1980). They calculated the relative permeability of different ionic species to that of Na^+ using the constant field equations. They demonstrated that the endplate nAChRs has a weak selectivity for monovalent cations with the following permeability ratios: Cs^+ (1.4) > Rb^+ (1.3) > K^+ (1.1) > Na^+ (1.0) > Li^+ (0.9). Compared to monovalent cations, divalent cations are significantly less permeant with the following sequence: Mg^{++} > Ca^{++} > Ba^{++} > Sr^{++} (Adams et al., 1980).

Hille and colleagues also found that the endplate nAChR is permeable to a number of large organic cations (Dwyer et al., 1980). In this extensive study, they calculated the relative permeability of over 45 organic cations to that of Na^+ at the

muscle endplate. They then constructed molecular models of the permeant ions based on the Corey-Pauling-Koltum (CPK) space-filling approach and found that there is an inverse relationship between the size of the molecules and their relative permeability through the endplate nAChR. Based on these molecular models, they estimated that the minimum size of the narrowest region of the open receptor to accommodate the largest permeating ion is most likely a square of approximately $6.5 \times 6.5 \text{ \AA}^2$ with cut off corners (Dwyer et al., 1980).

Ca⁺⁺ permeability of the muscle nAChRs:

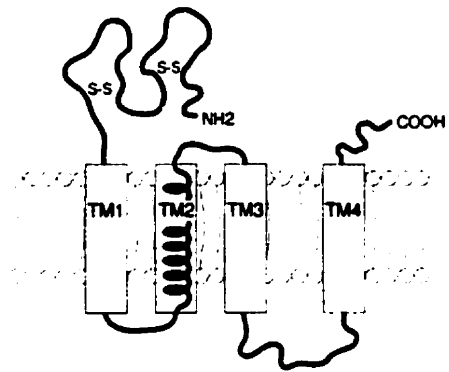
Muscle nAChRs have a low permeability to extracellular Ca⁺⁺. Early electrophysiological experiments on the frog neuromuscular junction suggested that the muscle nAChR has some permeability to extracellular Ca⁺⁺, since small amplitude spontaneous miniature endplate potentials (MEPPs) could be recorded in the presence of Ca⁺⁺ as the only charge carrier (Katz and Miledi, 1969). Later examination of Ca⁺⁺ permeability of the endplate nAChR revealed that the relative permeability of Ca⁺⁺ to Na⁺ (P_{Ca}/P_{Na}) is as low as 0.15- 0.3 (Lewis, 1979; Adams et al., 1980; Decker and Dani, 1990). Similar values for P_{Ca}/P_{Na} or P_{Ca}/P_{Cs} have reported from dissociated muscle fiber preparations (Villarroel and Sakmann, 1996) or from heterologously expressed muscle nAChRs (Costa et al., 1994). There is also evidence that the permeability of the muscle nAChRs to Ca⁺⁺ increases up to 2 fold during development and this change is caused by replacement of the fetal γ subunit with ϵ subunit in adult muscle (Villarroel and Sakmann, 1996). Since the pore size of the muscle nAChR is large enough to accommodate divalent cations, these results indicate that the muscle nAChR has an ionic filter that selects monovalent ions over divalent cations.

Muscle nAChR subunit genes and the overall membrane topology:

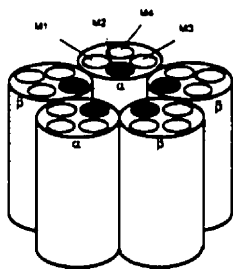
In the 1960's, 70's and 80's many laboratories used biochemical and molecular biological approaches to isolate the acetylcholine receptor (for reviews see: Karlin 1991). Two key discoveries immensely contributed to these studies: the discovery of a rich source of nicotinic receptors in the electric organ of the electric fish *Torpedo californica* and the identification of a high affinity ligand, α -bungarotoxin, that could irreversibly bind to the receptor and label it (for review see Changeux, 1981). These studies finally led to purification of the nAChR subunits (Weill et al., 1974) and identification of the first 54 amino acids of the receptor (Raftery et al., 1980). The knowledge of the amino acid sequence allowed the generation of synthetic DNA probes that were then used to screen a cDNA library of *Torpedo californica* electric organ. Using DNA hybridization methods, full-length cDNAs encoding nAChR subunit proteins were cloned (Noda et al., 1982; Sumikawa et al., 1982; Noda et al., 1983; Claudio et al., 1983). The identification of the amino acid sequence of muscle nAChR subunits provided important information about the structure of the receptor.

The muscle (or *Torpedo*) nAChR is formed by coassembly of four subunits α , β , δ , and γ (ϵ in adult receptor) with the stoichiometry of $\alpha_2\beta\gamma\delta$ or $\alpha_2\beta\gamma\epsilon$. All five subunits have a high degree of homology at the amino acid level and have a similar hydrophobicity profile. The predicted secondary structure for all subunits suggests the presence of a large hydrophilic extracellular amino terminal, four hydrophobic transmembrane domains (designated M1-M4), a large cytoplasmic loop between M3 and M4 and a short extracellular carboxy terminus (Fig. 1). Every receptor has two ACh binding sites that are formed mainly in the extracellular domain of the α -subunits marked by a pair of cysteine residues (for review see Karlin and Akabas, 1995). Based on the images reconstituted from electron micrographs of the receptor in closed and open states, the ion channel pore of the nAChR is formed in the center of the molecule facing all the subunits (Unwin, 1993). Several lines of evidence

A



B



C

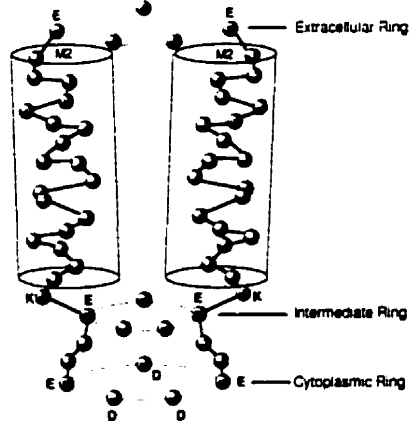


Figure 1.1. Membrane topology of nAChR subunits and putative structure of the M2 region. A. Each nAChR subunit has four transmembrane domains (M1 to M4), a large amino-terminus and a short carboxy-terminus. Co-assembly of five subunits forms B. The receptor. For heteromeric neuronal nAChRs two α subunits and three β subunits form the functional receptor. C. This figure shows a cartoon of the putative pore region. The two M2 segments correspond to the two α subunits. There are three rings of charged amino acids neighbouring the M2 segment: extracellular ring, intermediate ring and cytoplasmic ring. At these positions, the five charged residues corresponding to two α and three β subunits are shown. The circles connecting the charged residues are only to emphasize the ring-like formation of these residues.

indicate that the second transmembrane domain, M2, of each subunit lines the conductive pathway of the receptor.

The M2 membrane spanning segment lines the ion channel pore:

In the past two decades, a number of laboratories have provided evidence that the M2 hydrophobic segment forms the major part of the ion channel pore. These studies have used mainly three approaches to characterize the conducting pathway of the receptor: site-directed mutagenesis techniques, use of non-competitive open channel blockers and substituted-cysteine accessibility method (SCAM).

Site directed mutagenesis experiments:

One line of evidence pointing to the M2 as the main pore-forming segment of the receptor comes from several studies on recombinant nAChRs by Numa, Sakmann and colleagues in the mid to late 1980's by combining expression of recombinant receptors in *Xenopus* oocytes site-directed mutagenesis and single channel patch-clamp techniques. In their initial studies with recombinant *Torpedo* nAChR in *Xenopus* oocytes, Mishina et al. addressed the question of whether all four subunits are required for expression of a functional receptor. To test this, all four subunits or three subunits at a time were expressed in *Xenopus* oocytes and the responses to ACh were measured with the two-electrode voltage-clamp technique. In the absence of α or β subunits in the combination, no ACh-evoked responses were detected; however, α,β,γ and α,β,δ combinations did give rise to small but detectable ACh-evoked currents (Mishina et al., 1984). Thus it appeared that although γ and δ subunits can partially substitute each other, all four subunits are required for receptor function.

In their first attempt to locate the region of the subunit involved in the formation of the ion channel pore, Mishina et al. (1985) generated several α subunit mRNA constructs containing deletions in each of the transmembrane segments and in the cytoplasmic loop between M3 and M4. When these constructs were coinjected

with the other three wild type subunits in *Xenopus* oocytes, deletions in each of the transmembrane domains rendered the receptor non-functional (Mishina et al., 1985). Therefore, no conclusions could be made as to which region(s) of the subunit is involved in lining the pore of the receptor.

A major breakthrough came from experiments using chimeric δ -subunit constructs containing different regions corresponding to the *Torpedo* or bovine δ subunits (Imoto et al., 1986). The rationale was based on the finding that the coexpression of the bovine δ -subunit (but not α -subunit) with *Torpedo* α -, β - and γ -subunits resulted in a receptor with similar single channel conductance to that of the bovine nAChR. Therefore, by expressing chimeric bovine δ -subunit constructs that contain homologous regions of *Torpedo* δ -subunit, the domain of the subunit responsible for the change in the single channel conductance can be determined. Using this strategy, Imoto et al. demonstrated that the M2 transmembrane domain is involved in determining the single channel conductance of the receptor.

In subsequent studies, Imoto et al. (1988) provided further evidence for the involvement of the M2 region in the conductive pathway of the receptor by demonstrating that the negative charges surrounding the M2 region greatly influence the single channel conductance of the receptor. In the *Torpedo* nAChR ($\alpha_2\beta\gamma\delta$), alignment of the amino acid sequences of all the subunits suggests the presence of three ring-like accumulations of negatively charged residues, one on the extracellular side of M2 with three negative charges (the extracellular ring) and two on the cytoplasmic side of M2 each bearing four negative charges (the intermediate and the cytoplasmic ring) (Figure 1). Imoto and colleagues reasoned that if the M2 region is the major part of the conducting pathway, these negative charges may interact with conducting cations and thus influence the single channel conductance of the receptor. This hypothesis was addressed by substituting the negatively charged residues with neutral or positively charged residues and correlating the net charge change with the

single channel conductance of the receptor. The results indicated that all the negative charges are important for the single channel conductance. Interestingly but not unexpectedly, the extracellular ring mutations mainly affected the inward current, whereas the cytoplasmic ring mutations mainly affected the outward current. The intermediate ring mutations, however, had the largest effect and reduced both inward and outward currents. These results not only provided evidence for the essential role of the M2 region in forming the receptor pore, but also suggested that the intermediate ring residues are most likely located at a position where they can closely interact with the conducting cations (possibly at the narrowest part of the pore).

Later studies by Konno et al. (1991) and Wang and Imoto (1992) provided further support for the involvement of the rings of negatively charged residues in determining the permeability and ionic selectivity of the nAChR. Konno et al. studied the effect of charge substitution on the permeability and selectivity of the *Torpedo* nAChR for small monovalent cations. Their results indicated that the wild type receptor is weakly selective for K^+ and Na^+ over Li^+ or Cs^+ ; while Cs^+ has a higher relative permeability than K^+ , the single channel conductance for Cs^+ is about 25% less than that of K^+ . This selectivity is abolished in receptors that have a charge substitution in the intermediate ring (but not the extracellular or the cytoplasmic ring), further supporting the critical role of the intermediate ring residues in determining the conductance and permeability of the nAChR. Wang and Imoto examined the effect of charge substitutions on the permeability of large organic cations. Similar to previous findings for small monovalent cations, the conclusion was that the intermediate ring mutations have the greatest effect on relative permeability of large organic cations.

Taken together, these findings strongly suggested that the M2 region of each subunit is the major component that participates in forming the ionic pathway of the nAChR. Moreover, these results indicated that the rings of negatively charged

residues surrounding the M2 region, in particular the intermediate ring residues, are important for ionic conductance and permeability of the receptor.

Interaction of open channel blockers with the receptor:

Another line of evidence implicating the involvement of the M2 region in the ion-conducting pathway of the nAChRs is based on the interaction of the receptor with open channel blockers. The advantage of using these blockers is that they interact with the channel pore without affecting the binding of the ligand to the receptor.

The sedative antipsychotic drug Chlorpromazine (CPZ) is one such compound that was demonstrated to block the open nAChR (Koblin and Lester, 1979). CPZ can covalently bind to the open nAChR upon ultraviolet light irradiation (photolabeling) (Oswald and Changeux, 1981; Heidmann and Changeux, 1984). Therefore radioactively labeled CPZ, (³H)CPZ, can be used to label the receptor. Changeux and colleagues took advantage of this photolabeling method to identify the conducting pathway of the nAChR. They first demonstrated that all four subunits of the *Torpedo* nAChR can be photolabeled by (³H)CPZ in the presence of agonist, suggesting a site of interaction along the axis of the channel (Oswald and Changeux, 1981). Subsequently, Changeux and colleagues identified several residues on the α , β , δ , and γ subunits that interacted with CPZ (Giraudat et al., 1986; Giraudat et al., 1987; Revah et al., 1990). Interestingly, all these residues belong to the M2 segment of the subunits and correspond to a nonpolar ring of leucine residues and two polar rings of serine and threonine residues (Revah et al., 1990). Since these three identified rings of amino acids are three or four amino acids apart, it is plausible that the side-chains of these residues face the same side of an α -helical structure (Revah et al., 1990). Therefore, these results not only further implicated the M2 segment as the pore-forming region of the receptor, but also provided evidence for an α -helical structure of the M2 region.

Another open channel blocker that has been used to identify residues lining the pore of the nAChR is QX-222, a quaternary ammonium local anesthetic derivative (Neher and Steinbach, 1978; Leonard et al., 1988). Analysis of the action of local anesthetics on the nAChR at the neuromuscular junction had suggested that they only interact with the receptor when it is opened by ACh (Steinbach, 1968). Neher and Steinbach (1978) later confirmed these results at the single channel level. In the presence of QX-222, single channel openings appeared to be chopped into much briefer bursts of opening (Neher and Steinbach, 1978). These results indicated that QX-222 most likely interacts with the residues along the conducting pathway of the receptor.

Lester and colleagues used a combined approach of site-directed mutagenesis and electrophysiology to identify a residue(s) that would interact with QX-222 upon opening of the receptor. They took advantage of previous findings that pointed to the M2 region as the major part of the pore, and thus targeted residues in this region. First, they substituted a polar serine residue (α S248 and δ S262) 6 amino acids downstream of the cytoplasmic side of M2 with a neutral alanine residue in both α and δ subunits of mouse nAChR (Leonard et al., 1988). Mutated subunits were then coexpressed with the wild type subunits in *Xenopus* oocytes and the kinetics of the block by QX-222 were analyzed at both the single channel and the macroscopic level. The results indicated that each serine substitution progressively decreases the lifetime of the blocked state. These results suggested that the serine residues are important for interaction of QX-222 with the receptor and are therefore within the ion channel pore.

Lester and colleagues extended their findings by examining the effect of additional amino acid substitutions on the blocking kinetics of QX-222. QX-222 has two functional groups that are 5-6 Å apart: an ionizable amino group and a hydrophobic aromatic group (Charnet et al., 1990). Therefore, QX-222 can potentially interact with adjacent turns of an α -helix. To test this, Charnet et al.

mutated another serine residue four amino acids up-stream from α S248 (α S252 or β T263). Receptors with mutation of α S252 and β T263 to neutral alanines (α S252A and β T263A, respectively) affected the blocking kinetics of QX-222, suggesting that α S252 is also facing the lumen of the pore and is most likely on the same side of an adjacent α -helix structure. Interestingly, in contrast to α S248A, α S252A mutants showed a higher binding affinity and faster blocking kinetics for QX-222. This paradoxical effect can be attributed to a stronger interaction between the hydrophobic aromatic group of QX-222 with the nonpolar alanine side chain than the interaction with the polar OH group of serine. Altogether, these results indicated that the two functional groups of QX-222 most likely interact with an adjacent turn of an α -helix of the M2 region, thus providing further evidence for an α -helical structure for the M2 segment.

Substituted-cysteine accessibility experiments:

Finally, a third line of evidence that locates the M2 region in the conductive pathway of the nAChR is based on results of substituted-cysteine accessibility experiments. This method is based on the covalent interaction of small, charged, highly water soluble sulfhydryl-specific molecules (such as the positively charged methanethio-sulfonate ethylammonium, MTSEA) with exposed sulfhydryl group of cysteine residues (Akabas et al., 1992). If candidate residues along the conducting pathway of the receptor are substituted with cysteine residues, MTSEA can potentially bind to those residues while passing through the pore and block the ACh-evoked current through the receptor.

Using this method, Karlin, Akabas and colleagues mapped the entire M2 region of mouse muscle α -subunit (Akabas et al., 1994). One at a time, they substituted 22 amino acids spanning the M2 and flanking regions of the α -subunit. All but one construct resulted in functional nAChR receptors when combined with β , γ and δ subunits in *Xenopus* oocytes. When control ACh-responses were compared with those

measured following a 1 min treatment with extracellular MTSEA in the absence of ACh and 5 min wash, 10 mutant receptors containing a cysteine residue at one of ten positions from the extracellular ring to the intermediate ring showed a significant reduction in their response. This suggests that MTSEA can interact with the closed receptor at 10 different positions along the M2 segment. Based on the assumption that substituting cysteines have similar accessibility to that of the corresponding wild-type residues, the authors concluded that these ten residues normally face the lumen of the nAChR (Akabas et al., 1994). Although the cysteine accessibility assays provided a powerful tool to map the conducting pathway of ion channels, the question arose whether or not these substitutions had any effect on the overall tertiary structure of the protein. On the other hand, the consistency of these findings with data on previously identified residues facing the lumen of the nAChR and the proposed α -helical structure of the M2 transmembrane domain indicated that this method can be used reliably.

The location of the gate of the receptor

An important feature of the conducting pathway of all ion channels is the presence of a barrier or gate that allows the passage of ions only in the open state. Unwin has suggested that a ring of conserved leucine residues (*Torpedo* α L251) in the middle of the M2 forms the narrowest part and the gate of the receptor (Unwin, 1993). This suggestion is based mainly on the estimation of the position of an observed kink in the middle of the putative pore of the receptor at 9 Å resolution electron micrographs (Unwin, 1993). This idea also gains support from the results of photolabeling (Revah et al., 1990; White and Cohen, 1992) and site-directed mutagenesis experiments (Revah et al., 1991). In contrast, the results of the cysteine-substitution experiments demonstrated that all the residues facing the lumen of the pore up to the intermediate ring (α E241) can interact with extracellularly applied MTSEA in the closed state of

the receptor (Akabas et al, 1994). Therefore, the barrier or gate of the receptor is most likely more cytoplasmic than the originally proposed ring of leucine residues.

These conflicting results prompted Karlin and colleagues to further explore the location of the gate of the muscle nAChR (Wilson and Karlin, 1998). They substituted 6 residues at the cytoplasmic side of M2 including the intermediate ring residue (α S239 to α T244) with cysteines and expressed each mutant subunit with β , γ and δ subunits in human embryonic kidney (HEK-293) cells. The blocking effect of both intracellular and extracellular MTSEA on the mutant receptors was then measured using the whole-cell patch-clamp technique. To quantify the differences in the reactivities of the mutant receptors with MTSEA, they measured the rates of reaction with MTSEA at different concentrations and different application intervals. In the absence of ACh, extracellular MTSEA reacted with α T244C 2000-5500 times faster than with α K242C, α E241C and α G240C, whereas intracellular MTSEA reacted more than 100 times faster with α G240C than with α T244C. In the presence of ACh, all mutants reacted faster with MTSEA resulting in greater rate constants. The location of the substituted cysteines relative to the gate were then estimated by measuring the gate index, described as the ratio of the effect of ACh on the rate constant for the reaction of the extracellular MTSEA to the effect of ACh on the rate constant for the reaction of the intracellular MTSEA (Pascual and Karlin, 1998; Wilson and Karlin, 1998). The gate index places α G240C on the intracellular side of the gate and α T244C on the extracellular side of the gate. Based on these results the gate of the receptor is most likely at or close to the intermediate ring, consistent with the critical role of the intermediate ring in determining the single channel conductance (Imoto et al., 1988), ion selectivity (Konno et al., 1991) and permeability (Wang and Imoto, 1992) of the nAChR.

Basic science solves clinical problems

Studies on structure-function relationship of the muscle nAChR pioneered a large body of work on a variety of ligand-gated and voltage-gated ion channels. Our ability to study the structure-function relationship of ion channels using advanced molecular and patch-clamp electrophysiological techniques has allowed researchers to explore the role of these membrane proteins in many pathophysiological conditions. In recent years, this approach has led to identification of several ion channel related diseases (Ackerman and Clapham, 1997). Among these are several cases of congenital myasthenic syndromes that have been linked to mutations in the muscle nAChR (Vincent et al., 1997). Our understanding of the underlying cause of this disease would have been impossible without our knowledge of the structure-function relationship of the muscle nAChR.

Congenital myasthenic syndromes and muscle nAChR malfunction:

Congenital myasthenic syndromes (CMS) are genetic disorders that are characterized by defects at the neuromuscular junction. Similar to myasthenia gravis (MG), CMS are accompanied by severe muscle weakness and fatigue; however, unlike the autoimmune mediated MG, the underlying cause of CMS are defects in the pre- or post-synaptic apparatus (Engel et al., 1998; Boonyapisit et al., 1999). Slow channel syndrome is a form of CMS that is characterized by abnormally prolonged miniature endplate currents (MEPCs) and end plate myopathy (Engel et al., 1998). In the past decade, examination of patients with slow channel syndrome, mainly through the work of Engel, Sine and colleagues, has led to the identification of a number of mutations in the extracellular domain, the cytoplasmic loop, the M1 region and the M2 region of their muscle nAChRs (Vincent et al., 1997; Engel et al., 1998; Boonyapisit et al., 1999). Interestingly, mutations in the M2 region appear to cause more disabling symptoms than mutations in the M1 region and the extracellular

domain (Engel et al., 1998) consistent with the critical role of the M2 region in forming the ionic pore.

Using patch-clamp electrophysiology, Ohno et al. (1995) examined the intercostal muscle nAChRs of a 20-year-old patient suffering from slow-channel syndrome. When single channel records from end-plates of the CMS patient were compared to those of control specimen, CMS channels revealed a population of channels with significant prolongation of channel openings (Ohno et al., 1995). The mutational analysis of the nAChR subunits revealed the presence of a heterozygous single nucleotide transversion leading to the alteration of a conserved threonine residue in the M2 to a proline residue in the ϵ subunit (ϵ T264P). When recombinant mutant ϵ T264P or wild type ϵ were coexpressed with wild type α , β and δ subunits in HEK-293 (human embryonic kidney) cells, mutant receptors showed similar open channel properties to those recorded from CMS nAChRs, while wild type receptors in HEK cells were similar to the control nAChRs. These findings established a direct link between this mutation and the abnormally prolonged nAChR openings in the patient.

In a similar study, Milone et al. (1997) examined the single channel properties of the muscle nAChR of another CMS patient, a 12 year old boy, that had been confined to wheel-chair with extreme muscle fatigue. Similar to the previous case, single channel data from the patient's end-plates indicated a population of the receptors with more prolonged channel openings compared to normal end-plates. Mutational analysis of the patient's genomic DNA revealed the presence of a heterozygous nucleotide transversion in the α subunit resulting in alteration of a valine residue in the M2 region to a phenylalanine residue (α V249F). Surprisingly, this mutation was not detected in any of the patient's parents or relatives; however, closer examination of the father's genomic DNA by allele specific PCR (polymerase chain reaction) indicated mosaicism for α V249F. Therefore, for the son to be

affected, the α V249F mutation must have been carried by a sperm, suggesting that the father is a mosaic for both germ-line and somatic cells (Milone et al., 1997). Further single channel analysis of mutant receptors in HEK-293 cells indicated that α V249F both enhances ACh affinity at rest and stabilizes the open state of the receptor resulting in prolongation of channel openings (Milone et al., 1997). The increase in channel openings at the single channel level due to this mutation (also the case for ϵ T264P) is thought to underlie the prolonged MEPCs observed in slow channel CMS. These prolonged MEPCs in turn could lead to a depolarization block of transmission at physiologic rates and cationic overloading of the postsynaptic muscle resulting in end-plate myopathy (Engel et al., 1998). These results further highlight the critical role of the conducting pathway of the muscle nAChR for normal physiology of the neuromuscular junction.

Neuronal nAChRs:

Neuronal nAChRs are widely expressed in the peripheral and the central nervous system. The functional role of these receptors in the central nervous system (CNS) is still ambiguous; however, in the peripheral nervous system (PNS), it is well known that neuronal nAChRs underlie the excitatory synaptic currents in postsynaptic autonomic ganglionic neurons that receive cholinergic preganglionic innervation. Studies on the effect of drugs on ganglionic transmission date back to the late 1800's (Langley and Dickinson, 1890). Fast excitatory postsynaptic potentials (EPSPs) in the ganglionic neurons in the PNS are similar to the endplate potentials (EPPs) at the neuromuscular junction in that they are generated by presynaptic release of ACh (Feldberg and Gaddum, 1934). Released ACh interacts with postsynaptic receptors and increases the membrane conductance to Na^+ and K^+ (Eccles, 1963; Rang, 1981). However, ACh-evoked responses in muscle and neurons have different sensitivities to antagonists. The competitive antagonist hexamethonium is a more effective blocker of the autonomic ganglionic transmission than the neuromuscular transmission (Paton and Zaimis, 1951; Ascher et al., 1979; Rang and Rylett, 1984). On the other hand, the high affinity blocker of the muscle nAChRs, α -bungarotoxin, does not block the ganglionic transmission (Brown and Fumagalli, 1977; Carbonetto et al., 1978) despite the presence of high affinity binding sites for the toxin on many peripheral neurons (Fumagalli et al., 1976; Carbonetto et al., 1978; Ravdin and Berg, 1979). These findings strongly suggested that neuronal nAChRs most likely share many structural elements with the muscle nAChR, while having their own unique features. In addition, these findings suggested that neuronal nAChRs most likely comprise a heterogeneous population of receptors.

Neuronal nAChR subunit genes and the overall membrane topology

Molecular cloning of neuronal nAChR subunit genes has revealed the presence of a number of subunits in the PNS and the CNS. To date, 11 vertebrate genes have been

cloned that encode neuronal nAChR subunits: α 1- α 9 and β 2- β 4. Similar to muscle nAChRs, neuronal nAChRs are pentameric in structure, but unlike the muscle receptor a functional neuronal nAChR can be formed by coassembly of two α and three β subunits (Cooper et al., 1991). The exceptions to this stoichiometry are the α 7, α 8 and α 9 subunits, which can form homomeric receptors without incorporating any β subunits. Unlike the heteromeric neuronal nAChR subtypes, homomeric α 7, α 8 and α 9 show sensitivity to the muscle nAChR blocker α -bungarotoxin (α -BTX). In the PNS, α 3 and β 4 are the most abundant nAChR subunits (Boyd et al., 1988; Couturier et al., 1990; Mandelzys et al., 1995), whereas in the CNS, α 4 and β 2 are the most abundant subunits (Wada et al., 1989). α 7 is also present at high levels in both the PNS and the CNS (Bertrand et al., 1990; Seguela et al., 1993). These findings suggest that neuronal nAChR comprise a large family of receptors with pharmacological heterogeneity and functional diversity.

Neuronal nAChR subunits are highly homologous to the muscle subunits and have a similar membrane topology. The hydropathy profile of the subunits predicts an extracellular amino terminus, four transmembrane domains (M1-M4), and a short extracellular carboxy terminus (Fig. 1). Similar to the muscle nAChR α subunit, each neuronal α subunit has the characteristic pair of cysteine residues in their amino terminus that are involved in the binding of the agonist, and several studies have demonstrated that the M2 transmembrane domain is a critical part of the conducting pathway of these ion channels.

Ionic selectivity of the neuronal nAChRs

Although less extensively studied, it appears to a large extent that ion selectivity properties of neuronal nAChRs are similar to those of the muscle nAChR (Mathie et al., 1991; Nooney et al., 1992). Nutter and Adams measured the relative permeability of neuronal nAChRs for several monovalent and divalent cations in cultured rat cardiac parasympathetic ganglion neurons (Nutter and Adams, 1995). They found

that, similar to the muscle nAChRs, neuronal nAChRs have a weak selectivity for monovalent (alkali metals) and divalent (alkaline earth metals) cations. The striking difference between the muscle and neuronal nAChRs is their permeability to Ca^{++} (P_{Ca}) relative to that to monovalent alkali metals (P_{K}) (Fieber and Adams, 1991; Sands and Barish, 1991; Vernino et al., 1992; Trouslard et al., 1992).

Neuronal nAChRs are highly Ca^{++} permeable

Compared to muscle nAChRs, neuronal nAChRs have a much higher relative permeability to Ca^{++} , and the degree of their Ca^{++} permeability is dependent on the subunit composition of the receptor. High Ca^{++} permeability has been reported for neuronal nAChRs in cultured rat parasympathetic neurons (Fieber and Adams, 1991), PC12 cells (Sands and Barish, 1991), rat medial habenula neurons (Mulle et al., 1992), bovine chromaffin cells (Vernino et al., 1992) and cultured rat sympathetic neurons (Trouslard et al., 1993). In heterologous expression systems, Ca^{++} permeability of nAChRs shows strong subunit dependence, with $\alpha 7$ homomers having the highest ($P_{\text{Ca}}/P_{\text{Na}} = 10-20$) (Seguela et al., 1993; Bertrand et al., 1993) and $\alpha 3\beta 4$ the lowest ($P_{\text{Ca}}/P_{\text{Na}} = \sim 1$) (Costa et al., 1994) Ca^{++} permeability. More recently it has been demonstrated that incorporation of $\alpha 5$ subunit into $\alpha 3\beta 4$ or $\alpha 4\beta 2$ receptors causes an increase in $P_{\text{Ca}}/P_{\text{Na}}$ of the receptor (Gerzanich et al., 1998; Yu and Role, 1998). Therefore, the subunit composition of the native nAChRs expressed in different parts of the nervous system may in part underlie their different Ca^{++} permeability.

Molecular mechanisms underlying Ca^{++} permeability of neuronal nAChRs

Calcium influx through ion channels has been shown to trigger important signal transduction mechanisms involved in modulation of gene expression implicated in learning and memory. Despite the functional importance of the high Ca^{++}

permeability of neuronal nAChRs, the molecular mechanisms involved have not been extensively studied. In one study, Bertrand and colleagues, using site-directed mutagenesis and electrophysiology, identified two sites that appeared to be important for Ca^{++} permeability of the $\alpha 7$ receptor expressed in *Xenopus* oocytes (Bertrand et al., 1993). Interestingly, one of these sites is the intermediate ring that has been implicated in determining the single channel conductance and ion selectivity of the muscle nAChR (Konno et al., 1991; Wang and Imoto, 1992). Although, the homomeric nature of the $\alpha 7$ receptor is ideal for site directed mutagenesis experiments, the fast desensitization properties and the lack of reliable $\alpha 7$ single channel recordings has created a significant amount of inconsistency in interpreting electrophysiological recordings of this receptor. Also, since many of these experiments used the oocyte expression system, some of the results may have been contaminated by a contribution of the endogenous Ca^{++} -activated Cl^- current in oocytes (compare Seguela et al., 1993 and Costa et al., 1994). Similar experiments on heteromeric neuronal nAChRs, that could point to subunit specificity and minimum net negative charge on the intermediate ring affecting Ca^{++} permeability, are lacking. It is plausible to hypothesize that the number of charges at the intermediate ring may correlate with the degree of Ca^{++} permeability of the receptor.

Neuronal nAChR are modulated by extracellular Ca^{++}

In addition to having high permeability to Ca^{++} , nAChRs appear to be modulated by extracellular Ca^{++} (Mulle et al., 1992a; Vermino et al., 1992). Increasing the concentration of extracellular Ca^{++} in the low millimolar range potentiates the ACh-evoked responses of neuronal nAChRs. Changeux and colleagues examined the effect of extracellular Ca^{++} on ACh-evoked currents in neurons from the rat medial habenular nucleus using single channel recording techniques (Mulle et al., 1992). These results indicated that the potentiation of macroscopic ACh-evoked currents is due to an increase in the frequency of channel opening at the single channel level.

This effect was unlikely due to a cytoplasmic action of Ca^{++} , since it was instantaneous in outside out patches and persisted in the presence of Ca^{++} chelators in the recording electrode. Therefore, Changeux and colleagues proposed an allosteric modulatory role for extracellular Ca^{++} , whereby Ca^{++} can bind to an extracellular site on the receptor and cause a conformational shift to a state that favours higher frequency opening of the receptor (Mulle et al., 1992a).

Bertrand Changeux and colleagues have explored the site of action of extracellular Ca^{++} in at least two studies. Eisele et al. (1993) constructed a chimeric receptor that contained the N-terminal region of the nicotinic $\alpha 7$ receptor (up to M1) and the complementary C-terminal segment of the serotonergic receptor, 5HT3 (including all four transmembrane domains and the C-terminus). When expressed in *Xenopus* oocytes, this chimeric receptor exhibited an $\alpha 7$ -like pharmacological profile: both ACh and nicotine activated the receptor and α -BTX blocked the ACh-evoked response. However, the selectivity and conductance profile of the receptor were similar to those of the wild type 5HT-3 receptor: a very mild inward rectification and a very low Ca^{++} permeability. Eisele et al. reasoned that if the modulatory site for the action of Ca^{++} is in the extracellular region of the receptor, the ACh-evoked current in the chimeric receptor should exhibit potentiation in response to increasing extracellular Ca^{++} concentrations. To test this hypothesis, they rapidly exposed the chimeric receptor to different concentrations of Ca^{++} following activation by ACh. The results suggested a Ca^{++} -dependent increase in the inward currents at -100 mV. This increase in the amplitude of the inward current may have been in part contaminated by the Ca^{++} -dependent chloride current in the oocytes, since only small amounts of Ca^{++} is enough to trigger large inward Cl^- currents at -100 mV (E_{rev} for Cl^- is $\sim -20\text{mV}$ in oocytes). One control for this contamination would have been to examine this potentiation at a range of membrane potentials in the presence and absence of extracellular Cl^- ; a lack of shift in the E_{rev} of the ACh-evoked I-V curves

then would have suggested minimal contribution by Cl^- current. If we assume the contribution of Cl^- currents to this potentiation to be negligible, these results suggest that extracellular Ca^{++} acts on the extracellular region of the receptor to potentiate the ACh-evoked response.

More recently, Galzi et al. (1996) identified a region in the extracellular domain of $\alpha 7$ subunit that appears to contain a modulatory binding site for extracellular Ca^{++} . This site spans amino acids 161-172 and overlaps with parts of the ACh binding pocket. Thus, one mechanism for potentiation of the receptor by extracellular Ca^{++} is likely through an interaction between extracellular Ca^{++} and the agonist at this site (Galzi et al., 1996).

M2 segment lines the pore of the neuronal nAChRs

Since the cloning and characterization of neuronal nAChR subunit genes, several groups have used a combination of site-directed mutagenesis and electrophysiological techniques on heterologously expressed recombinant neuronal nAChRs to elucidate the conducting pathway of these receptors.

In one of the initial studies, Cooper and colleagues demonstrated that, similar to the muscle nAChR, removal or addition of negative charges at the extracellular ring ($\alpha\text{E}266$ and $\beta\text{K}260$) of $\alpha 4\beta 2$ neuronal nAChR subtype has significant effects on the single channel conductance of the receptor (Cooper et al, 1991). Substitution of the glutamic acid in the extracellular ring of the α subunit to a lysine residue ($\alpha 4\text{E}266\text{K}$) caused a 50% reduction in the single channel conductance, whereas substitution of a lysine residue at the corresponding position on the β subunit ($\beta 2\text{K}260\text{E}$) doubled the single channel conductance. Since each of the conductance mutant $\alpha 4$ or $\beta 2$ subunits introduced a new single channel conductance level, Cooper et al. reasoned that by coexpressing a mutant and wild type $\alpha 4$ or $\beta 2$ subunit in the same oocyte the number of single channel conductance states can be used as an

indication of how many $\alpha 4$ or $\beta 2$ subunits have been incorporated into the receptor complex. When $\alpha 4E266K$ and wild type $\alpha 4$ subunits were coexpressed with $\beta 2K260E$ subunits in *Xenopus* oocytes, only three distinct single channel conductance levels were detected: one corresponding to the single channel conductance of $\alpha 4\beta 2K260E$ receptor, one corresponding to the single channel conductance of $\alpha 4E266K\beta 2K260E$ and one intermediate conductance most likely corresponding to $\alpha 4\alpha 4E266K\beta 2K260E$. On the other hand, when $\beta 2K260E$ and wild type $\beta 2$ subunits were coexpressed with one $\alpha 4$ subunit, four different single channel conductance states were measured. Based on possible arrangements of subunits in one complex these results indicated that the receptor is most likely a pentamer made up of two $\alpha 4$ and three $\beta 2$ subunits (Cooper, 1991).

Subsequently, Ballivet, Bertrand, Changeux and colleagues used site-directed mutagenesis and electrophysiology to identify important amino acids in the conducting pathway of $\alpha 7$ receptor (Revah et al., 1991; Galzi et al., 1992; Bertrand et al., 1992; Eisele et al., 1993; Corringer et al., 1999). Revah et al. (1991) mutated several residues in the M2 region of $\alpha 7$ that would be facing the ion channel pore based on sequence homology to the muscle (*Torpedo*) nAChR. They found that a ring of leucine residues in the middle of the M2 segment is important for the desensitization kinetics of the receptor. When this non-polar residue was substituted with a more polar serine or threonine residue, the mutant receptor expressed in *Xenopus* oocytes exhibited significantly less desensitization than the wild type $\alpha 7$ receptor in response to application of the agonist. Examination of the mutant receptors at the single channel level suggested the presence of an additional open channel state at levels of ACh that causes desensitization of the wild type $\alpha 7$ receptor (Revah et al., 1991). These recording were only done in the cell attached configuration, a method of recording that usually activates intrinsic stretch-activated receptors in oocytes that appear to have very similar characteristics as the ACh-

activated single channels (Methfessel et al., 1986). It is not clear in this report what measures were taken to control for these endogenous currents. In addition, the single channel properties of the wild type $\alpha 7$ receptor have not been extensively examined; therefore, it is difficult to make conclusive interpretations when comparing the single channel properties of the mutant and wild type receptors. Despite these technical complexities, the authors speculated that the additional open state observed in $\alpha 7L247T$ is normally blocked by the leucine residues in the wild type receptor; therefore, substitution of these leucines with smaller, more polar amino acids allows the transition to this open state resulting in an apparent removal of desensitization.

In subsequent studies, Galzi et al. (1992) explored the region(s) in the receptor that determine(s) cation-selectivity of the $\alpha 7$ receptor. Cation conducting muscle and neuronal nAChRs have a high degree of homology in their pore region with anion conducting GABA_A and glycine receptors; however, there are several residues in this region that are not shared between the two types of receptors. Galzi et al reasoned that the substitution of these residues in the M2 of the $\alpha 7$ receptor with the corresponding residues of the M2 region of GABA_A and glycine receptors may be sufficient to change the charge selectivity of $\alpha 7$ from cationic to anionic. The chloride permeabilities of the mutant and wild-type receptors were examined electrophysiologically upon expression in *Xenopus* oocytes. When extracellular chloride was replaced with isothionate or mannitol (impermeable through nAChRs) the reversal potential for the mutant receptor, but not the wild type receptor, showed a large positive shift indicating high Cl⁻ permeability of the receptor. A positive shift in the E_{rev} of ACh-activated single channels in the mutant receptor was also observed. These results indicated that only three amino acid changes are sufficient to change the $\alpha 7$ receptor to an anion selective channel: introduction of an additional proline residue adjacent to the intermediate ring, substitution of the negatively charged residues of the intermediate ring to neutral alanines, and substitution of a nonpolar

valine in the M2 region to a polar threonine residue. These results again suffer from the same technical complexities involved with recordings from the $\alpha 7$ receptor. In particular, the single channel records in this report are less convincing for two reasons. First the data only represent recordings from two patches, and secondly there is no recordings from the wild-type receptor that could be used for comparison.

Corringer et al. (1999) have further examined the selectivity filter of the $\alpha 7$ receptor. The important finding of these experiments is that the insertion of the proline residue can only be done between the positions 234 to 238 in order to construct a functional anion selective receptor. Insertions up stream of 234 yielded cationic receptors and insertions down stream of 238 resulted in non-functional receptors (Corringer et al., 1999). These results are consistent with the role of the corresponding region of the muscle nAChR in forming the selectivity filter and gate of the receptor (Wilson and Karlin, 1998).

Taken together, these results indicate the importance of the M2 region in determining the conductance and selectivity of neuronal nAChRs, as is the case for the muscle nAChR. These studies also suggest that there is a high degree of homology between the overall pore geometry among anion- and cation-selective members of the ligand-gated ion channel super family.

Neuronal nAChRs and diseases of the nervous system

The function of neuronal receptors in the CNS remains unclear, despite the accumulating evidence implicating neuronal nAChRs in a variety of physiological and pathophysiological conditions. A large body of evidence in the past two decades suggests that most central neuronal nAChRs are located presynaptically and are involved in the modulation of neurotransmitter release (Role and Berg, 1997; McDermott et al., 1999). Recent findings, showing linkage between two mutations in the $\alpha 4$ subunit gene and autosomal dominant nocturnal frontal lobe epilepsy

(ADNFLE). have provided the first direct evidence for involvement of neuronal nAChRs in causing disease (Steinlein et al., 1995; Steinlein et al., 1997), highlighting the important role of these receptors for normal physiology of the nervous system.

ADNFLE is caused by mutations in the M2 region of the $\alpha 4$ subunit:

Autosomal dominant nocturnal frontal lobe epilepsy (ADNFLE) is an idiopathic partial epilepsy that is characterized by clusters of brief motor seizures during sleep. Clinical onset of this disorder is usually in childhood with persistence of symptoms through adulthood (Sheffer et al., 1994). Recently, two mutations in the $\alpha 4$ subunit gene have been linked to ADNFLE (Steinlein et al., 1995; Steinlein et al., 1997). The first mutation, found in all affected members of a large Australian pedigree with ADNFLE (Philips et al., 1995), is a single nucleotide missense mutation in the $\alpha 4$ subunit gene leading to substitution of a serine to a phenylalanine in the middle of the M2 region ($\alpha 4$ S248F) (Steinlein et al., 1995). The second mutation, found in a Norwegian family, is a three nucleotide insertion mutation of the $\alpha 4$ subunit gene leading to the insertion of a leucine residue near the extracellular end of the M2 region ($\alpha 4$ L264ins) (Steinlein et al., 1997). The functional consequence of these mutations have been studied by electrophysiological examination of the mutant subunits coexpressed with the $\beta 2$ subunit in *Xenopus* oocytes (Weiland et al., 1996; Steinlein et al., 1997; Kuryatov et al., 1997; Figl et al., 1998). The results of these experiments indicate that both mutations lead to an increase in the rate of desensitization and a decrease in Ca^{2+} permeability of the receptor (Weiland et al., 1996; Steinlein et al., 1997; Kuryatov et al., 1997; Figl et al., 1998). Therefore, it appears that the net effect of these mutations is an attenuation of the nicotinic response in the regions of the brain that these mutant genes are expressed. Therefore, if nAChRs in these regions normally potentiate an inhibitory nerve terminal, it is plausible that the lack of an appropriate nicotinic response can lead to over excitation and possibly seizure-like activity in those regions.

An alternative mechanism by which these mutations can lead to epileptic seizures has been proposed by Figl et al. (1998). Electrophysiological experiments have revealed a use-dependent potentiation of the ACh response in both mutant receptors α 4S252F β 2 and α 4L264ins β 2 compared to the wild type α 4 β 2 (Figl et al., 1998). In contrast to the wild type receptor, both mutant receptors show a significant increase in their response to ACh upon repeated applications of ACh in a reversible manner. The degree of this use-dependent potentiation is decreased by either prolonging the interval between applications or by increasing the concentration of ACh (Figl et al., 1998). Therefore, in regions of the brain where these mutant receptors are expressed, high rates of stimulation of the nAChRs can produce higher levels of excitation leading to epileptic seizures.

Inward Rectification of Neuronal Nicotinic Receptors:

In spite of many structural and functional similarities, muscle and neuronal nAChRs exhibit drastically different current-voltage relationships (I-V curves). When macroscopic ACh-evoked currents are measured at different voltages from the endplate muscle, a nearly linear current-voltage relationship (I-V curve) is obtained. This indicates that muscle nAChRs allow the passage of cations into and out of the cell equally well. In contrast, when one records whole-cell ACh-evoked currents from a neuron, there is no detectable outward current at positive membrane potentials, a process known as inward rectification.

Macroscopic inward rectification has been reported for native neuronal nAChRs from rat superior cervical ganglion (SCG) neurons (Selyanko et al., 1979; Mathie et al., 1987), rat adrenal chromaffin cells (Hirano et al., 1987) and rat pheochromocytoma cells (PC12) (Cachelin and Neuhaus, 1989; Ifune and Steinbach, 1990; Sands and Barish, 1992) as well as for heterologously expressed receptors in *Xenopus* oocytes (Forster and Bertrand, 1995) and HEK-293 cells (Buisson et al., 1996).

This strong inward rectification is lost in ACh-evoked single channel currents recorded from excised patches (Mathie et al., 1990; Ifune and Steinbach, 1992; Sands and Barish, 1992). Colquhoun and colleagues analyzed the single channel properties of the ACh-evoked single channel currents in cultured sympathetic neurons using the outside out patch-clamp technique (Mathie et al., 1990). They found no significant differences between the single channel conductance, open channel burst times and open channel frequency at negative and positive membrane potentials for ACh-activated single channels. Similarly, Ifune and Steinbach (1992) found that in outside out patches from PC12 cells ACh-activated single channels show similar single channel conductance and open channel probability at positive and negative membrane potentials. These results strongly suggested that the single channel properties of

neuronal nAChRs cannot explain the ACh-evoked macroscopic inward rectification leading to the hypothesis that an intracellular diffusible blocking agent may be involved.

Consequently, several groups examined the effect of divalent cations, specifically Mg^{2+} on inward rectification. Analysis of the effect of Mg^{2+} at the single channel level revealed that intracellular Mg^{2+} (2-10 mM) can moderately reduce the ACh-evoked single channel conductance at positive membrane potentials in both sympathetic neurons and PC12 cells (Mathie et al., 1990; Neuhaus and Cachelin, 1990; Ifune and Steinbach, 1991). However, the common finding was that at the whole cell level, inward rectification persisted in divalent free solutions in the presence of chelating agents for intracellular Mg^{2+} (Neuhaus and Cachelin, 1990; Mathie et al., 1990; Forster and Bertrand, 1995). These results indicated that a intracellular Mg^{2+} is not a likely candidate to underlie the strong macroscopic rectification, and that its effect could be mainly a charge screening effect as opposed to a blocking effect (Imoto et al., 1988; Neuhaus and Cachelin, 1990).

In a further attempt to characterize the mechanism of rectification, Sands and Barish (1992) and Ifune and Steinbach (1993) demonstrated that macroscopic inward rectification can be partially removed in PC12 cells when cells are dialyzed with Na_2 -ATP as a chelating agent. Ifune and Steinbach addressed the possibilities for the action of ATP. They argued that it is unlikely that this partial removal of rectification could be due to receptor phosphorylation, or involvement of a GTP-binding protein; thus, they suggested that the loss or degradation of other cytoplasmic factor(s) may be involved.

These results of the single channel analysis together with the partial removal of rectification at the macroscopic level suggest that the strong macroscopic inward rectification of neuronal nAChRs is not due to an intrinsic property of the receptor and most likely involves an intracellular factor(s) that is lost in excised patches. If this

is the case, then the degree of inward rectification of neuronal nAChRs can be modulated under different physiological or pathophysiological conditions. This modulation can in turn have important consequences for the synaptic function of neuronal nAChRs.

Polyamines and Inward Rectification

Polyamines comprise a class of ubiquitous organic cations that have been implicated in a variety of physiological and pathophysiological conditions. Endogenous polyamines, spermidine and spermine and the diamine putrescine, are present in all vertebrate cells and are involved in important functions from DNA synthesis to cell growth and differentiation (Shaw, 1979; Pegg, 1986). Polyamines are found at millimolar concentrations in the mammalian brain and have been demonstrated to be released from cerebral cortex slices (Shaw and Pateman, 1973; Harman and Shaw, 1981; Yoneda et al., 1991; Gilad and Gilad, 1991). Polyamines have also been implicated in several pathophysiological conditions, particularly in induction of tumors (Pegg, 1986). Because of the potential role of polyamines in disease, many attempts have been made to control the level of polyamines by targeting enzymes in their biosynthesis pathway (McCann and Pegg, 1992; Swärd et al., 1997). These efforts have encountered many difficulties partly because polyamines are normally present at high levels and are highly compartmentalized within cells (Pegg, 1986; Davis, 1990; Watanabe et al., 1991; Swärd et al., 1997). In addition, highly positively charged polyamines have a high binding affinity for negatively charged membraneous, cytoplasmic and nuclear macromolecules including DNA, RNA, phospholipids and ATP (Watanabe, 1991; Meksuriyen, 1998).

In the past decade, a number of studies have implicated polyamines in modulation and block of several ion channels (Williams, et al., 1990; Ficker et al., 1994; Bowie and Mayer, 1995). More relevant to my study, intracellular polyamines

have been implicated recently in blocking inward rectifier potassium channels and Ca^{++} permeable α -amino-3-hydroxy-5-methyl-4-isoxazolepropionic acid (AMPA) and kainate glutamate receptors (for reviews see Nichols and Lopatin, 1997; Dingledine et al., 1999). This block has been demonstrated to be a high affinity block with strong voltage dependence. Results from several studies strongly suggest that the voltage-dependent block by intracellular spermine and spermidine underlies the inward rectification of inward rectifier potassium channels and AMPA and kainate glutamate receptors (Falker et al., 1995; Bowie and Mayer, 1995).

Polyamines cause the inward rectification of Inward rectifier K^+ channels

Inward rectifier potassium channels constitute a family of potassium channels (Kir family) that are responsible for maintaining the membrane potential close to the K^+ reversal potential (Nichols et al., 1993; Kubo et al., 1993; Wang et al., 1993; Ashfort et al., 1994; for review see Nichols and Lopatin, 1997). These ion channels conduct inward currents at membrane potentials negative to potassium reversal potential (E_k), small outward current at potentials slightly more positive than E_k and close at more depolarized membrane potentials. This unique inward rectification profile has important physiological consequences. In cardiac ventricular cells, where Kir channels are primary potassium channels, the lack of a large outward current at depolarized potentials leads to a lengthening of the action potential duration (Kurachi, 1985; Vandenberg, 1987; Hille, 1992). In addition, the current profile of Kir channels near E_k , both prevents overhyperpolarization by giving rise to inward currents at potentials negative to E_k and opposes small depolarizations by conducting outward currents at potentials positive to E_k ; in other words, Kir channels clamp the membrane resting potential near E_k .

The mechanism of rectification of Kir potassium channels has been the focus of a number of studies in the past decade (Vandenberg, 1987; Matsuda, 1991; Lopatin

et al., 1994; Falker et al., 1995). In excised membrane patches, Kir potassium channels lose their inward rectification and do not exhibit any intrinsic voltage-dependence (Matsuda et al., 1988; Lopatin et al., 1994; Ficker et al., 1994) suggesting that a diffusible intracellular factor may act as a gating molecule. Ruppersberg and colleagues elegantly demonstrated that the inward rectification can be restored to excised patches of *Xenopus* oocytes expressing Kir2.1 channels upon exposure of the cytoplasmic side of the patch to oocyte cell extracts (Falker et al., 1995). They further showed that including strong chelators of Mg^{++} in the cell extracts did not have any effect on the inward rectification, whereas the addition of Na_2 -ATP to the extracts partially removed the inward rectification suggesting that polyamines are involved. The effect of polyamines was then directly tested in excised patches by including different concentrations of spermine and spermidine in the recording electrode. The results together with previous analysis of polyamine block of Kir2.1 channels (Falker et al., 1994) indicated that both spermine ($IC_{50}=40$ nM at +50 mV) and spermidine (with less affinity) block Kir2.1 channels at physiological concentrations in a voltage-dependent manner, and thus underlie the macroscopic inward rectification of Kir2.1 channels.

Since the identification of polyamines as the intracellular agents conferring rectification to Kir channels, several studies have focused on characterizing the structural element(s) of the channel that interact with polyamines. One such element is a negatively charged aspartate residue (D172) in the second transmembrane domain of Kir2.1 (Wible et al., 1994; Lopatin et al., 1994; Falker et al., 1994; Yang et al., 1995). Substitution of this negatively charged residue with neutral glutamine (Q) significantly decreases the affinity of spermine for the receptor and results in a shallower rectification; interestingly one native subtype of Kir family, Kir1.1, has a neutral amino acid at this site and exhibits very little rectification (Falker et al., 1994; Lopatin et al., 1994; Falker et al., 1995). These results suggest that positively charged

polyamines interact with negatively charged residues within the conducting pathway of the ion channel.

Polyamines cause the inward rectification of AMPA and kainate receptors

Another subfamily of ion channels that exhibit strong inward rectification are Ca⁺⁺ permeable subtypes of AMPA/kainate receptors (Hume et al., 1991; Dingledine et al., 1999). The mechanism of inward rectification of AMPA/kainate receptors has been explored in a number of recent studies. Similar to neuronal nAChRs and inward rectifier K⁺ channels, inward rectification of both native and recombinant AMPA/kainate receptors is lost in excised patches, suggesting that a diffusible cytoplasmic factor most likely accounts for the macroscopic inward rectification (Bowie and Mayer, 1995; Donevan and Rgawski, 1995; Isa et al., 1995; Kamboj et al., 1995; Koh et al., 1995). Based on the effect of polyamines on Kir channels, Bowie and Mayer hypothesized that polyamines may have a similar effect on AMPA/kainate receptor. In an extensive study, they examined the effect of polyamines on inward rectification of homomeric GluR6 receptors expressed in HEK-293 cells using outside out patch clamp technique. They found that in outside-out patches both spermine and spermidine block GluR6 receptors when applied to the cytoplasmic side of the patch. To further analyze their results, they used a derivation of the Woodhull model for voltage-dependent ion channel block (Woodhull, 1973).

This model predicts that a blocker can enter the open receptor and bind to a site within the membrane electrical field. This binding occludes the ion channel and its strength depends on the membrane potential according to the following equation:

$$G/G_{\max} = 1 / \{1 + [S]/K_d\}$$

where

$$K_d = K_{d(0)} \exp\{-V_m z \delta F / [RT]\}$$

and G is the conductance in the presence of the blocker at any given V_m , G_{\max} is the maximum unblocked conductance, $[S]$ is the internal concentration of the blocker, K_d is the dissociation constant at a given V_m , $K_{d(0)}$ is the dissociation constant at 0 mV, z is the valence of the blocker, δ is the fraction of the membrane electric field sensed by the blocker, and F , R and T have their usual meanings.

Using this model, Bowie and Mayer fit the conductance-voltage curves (G-V curves) at different concentrations of spermine and spermidine for GluR6 and calculated the $K_{d(0)}$ and δ values for the block by spermine and spermidine. Using these values, they estimated the whole-cell concentration of intracellular spermine and spermidine by fitting the macroscopic G-V curves to the Woodhull equation. These values, 64 μM for spermine and 322 μM for spermidine, are well within the physiological concentrations of these polyamines in mammalian cells (Watanabe et al., 1991). Therefore, the authors concluded that the voltage-dependent block by spermine and spermidine is the underlying mechanism of inward rectification of AMPA/kainate receptors. These conclusions have been supported by findings of a number of similar studies on both native and recombinant AMPA/kainate receptors (Isa et al., 1995; Kamboj et al., 1995; Koh et al., 1995).

In the mammalian brain, there are four known genes encoding AMPA receptor subunits (GluR1-4) and five genes encoding kainate receptor subunits (GluR5-GluR7, KA1 & KA-2) (Hollmann and Heinemann, 1994; Dingledine et al., 1999). Structure of glutamate receptors is different from that of the nAChR superfamily; each subunit has a large extracellular N-terminus with four hydrophobic domains (M1-M4). M1, M3 and M4 are transmembrane which leaves the C-terminus in the cytoplasm. The M2 domain, however, forms a reentrant loop into the membrane (similar to the *P*-loop of K^+ channels) and is thought to line the ion channel pore (Bennett and Dingledine, 1995; Dingledine et al., 1999).

All AMPA and kainate subunits (except for GluR2, GluR5 and GluR6) whether in a homomeric receptor or a heteromeric receptor show a strong inward rectification and high calcium permeability in heterologous expression systems (Dingledine et al., 1999). However, the majority of GluR2, GluR5 and GluR6 subunits naturally undergo RNA editing; this editing changes a glutamine (Q612) residue to an arginine (R) within the M2 pore forming region of the subunit. Expression of edited subunits in homomeric receptors or in combination with other subunits leads to a drastic decrease in the single channel conductance, removal of inward rectification and a substantial decrease in Ca^{++} permeability of the receptor (Hume et al., 1991; Verdoorn et al., 1991; Egebjerg and Heinemann, 1993; Swanson et al., 1996). Consistent with the role of polyamines in inward rectification of AMPA and kainate receptors, intracellular polyamines have no effect the non-rectifying Q/R edited GluR2, and GluR6 in outside out patches (Bowie and Mayer, 1995; Washburn et al., 1997). Examination of native AMPA receptors in hippocampal interneurons using the single cell PCR method combined with patch-clamp electrophysiology suggests that differential expression of Q/R edited GluR2 and GluR5 is a major determinant of both Ca^{++} permeability and rectification properties of the native heteromeric receptors (Geiger et al., 1995; Washburn et al., 1997). These results indicate that polyamines also act as gating molecules to block neurotransmitter receptors in a voltage dependent manner, leading to inward rectification.

Hypothesis and Outline of the Proposed Experiments

Mechanism of inward rectification of neuronal nAChRs

Hypothesis:

Polyamines can interact with neuronal nAChRs in a voltage-dependent manner to confer inward rectification to neuronal nAChRs.

Rationale:

At least two lines of evidence support this hypothesis. First, the partial removal of ACh-evoked inward rectification in PC12 cells upon dialysis with Na₂-ATP (Sands and Barish, 1992; Ifune and Steinbach, 1993) and the fact that ATP is a good chelator of polyamines spermine and spermidine (Nakai and Glinsmann, 1977; Watanabe et al., 1991; Meksuriyen et al., 1998) suggest that positively charged polyamines may be involved in conferring rectification to neuronal nAChRs. Second, a large body of evidence indicates that polyamines, spermine and spermidine, confer inward rectification to inward rectifier K⁺ channels and Ca²⁺-permeable AMPA/kainate receptors.

Experimental outline:

I will test this hypothesis using whole-cell and outside-out single channel patch-clamp techniques on native nAChRs expressed by SCG neurons as well as recombinant neuronal nAChRs expressed in *Xenopus* oocytes. If cytoplasmically applied polyamines show a voltage-dependent blocking effect on nAChRs in outside-out patches, I will fit the data to the Woodhull model to find the dissociation constant of this block. Finally, to test whether this effect can account for the macroscopic inward rectification of nAChRs, I will estimate the concentrations of polyamines needed to confer inward rectification to nAChRs at the whole-cell level and compare those values to the physiological levels of intracellular polyamines. I will describe these results in the second chapter of my thesis.

Characterization of the site of interaction of polyamines

Hypothesis:

Two ring-like collections of negatively charged residues at the intracellular mouth of the pore are essential for the interaction of intracellular polyamines with neuronal nAChRs.

Rationale:

Results from studies on both inward rectifier K^+ channels and AMPA/kainate receptors suggest that polyamines interact with negatively charged (or polar) residues in the conductive pathway of the ion channel. For both muscle and neuronal nAChRs two rings-like accumulations of negatively charged residues (cytoplasmic and intermediate rings) near the cytoplasmic mouth of the pore influence the single channel conductance and ion selectivity of the receptor (Imoto et al., 1988; Konno et al., 1991; Bertrand et al., 1993). Therefore, it is likely that these negatively charged residues interact with intracellular polyamines.

Experimental outline:

I will use a combined approach of site-directed mutagenesis and electrophysiology to test this hypothesis on recombinant neuronal nAChRs expressed in *Xenopus* oocytes. I will use the two-electrode voltage clamp technique to examine the inward rectification properties of mutant receptors. In addition, I will use ion substitution experiments to examine the Ca^{++} permeability of the wild type and mutant receptors. I will describe these results in the third chapter of my thesis.

Permeability and block by large organic cations, extracellular polyamines and polyamine-related toxin, Joro toxin, of neuronal nAChRs:

Hypothesis:

Joro toxin blocks neuronal nAChRs with high affinity as an open channel blocker.

Rationale:

A number of studies implicate extracellular polyamines and polyamine-related neurotoxins, including the Joro spider toxin (JSTX), to have inhibitory effects on cation selective neurotransmitter receptors (Scott et al., 1993). In particular, these molecules have been shown to block Ca^{++} permeable, inward rectifying AMPA/kainate receptors with high affinity (Blaschke et al., 1993; Tsubokawa et al., 1995), suggesting that these toxins may also target neuronal nAChRs.

Experimental outline:

To test this hypothesis, I will examine the effect of JSTX on ACh-evoked currents using electrophysiological techniques and recombinant neuronal nAChRs expressed in *Xenopus* oocytes. I will discuss these results in the fifth chapter of my thesis.

CHAPTER 2

Neuronal Nicotinic Acetylcholine Receptors Are Blocked By Intracellular Spermine In A Voltage-Dependent Manner

Abstract

A common feature of neuronal nicotinic acetylcholine receptors (nAChR) is that they conduct inward current at negative membrane potentials but little outward current at positive membrane potentials, a property referred to as inward rectification. Physiologically, inward rectification serves important functions, and the main goal of our study was to investigate the mechanisms underlying the rectification of these receptors. We examined recombinant $\alpha_3\beta_4$ and $\alpha_4\beta_2$ neuronal nAChR subtypes expressed in *Xenopus* oocytes and native nAChRs expressed on superior cervical ganglion (SCG) neurons. Whole-cell ACh-evoked currents recorded from these receptors exhibited strong inward rectification. In contrast, we showed that single channel currents from these neuronal nAChRs measured in outside-out patches outwardly rectify. Based on recent findings that spermine, a ubiquitous intracellular polyamine, confers rectification to glutamate receptors and inwardly-rectifying potassium channels, we investigated whether spermine causes neuronal nAChRs to inwardly rectify. When spermine was added to the patch electrode in outside-out recordings, it caused a concentration- and voltage-dependent block of ACh-evoked single channel currents. Using these single channel data and physiological concentrations of intracellular spermine, we could account for the inward rectification of macroscopic whole-cell ACh-evoked conductance-voltage relationships. Therefore, we conclude that the voltage-dependent block by intracellular spermine underlies inward-rectification of neuronal nAChRs. We also found that extracellular spermine blocks both $\alpha_3\beta_4$ and $\alpha_4\beta_2$ receptors; this finding points to a mechanism whereby increases in extracellular spermine, perhaps during pathological conditions, could selectively block these receptors.

INTRODUCTION

Neuronal nicotinic acetylcholine receptors (nAChRs) are widespread in the nervous system where they function as postsynaptic receptors to excite neurons or as presynaptic receptors to modulate neurotransmitter release (Role and Berg, 1996). Structurally, neuronal nAChRs are pentamers (Anand et al., 1991; Cooper et al., 1991); however, the precise subunit composition of functional nAChRs on a given neuron has not been fully resolved (McGehee and Role, 1995). In the peripheral nervous system (PNS), α_3 and β_4 are the most abundant transcripts (Boyd et al., 1988; Couturier et al., 1990; Mandelzys et al., 1994), and most nAChRs are located postsynaptically at synapses formed between cholinergic preganglionic nerve terminals and postganglionic autonomic neurons. In the central nervous system (CNS), α_4 and β_2 transcripts are the most abundant (Wada et al., 1989; Flores et al., 1992), and many nAChRs appear to be located on presynaptic nerve terminals (McGehee et al., 1995; McGehee and Role, 1996). The recent finding that a missense mutation in the α_4 gene underlies autosomal dominant nocturnal frontal lobe epilepsy highlights the importance of neuronal nAChRs for normal CNS function (Steinlein et al., 1995; Weiland et al., 1996).

One striking feature common to all functional neuronal nAChRs, regardless of whether they are expressed on neurons or heterologously in non-neuronal cells, is the strong inward rectification that results from a progressive reduction in channel conductance as the membrane potential depolarizes over the physiological range (Bertrand et al., 1990; Mathie et al., 1990; Ifune and Steinbach, 1991; Ifune and Steinbach, 1992; Sands and Barish, 1992). Physiologically, this inward rectification serves important functions. For presynaptic receptors, inward rectification ensures that the receptors will not depress transmitter release by decreasing the input resistance of the terminal. For postsynaptic receptors, fluctuations in membrane potential near rest change the receptors' conductance and consequently affect

synaptic effectiveness. The factors that cause neuronal nAChRs to rectify have not been fully characterized. If rectification is not constant, then changes in rectification can alter synaptic efficacy.

Previous studies suggest that both intrinsic channel properties and block by intracellular Mg^{++} contribute to inward rectification of neuronal nAChR channels (Mathie et al., 1990; Ifune and Steinbach, 1991; Sands and Barish, 1992). However, these factors only partially account for the rectification, suggesting that unidentified factors are involved (Ifune and Steinbach, 1993). Interestingly, inward rectification of whole-cell ACh-evoked currents in rat pheochromocytoma (PC12) cells was reduced when cells were extensively dialyzed with Na_2ATP (Sands and Barish, 1992; Ifune and Steinbach, 1993). ATP is known to effectively chelate spermine, a ubiquitous polyamine (Watanabe et al., 1991). Therefore, it is conceivable that intracellular free spermine contributes to the inward rectification of neuronal nAChRs, as demonstrated for inward rectifier potassium channels and glutamate receptors (Ficker et al., 1994; Falker et al., 1995; Bowie and Mayer, 1995). The objective of our study was to examine whether intracellular spermine produces inward rectification of neuronal nAChRs. We studied $\alpha_4\beta_2$ and $\alpha_3\beta_4$ receptors expressed in *Xenopus* oocytes, as well as native nAChRs expressed on rat superior cervical ganglion (SCG) neurons. Our results suggest that inward rectification of neuronal nAChRs can result from a voltage-dependent block by intracellular spermine. We have reported our preliminary results previously (Haghighi and Cooper, 1997).

METHODS and MATERIALS

Preparation of SCG Neurons

SCG ganglia were dissected from postnatal day 18-26 Sprague-Dawley rats (Charles River, Canada) and dissociated mechanically and enzymatically as previously described (McFarlane and Cooper, 1992). Briefly, the ganglia were dissected under sterile conditions from animals sacrificed by cervical dislocation. The ganglia were dissociated at 37°C either in collagenase (1 mg/ml, type I, Sigma, St. Louis, MO) for 15min followed by dispase (2.4 mg/ml, grade II, Boehringer-Mannheim, Indianapolis, IN) for 30-45min or in an enzyme mixture containing trypsin (1mg/ml, Sigma), deoxyribonuclease (5µg/ml, Sigma) and bovine serum albumin (6mg/ml, Sigma) (Mathie et al., 1990) for 45min. All enzymes were dissolved in Hank's balanced salt solution (HBSS, without Ca⁺⁺ or Mg⁺⁺). The ganglia were gently triturated following the enzyme treatment using a fire-polished Pasteur pipette until they were completely dissociated. Dissociated neurons were washed with L-15 medium supplemented with 10% horse serum and plated onto laminin-coated (40 µg/ml, overnight at 4°C; gift of Dr. S. Carbonetto, McGill University) Aclar coverslips (Allied Chemicals, Clifton, NJ) in modified petri dishes. The neurons were incubated in 1.5 ml of L-15 medium supplemented with 5% rat serum, vitamins, cofactors, penicillin, streptomycin, and sodium bicarbonate as described previously (Hawrot and Patterson, 1979). The media was also supplemented with nerve growth factor (2.5S NGF, 25 ng/ml; gift of Dr. S. Carbonetto). The cultures were maintained at 37°C in a humidified incubator with an atmosphere of 5% CO₂ and 95% air. Neurons were used for electrophysiology within 48h (often within 24h) after plating.

Preparation and Nuclear Injection of Oocytes

Xenopus oocytes were defolliculated and prepared as described by Bertrand et al. (1991). We injected 1-3 ng of pairwise combinations of cDNAs coding for neuronal

nAChR subunits α_4 and β_2 , α_4 and β_2 E260 or α_3 and β_4 into the nucleus of oocytes. In β_2 E260, the lysine (K) residue at the position 260 (part of the extracellular ring of charged residues) has been substituted with an glutamic acid residue (E), which increases the single channel conductance (Cooper et al., 1991). Rat α_3 and β_4 cDNAs were cloned into the pCDNA1 expression vector (Invitrogen, San Diego, CA), and chick α_4 , β_2 and β_2 E260 were cloned into derivatives of pSV2.cat expression vectors (Bertrand et al., 1991). Oocytes were incubated at 19°C for 48-72h before recording. For single channel experiments, the vitelline membrane surrounding the oocytes was removed.

Electrophysiology

Whole-cell recordings from oocytes: In order to measure the macroscopic ACh-evoked currents in oocytes, we used two-electrode voltage clamp techniques (Bertrand et al., 1991). These experiments were performed at room temperature (22-24°C) using a standard voltage-clamp amplifier (built by Mr. A. Sherman, McGill University). During the recordings, oocytes were perfused with control perfusion solution or agonist solutions at 10-20ml/min; switching from one solution to another was done manually. Currents were sampled at 100-350Hz on-line with a 386-based PC computer (AT class running at 33MHz and a 64K cache and A/D card; Omega, Stamford, CT). The program PATCHKIT (Alembic Software, Montréal) was used for stimulation and data acquisition. Recording electrodes had tip diameters of 10-15 μ m and were filled with 3M KCl. Only oocytes that gave rise to large inward currents (>1 μ A in response to 1 μ M ACh for $\alpha_4\beta_2$ expressing oocytes or 10 μ M ACh for $\alpha_3\beta_4$ expressing oocytes when voltage clamped at -60mV) were used for single channel recordings. External perfusing solution contained 96mM NaCl, 2mM KCl, 1mM NaH₂PO₄, 1mM BaCl₂, 10mM HEPES and 1 μ M atropine; pH was adjusted with

NaOH to 7.4-7.5. Spermine (Sigma) was dissolved in sterile water and aliquots were kept frozen at -20°C .

Single channel recordings from oocytes: Outside-out recordings were carried out using a List EPC-7 amplifier at room temperature ($22-24^{\circ}\text{C}$) (Hamill et al., 1981). Pipette resistance ranged from 5-10M Ω for outside-out recordings, and electrodes were coated with Sylgard (Dow Corning). Recordings were obtained in the continuous presence of ACh (0.1-0.2 μM) in the recording bath. ACh-evoked single channel activity gradually diminished in 2-5min after excision of the patch. Signals were digitized with a PCM (501, Sony) and stored on VCR tapes. For off-line analysis, the stored signals were first filtered at 1.5-2kHz with an eight-pole Bessel filter (Frequency Devices Inc.) and sampled at 10-20kHz using a 386-based PC computer. The program PATCHKIT was used for stimulation and data acquisition. External solution contained 100mM KCl, 1mM CaCl₂, 10 HEPES and 1 μM atropine, and pH was 7.4 adjusted with KOH. Recording electrodes contained 80mM KF, 20mM KAcetate, 10mM HEPES and 10mM EGTA; pH=7.4 adjusted with KOH.

Whole-cell recordings from SCG neurons: Whole-cell patch-clamp recordings on SCG neurons were performed at room temperature ($22-24^{\circ}\text{C}$) using a List EPC-7 amplifier (Hamill et al., 1981). Throughout the recordings neurons were perfused with the external solution at a rate of 1ml/min, and agonists were applied by pressure ejection from pipettes with tip diameters of 20-30 μm (Mandelzys et al., 1995). Currents were filtered at 1.5kHz with an eight-pole Bessel filter (Frequency Devices Inc.), sampled at 2.5-5kHz, displayed and stored on-line with a 386-based PC computer. The program PATCHKIT was used for stimulation and data acquisition. The resistance of patch pipettes ranged from 2-6 M Ω , and 50-60% of the series resistance was compensated. External perfusing solution contained 140mM NaCl, 5.4mM KCl, 0.33mM NaH₂PO₄, 0.44mM KH₂PO₄, 2.8mM CaCl₂, 10 mM HEPES, 5.6 mM glucose, 2 mM glutamine, 0.5-1 μM TTX (Sigma) and 1 μM atropine; pH

was adjusted to 7.4. ACh (acetylcholine iodide, Sigma) was dissolved in the same external perfusing solution (100 μ M). Recording electrodes were filled with intracellular solution containing 70mM KF, 65mM KAcetate, 5mM NaCl, 1mM MgCl₂, 10mM EGTA and 10mM HEPES; pH=7.4 was adjusted with KOH.

Single channel recordings from SCG neurons: Outside-out recordings were performed on SCG neurons as described above for oocytes. Agonists were applied by a manual switch through a micropipette, and neurons were washed with control solutions between each recording. Recording electrodes were fire polished after coating with Sylgard. SCG outside-out patches also showed a rapid run-down of single channel activity (2-4min) in all cases. External solution was identical to that described for whole-cell experiments except that the ACh concentrations were 5-20 μ M. Recording electrodes contained 70mM CsGluconate, 70mM CsF, 1mM MgCl₂, 10mM HEPES and 10 EGTA. pH=7.4 was adjusted with CsOH.

Voltage-Clamp Protocols: For I-V curves we measured ACh-evoked currents either by holding the membrane potentials (V_m) at different levels, or in response to voltage ramps. Voltage ramp protocols were as follows: Whole-cell oocytes, 333mV/s; whole-cell neurons, 333 or 200mV/s; outside-out recordings, 1V/S, 333mV/s or 200mV/s. We also used voltage-step protocols where we switched the holding potential rapidly between ± 40 , ± 50 or ± 60 mV, and held at each potential for 1s.

.Analysis

Whole-cell and single channel ramp I-Vs were obtained by subtracting the current in the absence of agonist from that in the presence of agonist. All I-V curves were fit by eye to a polynomial function using Origin 4.1 graphics software (MICROCAL™ Software, Inc.). To measure the amplitude of single channel currents, we used either all-points histograms of open and closed distributions, or we measured the amplitude of the channel openings individually using PATCHKIT and then plotted values (>50

openings) on a histogram. Histograms were fit by Gaussian curves using Origin 4.1 graphics software. Some outside-out patches, especially from SCG neurons, gave rise to a non-specific steady-state conductance at potentials above +20mV, which made the clear detection of ACh-evoked single channel openings difficult.

In order to measure the relative open channel probability (P_{open}), we used single channel recordings in response to 1 s voltage steps between ± 40 , ± 50 and ± 60 mV. At each V_m , we integrated the area under the all-points amplitude histograms corresponding to closed and open states of the receptors and then divided the open state's area by the total area. Then we calculated the relative P_{open} for ± 40 , ± 50 and ± 60 mV by dividing the P_{open} at the positive V_m by that at the corresponding negative V_m . The conductance (G) was determined from $G=I/(V_m-E_{rev})$.

We used a derivation of the Woodhull (1973) equation (see results) in order to fit the G - V relationships. All fits were performed using Origin 4.1 based on a Levenberg-Marquardt algorithm, and the best fit was achieved by χ^2 minimization. Statistical significance was examined using analysis of variance.

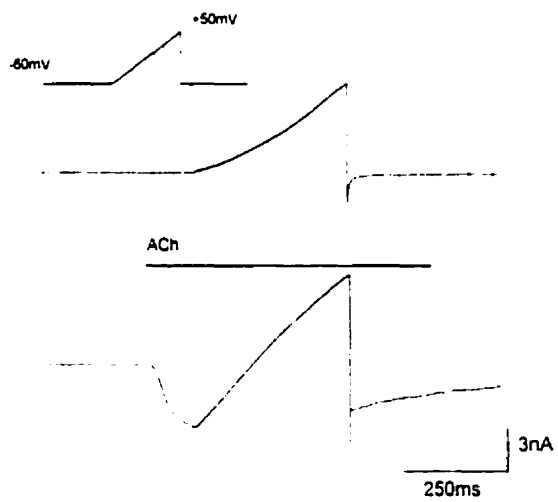
RESULTS

Inward Rectification of Macroscopic ACh Currents

ACh-evoked currents through nicotinic receptors on neurons are carried by small monovalent and divalent cations. A property common to all functional neuronal nicotinic receptors is that they conduct inward current when the membrane potential (V_m) is negative, but pass little outward current when V_m is positive. To observe the rectification on neonatal rat SCG neurons, we applied voltage ramps to change V_m from -60mV to $+50\text{mV}$ at a rate of 333mV/s before and during ACh application (Fig. 1A). We obtained the current-voltage (I-V) curve by subtracting the control current from the current during the ACh application (Fig. 1B). The small amount of desensitization of the ACh-evoked current had minimal effect on the shape of the I-V curve. The ratio of the whole-cell ACh-evoked current at $+50\text{mV}$ to that at -60mV is 0.01 ± 0.008 ($n=10$). Similar rectification is observed when V_m is held steady at different potentials during ACh application (data not shown). Comparable inward rectification has been reported previously for ACh-evoked currents in adult rat sympathetic neurons (Mathie et al., 1990 & 1991), rat adrenal chromaffin cells (Hirano et al., 1987) and in rat PC12 cells (Neuhaus and Cachelin, 1990; Sands and Barish, 1992; Ifune and Steinbach, 1992).

Recombinantly expressed neuronal nAChRs also exhibit strong inward rectification. Figures 2A and 2B show an example of an ACh-evoked I-V curve and the corresponding chord conductance-voltage (G-V) curve for $\alpha_3\beta_4$ receptors expressed in *Xenopus* oocytes. Figures 2C&D show an example of an ACh-evoked I-V curve and the G-V curve for $\alpha_4\beta_2$ receptors expressed in *Xenopus* oocytes. These figures demonstrate that both $\alpha_4\beta_2$ and $\alpha_3\beta_4$ receptors show strong inward rectification, and the conductance of these receptors progressively decreases as V_m depolarizes from -80mV . We have also investigated a mutant $\alpha_4\beta_2$ receptor in which

A



B

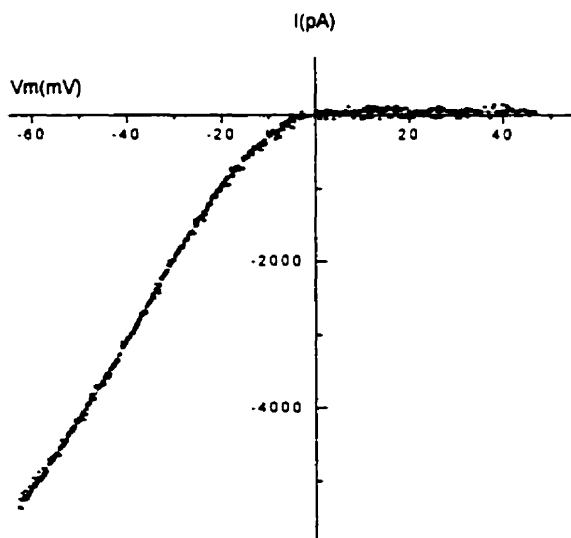
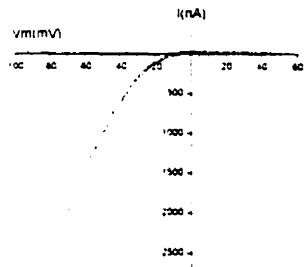
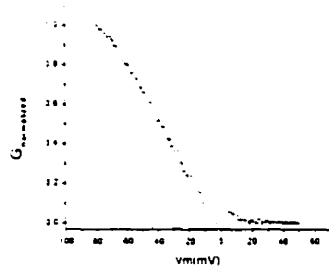


Figure 2.1. Macroscopic ACh-evoked currents recorded from SCG neurons show strong inward rectification. A, Whole-cell currents were recorded from an SCG neuron while the membrane potential was ramped from -60 to +50mV (333mV/s). The upper panel shows the response of the neuron in the absence of agonist, and the lower trace shows the response to 100 μ M ACh. B, This figure shows the current-voltage (I-V) relationship for the neuron in A. The whole-cell I-V curve was obtained by subtracting the current in control solution from the current in the presence of ACh. during the voltage ramp. The I-V plot shows strong inward rectification.

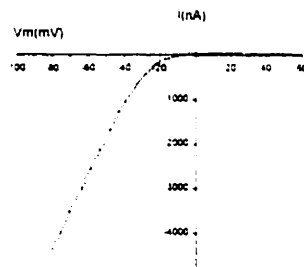
A α, β_1



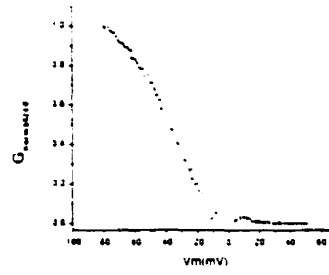
B



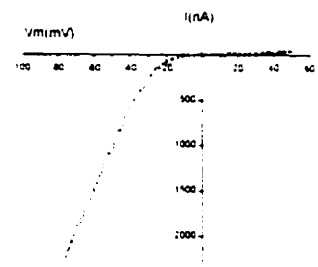
C α, β_2



D



E α, β_2 E260



F

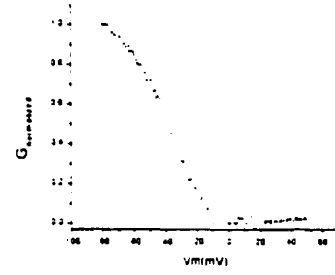


Figure 2.2. Whole cell ACh-evoked current-voltage relationships for recombinant $\alpha_3\beta_4$, $\alpha_4\beta_2$ and $\alpha_4\beta_2$ E260 expressed in *Xenopus* oocytes show strong inward rectification. Figures A, C and E show whole-cell I-V curves for three oocytes expressing recombinant $\alpha_3\beta_4$, $\alpha_4\beta_2$ and $\alpha_4\beta_2$ E260, respectively. Macroscopic currents were recorded in response to voltage ramps from -80 to +50mV (333mV/s) in the absence or presence of ACh (1 μ M for $\alpha_4\beta_2$ and $\alpha_4\beta_2$ E260, and 20 μ M for $\alpha_3\beta_4$), and the net currents were obtained as explained in figure 1. Figures B, D and F show the corresponding conductance-voltage relationships (G-V plot) for $\alpha_3\beta_4$, $\alpha_4\beta_2$ and $\alpha_4\beta_2$ E260, respectively. Conductance at each holding potential is normalized to the conductance at -80mV.

the lysine at position 260 on the β_2 subunit has been changed to a glutamic acid; this mutation increases the single channel conductance of the $\alpha_4\beta_2$ receptors (Cooper et al., 1991; also see Fig. 3), and we refer to it as $\alpha_4\beta_2$ E260. Our reason for using this mutant receptor is that altering charged residues at the extracellular mouth of the pore has been shown to influence rectification of muscle nAChRs (Imoto et al. 1988). Figure 2E shows an example of an I-V curve for $\alpha_4\beta_2$ E260 receptors expressed in *Xenopus* oocytes. Qualitatively, $\alpha_4\beta_2$ E260 receptors rectify in a manner similar to wild-type $\alpha_4\beta_2$ receptors. Similarly, the G-V plot in figure 2F demonstrates that the conductance of $\alpha_4\beta_2$ E260 receptors decreases progressively as V_m depolarizes. At very positive potentials ($>+60\text{mV}$), all three receptors conduct some outward current (data not shown). The $V_{1/2}$ values obtained from the G-V curves are not significantly different for $\alpha_3\beta_4$, $\alpha_4\beta_2$, $\alpha_4\beta_2$ E260 subtypes and for native nAChRs on SCG neurons: this suggests that their inward rectification properties are similar.

Lack of Inward Rectification in Single nAChRs Measured from Outside-Out Patches of *Xenopus* oocytes

In contrast to what we observed at the macroscopic level, single nAChRs measured in outside-out patches conducted current in both directions equally well through the receptor. Figure 3 shows examples of single channel currents from $\alpha_3\beta_4$, $\alpha_4\beta_2$ and $\alpha_4\beta_2$ E260 receptors recorded from outside-out patches held at 4 different potentials (Fig. 3A,C&E) and the corresponding single channel I-V curves (Fig. 3B,D&F). These records were obtained in symmetrical K^+ concentrations (100mM), with K^+ being the main charge carrier. Under these conditions, $\alpha_3\beta_4$ receptors (Fig. 3A) have a single channel conductance of $45\pm 0.87\text{pS}$ (mean \pm SE, at -100mV) and rectify slightly outwards ($I@+60\text{mV}/I@-60\text{mV}=1.2\pm 0.13$). Similarly, both $\alpha_4\beta_2$ and $\alpha_4\beta_2$ E260 receptors in outside-out patches conducted current in both directions (Fig. 3C & 3E). The single channel conductance for $\alpha_4\beta_2$ receptors recorded in

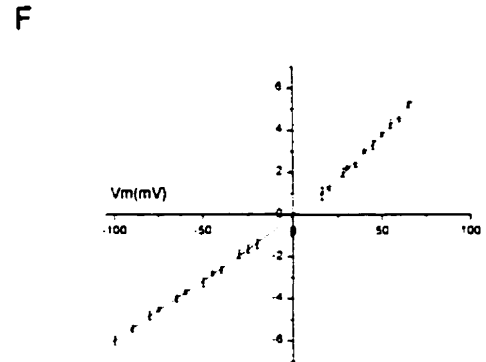
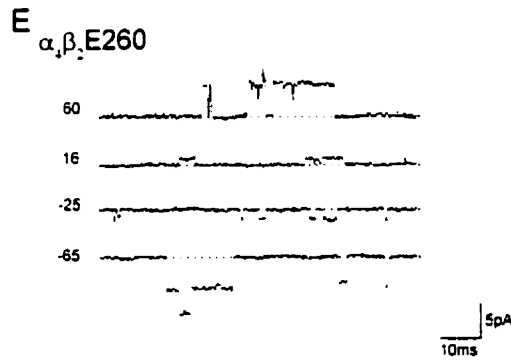
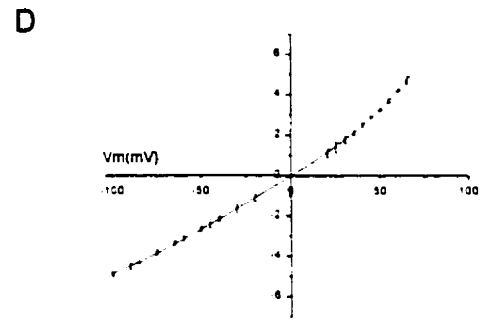
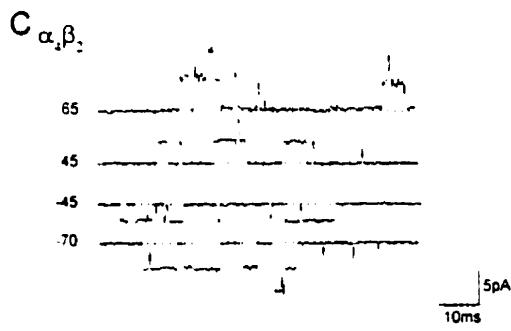
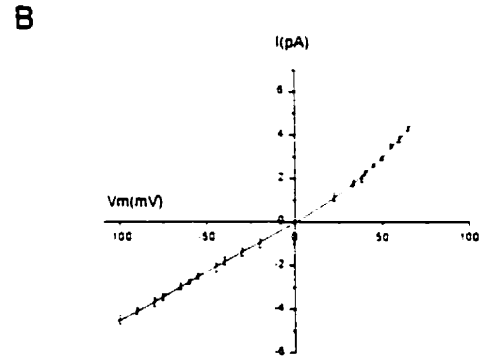
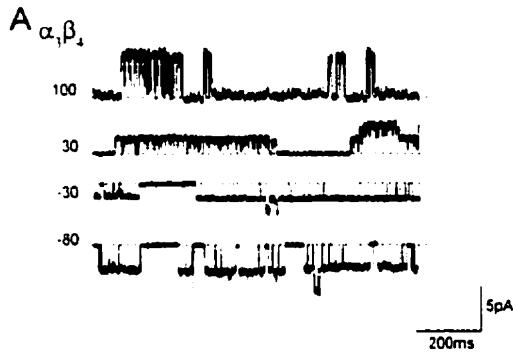


Figure 2.3. Outside-out single channel currents from *Xenopus* oocytes expressing $\alpha_3\beta_4$, $\alpha_4\beta_2$ and $\alpha_4\beta_2$ E260 do not show inward rectification. Figures A, C and E show steady-state single channel recordings from outside-out patches of oocytes expressing $\alpha_3\beta_4$, $\alpha_4\beta_2$ or $\alpha_4\beta_2$ E260, respectively. These recordings were performed in the continuous presence of ACh: 100-200nM for $\alpha_4\beta_2$ and $\alpha_4\beta_2$ E260 and 1-2 μ M for $\alpha_3\beta_4$. Numbers on the left of each trace correspond to the holding potential at which that recording was obtained. The dotted lines mark the zero current level for each trace. Figures B, D and F show the single channel I-V plots for $\alpha_3\beta_4$, $\alpha_4\beta_2$ or $\alpha_4\beta_2$ E260, respectively. These I-V plots, in contrast to the corresponding macroscopic I-Vs (Fig. 2A, C and E), show a slight outward-rectification. Each point in the plots represents the mean \pm standard error (SE) of single channel current amplitudes from 4 patches for $\alpha_3\beta_4$, 8 patches for $\alpha_4\beta_2$ and 8 patches for $\alpha_4\beta_2$ E260.

symmetrical K^+ was 49 ± 0.68 pS, and that for $\alpha_4\beta_2$ E260 was 61 ± 0.81 pS. All three receptors showed a smaller single channel conductance when extracellular K^+ was substituted with Na^+ (Cooper et al., 1991) or Cs^+ (data not shown). The I-V curve for $\alpha_4\beta_2$ E260 receptors shows less outward rectification than those for $\alpha_3\beta_4$ and $\alpha_4\beta_2$ receptors as a result of introducing negative charges to the extracellular ring of the pore (Imoto et al., 1988).

The results in figure 3 indicate that inward rectification of macroscopic ACh-evoked currents is not because neuronal nAChRs cannot pass outward currents. Similar results have been reported for nAChRs on adult rat sympathetic neurons (Mathie et al., 1990 & 1991), rat adrenal chromaffin cells (Hirano et al., 1987) and on rat PC12 cells (Neuhaus and Cachelin, 1990; Ifune and Steinbach, 1991; Ifune and Steinbach, 1992; Sands and Barish, 1992).

We investigated whether the rectification of macroscopic ACh-evoked currents occurs because these receptors have a decreased open channel probability (P_{open}) at depolarized potentials. For these experiment, we recorded single channel currents from $\alpha_4\beta_2$ and $\alpha_4\beta_2$ E260 receptors in outside-out patches while repeatedly stepping V_m between ± 40 , ± 50 (Fig. 4A) and ± 60 mV. The results indicate that there is a 25-30% reduction in P_{open} at +40, +50 and +60 potentials compared to P_{open} at the corresponding negative potentials: $P_{open(+40)}/P_{open(-40)} = 0.72 \pm 0.3$; $P_{open(+50)}/P_{open(-50)} = 0.75 \pm 0.2$; $P_{open(+60)}/P_{open(-60)} = 0.71 \pm 0.4$ ($n=3$ patches, 10-20 steps per patch). This reduction of P_{open} at depolarized potentials, however, is too small to account for the inward rectification observed at the whole-cell level.

In a few experiments, we also measured ACh-evoked currents from macropatches in outside-out configuration while ramping the membrane potential (Fig. 4B). Consistent with what we observed for P_{open} in the experiments above, the ACh-evoked currents from these macropatches exhibited only a small degree of rectification.

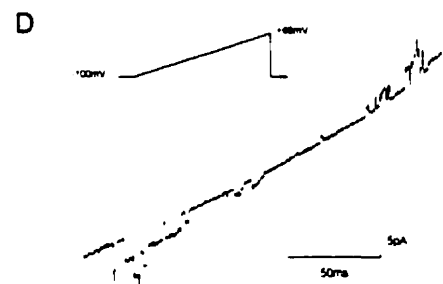
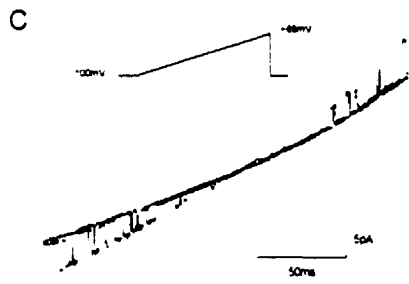
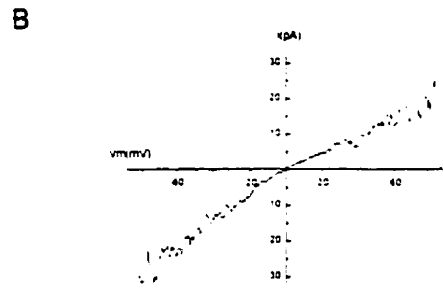


Figure 2.4. Voltage-dependence at the single channel level cannot account for the macroscopic inward-rectification. A. Representative trace showing $\alpha_4\beta_2$ single channel recordings from an outside-out patch while V_m was stepped between -50 and +50mV (1s at each V_m). Dotted lines mark the zero current level. B. This trace shows currents recorded from an outside-out macro-patch expressing $\alpha_4\beta_2$ nAChR subtypes. The current was recorded in response to 200nM ACh while V_m was ramped from -85 to +85mV at 1V/s. The IV curve was obtained by subtracting the current after run-down of single channel activity from the current obtained 30s after excision of the patch. C. This trace shows two superimposed $\alpha_4\beta_2$ single channel recordings from an outside-out patch while the V_m was ramped from -100 to +90mV (1V/s). These traces were obtained in the continuous presence of 100nM ACh. D. This figure shows single channel currents from an outside-out patch expressing $\alpha_4\beta_2$ E260 (ACh=200nM) while V_m was ramped from -100 to +90mV (1V/s). For this patch, 1mM Mg^{2+} had been added to the recording pipette. Note: outward single channel openings at positive membrane potentials are smaller than those in control recordings suggesting a moderate block by intracellular Mg^{2+} .

To test whether fast changes in the membrane potential can affect the opening of the receptors, we recorded ACh-evoked single channels from outside-out patches while rapidly ramping the patch holding potential from -100 to +90mV. Figure 4C shows two superimposed $\alpha_4\beta_2$ single channel records measured under these conditions. These records illustrate opening of single channel $\alpha_4\beta_2$ receptors while the membrane potential is rapidly changed from -100 to +90 mV at 1V/s. The average frequency of opening at positive potentials was 20-25% less than that at negative potentials.

The results of these cell-free single channel experiments suggest that inward rectification of the ACh-evoked current is due to an intracellular(s) mediator. It had been suggested that intracellular Mg^{++} could cause a moderate rectification at single channel level through a voltage-dependent blocking mechanism (Mathie et al., 1990; Ifune and Steinbach, 1991). However, extensive chelation of intracellular Mg^{++} had very little effect on the rectification properties of the whole-cell currents (Mathie et al., 1990; Neuhaus and Cachelin, 1990). We found that including Mg^{++} (up to 1mM) in the pipette solution in outside-out recordings had little effect on either the single channel I-V curves for both $\alpha_4\beta_2$ and $\alpha_4\beta_2E260$ receptors (figure 4D) or on P_{open} at depolarized potentials (data not shown). These findings confirm previous results that intracellular Mg^{++} is not a mediator of inward rectification of macroscopic ACh-evoked currents.

Intracellular Spermine Blocks Neuronal nAChRs Expressed in *Xenopus* Oocytes

Recent studies have reported that intracellular spermine, an intracellular polyamine, can block inwardly-rectifying K^+ channels and α -amino-3-hydroxy-5-methylisoxazole-4-propionate (AMPA) and kainate receptors in a voltage-dependent manner (Ficker et al., 1994; Fakler et al., 1995; Bowie and Mayer, 1995; Kamboj et al., 1995). We investigated whether spermine also blocks neuronal nAChRs. To test

this, we recorded single channel currents from $\alpha_4\beta_2$ and $\alpha_4\beta_2$ E260 receptors in outside-out patches with different concentrations of spermine (100nM-100 μ M) added to the pipette solution. Figure 5A shows an example of single channel currents for $\alpha_4\beta_2$ E260 receptors recorded with 33 μ M spermine in the recording electrode: the presence of 33 μ M spermine abolished single channel current at holding potentials greater than 0mV. At lower concentrations (1 to 3.3 μ M), spermine reduced the amplitude of the single channel openings (Fig. 5B). The fact that the outward currents are reduced in size, as seen in figure 5B, suggests that spermine acts with fast kinetics (Hille, 1992). The single channel I-V curves for $\alpha_4\beta_2$ receptors obtained from 14 outside-out patches in the presence of 3 different spermine concentrations are shown in the figure 5C: for concentrations of spermine equal or greater than 10 μ M, outward currents are abolished for V_m from 0mV to +50mV. In addition, by comparing data in control solutions, it is clear that spermine causes some reduction of the inward current at negative V_m . The effects of spermine on the single channel I-V curves of $\alpha_4\beta_2$ and $\alpha_4\beta_2$ E260 receptors (n=12) were similar.

The effects of spermine are voltage- and concentration-dependent. Figure 6A shows the single channel G-V relationship for $\alpha_4\beta_2$ receptors with increasing spermine concentrations. At each V_m , every point represents the single channel conductance in the presence of spermine as a fraction of the control: all points are normalized to their single channel conductance at -100mV. In control solutions without spermine, the single channel conductance shows slight outward rectification. However, with spermine in the recording electrode the single channel conductance decreases with depolarization in a sigmoidal fashion and falls to near zero at positive potentials (except for spermine concentrations < 3.3 μ M). Higher concentrations of spermine result in parallel leftward shifts of the G-V curves. With spermine concentrations greater than 3.3 μ M the sigmoidal G-V curve at the single channel level resembled the G-V curves measured at the macroscopic level (compare with

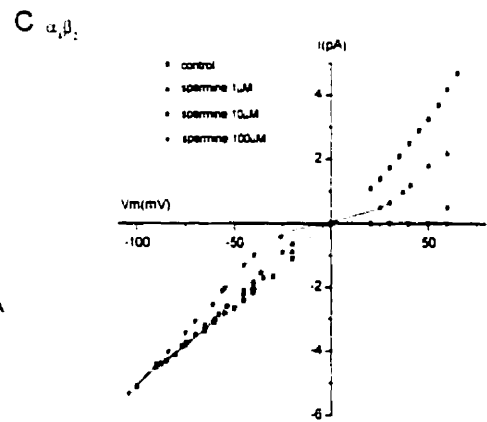
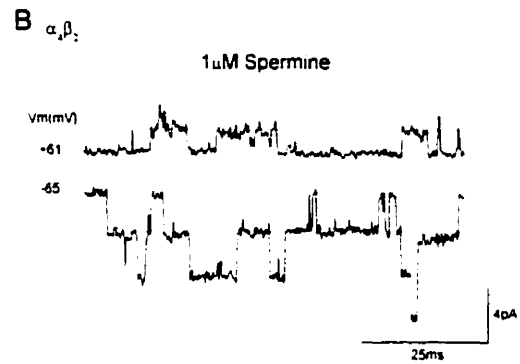
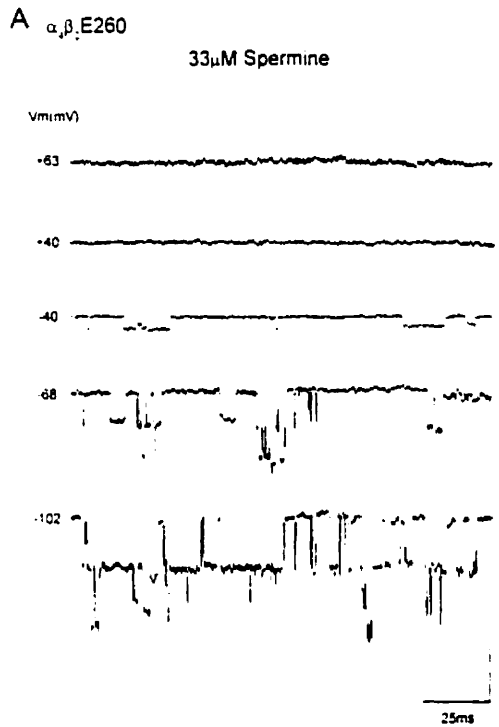


Figure 2.5. Spermine causes inward rectification of ACh-evoked currents in outside-out patches. A, These traces are outside-out single channel recordings (100nM ACh) at different holding potentials from an oocyte expressing $\alpha_4\beta_2$ E260 receptors with 33 μ M spermine added to the intracellular pipette solution. Dotted lines mark the zero current level. B, This figure shows outside-out recordings (ACh 100nM) from an oocyte expressing $\alpha_4\beta_2$ receptors with 1 μ M spermine added to the recording electrode; the outward $\alpha_4\beta_2$ single channel currents at +60mV are reduced by ~40%. Dotted lines mark the first open channel level for each trace. C, This figure shows the steady-state single channel I-V relationship for $\alpha_4\beta_2$ receptors in the absence (squares, n=12) or in the presence of 1 μ M (up triangles, n=4), 10 μ M (circles, n=6) or 100 μ M (down triangles, n=4) spermine in the recording patch electrode. I-V plots show progressive inward-rectification of single channel current with increasing concentrations of intracellular spermine. Solid lines are polynomial fits.

figure 2) suggesting that the voltage-dependent block by intracellular spermine may underlie the inward rectification observed for the whole-cell ACh-evoked currents. At membrane potentials positive to +50mV (+20mV for <3.3μM spermine), we observed an increase in the conductance. Small outward currents were also apparent at these potentials at the whole-cell level (data not shown).

In order to analyze the effects of spermine at the single channel level we used a derivation of the Woodhull model (Equation 1) for voltage-dependent ion channel block (Woodhull, 1973; Johnson and Ascher, 1990):

$$G/G_{\max} = 1 / \{ 1 + [S] / K_D \} \quad (1)$$

where

$$K_D = K_{D(0)} \exp \{ -V_m z \delta F / [RT] \}$$

and [S] is the internal spermine concentration; K_D is the dissociation constant at a given V_m ; $K_{D(0)}$ is the dissociation constant at 0mV; z is the valence of spermine; δ is the fraction of the membrane electrical field sensed by spermine from the intracellular side; and R , T and F have their usual meaning.

The solid lines in figure 6A show that Eq. 1 provides a good description of the single channel G-V curves. Assuming the valence of spermine, z , to be 3.8 at physiological pH (Bowie and Mayer, 1995), this analysis estimates $K_{D(0)}$ and δ to be $3.64 \pm 0.25 \mu\text{M}$ and 51%, respectively ($z\delta = 1.93 \pm 0.3$), and is based on data from 25 outside-out patches expressing $\alpha_4\beta_2$ receptors at 8 different concentrations of spermine. Analysis of the spermine block of $\alpha_4\beta_2\text{E260}$ receptors gave very similar results: $K_{D(0)} = 3.58 \pm 0.20$ and $z\delta = 1.85$. Figure 6B shows the effects of V_m on the affinity of the receptor for spermine (K_D). Within a range of V_m from -80mV to +30mV, the concentration-dependent block by spermine was well described by a single binding isotherm (solid lines), with the K_D decreasing with increasing

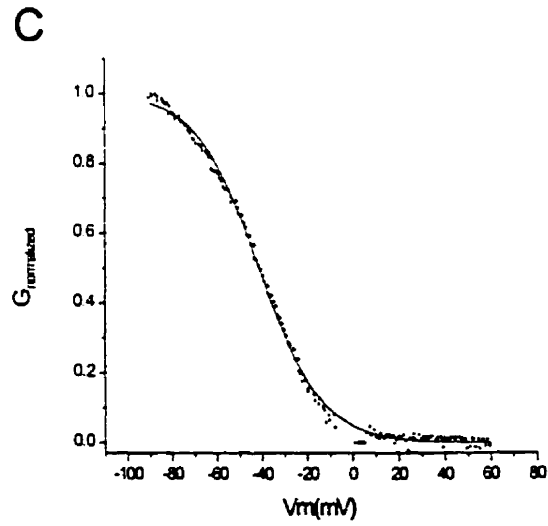
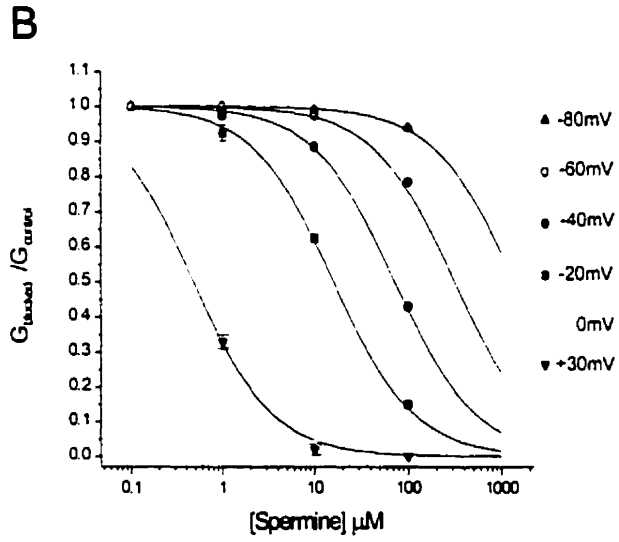
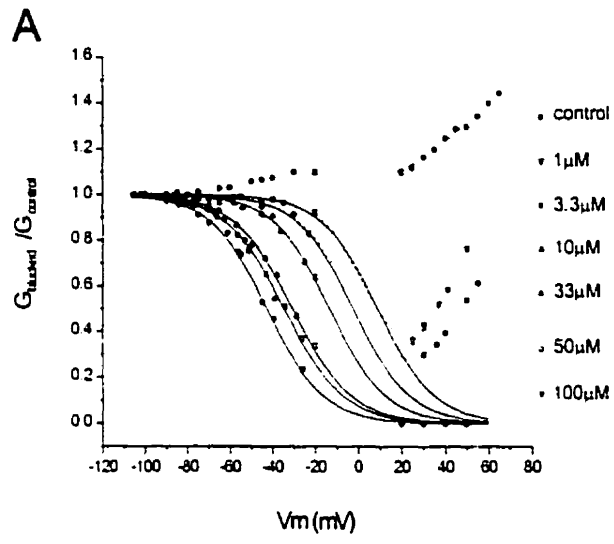


Figure 2.6. Analysis of voltage- and concentration-dependent block by intracellular spermine. A, This figure shows single channel G-V relationships for $\alpha_4\beta_2$ neuronal nAChR subtypes in the absence or the presence of 1, 3.3, 10, 33, 50 or 100 μ M spermine in the recording electrode. Single channel conductance in control patches increases with depolarization (n=14), whereas single channel conductance in the presence of spermine is progressively decreased with depolarization. Increasing the concentration of spermine causes a leftward shift of the G-V relationship. Solid lines are fits to data points using equation 1 (see results). Points represent the single channel conductance in the presence of spermine as a fraction of the control conductance for each holding potential; all points are normalized to the conductance at -100mV. Data are obtained from 3-6 outside-out patches for every spermine concentration (mean \pm SE). Dotted lines are polynomial fits to the data. B. This figure shows the concentration-response relationship for spermine at different holding potentials. Affinity of spermine for $\alpha_4\beta_2$ receptors is increased with depolarization. Data points are the corresponding points in A, and solid lines are fits using equation 1. The dotted line is the theoretical fit at 0mV predicted by equation 1 (see results). C. This figure shows a representative G-V plot of the macroscopic ACh-evoked current recorded from an oocyte expressing $\alpha_4\beta_2$ receptors. We fit this G-V curve with equation 1 using the K_{d0} , and $z\delta$ values obtained from single channel analysis (solid line).

depolarization: 1399, 316, 71.4, 16.1, 3.64 and 0.39 μM for -80 , -60 , -40 , -20 , 0 and $+30$ mV, respectively. These values are comparable to those for recombinantly expressed AMPA and kainate receptors (Bowie and Mayer, 1995).

Using the values for $z\delta$ and $K_{d(0)}$ from the single channel measurements above, we fit the G-V curves for macroscopic ACh-evoked currents for $\alpha_4\beta_2$ receptors using equation 1. Figure 6C shows that Eq. 1 describes the data well assuming an intracellular spermine concentration [S] of 82 ± 5 μM ($n=8$). It should be noted that this fit does not take into account the possible contribution of other polyamines such as spermidine and putrescine or the moderate voltage-dependent decrease in single channel P_{open} .

Spermine Blocks Native neuronal nAChRs On Sympathetic Neurons

Our results on recombinant receptors indicated that intracellular spermine blocks neuronal nAChRs in a voltage-dependent manner thereby producing inward rectification of the ACh-evoked currents. To determine whether spermine has a similar action on native receptors expressed on neurons, we examined the effects of intracellular spermine on nAChRs expressed by sympathetic neurons. Figure 7A shows that single nAChR currents measured in cell-free outside-out patches flow in both directions equally well, as has been reported previously (Mathie et al., 1990). The single channel conductance measured in outside-out patches from SCG neurons was 32.5 ± 1.35 pS at -60 mV ($n=12$). Spermine ($100\mu\text{M}$) added to the recording electrode, completely abolished single channel current at V_m greater than 0 mV (Fig. 7B). These results suggest that intracellular spermine in sympathetic neurons can block nAChRs from the inside and produce inward rectification of the ACh-evoked currents. We plotted the single channel I-V curves using data from 7 control outside-out patches and 4 outside-out patches in the presence of spermine (Fig. 7C). The control I-V curve shows slight outward rectification, whereas the single channel I-V

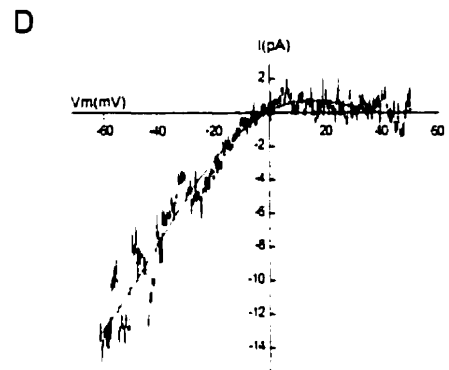
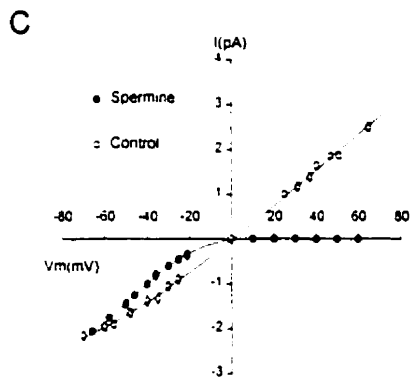
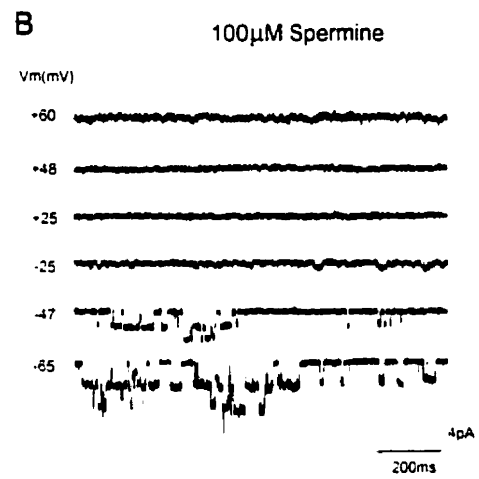
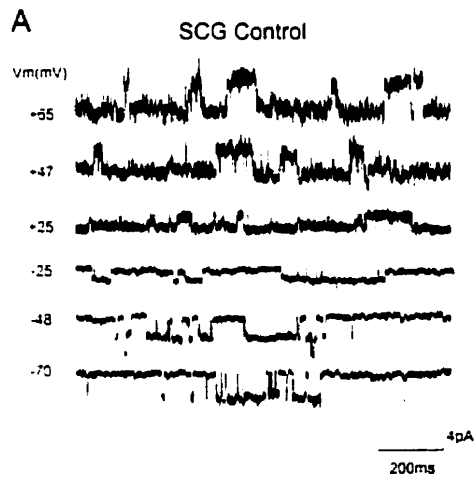


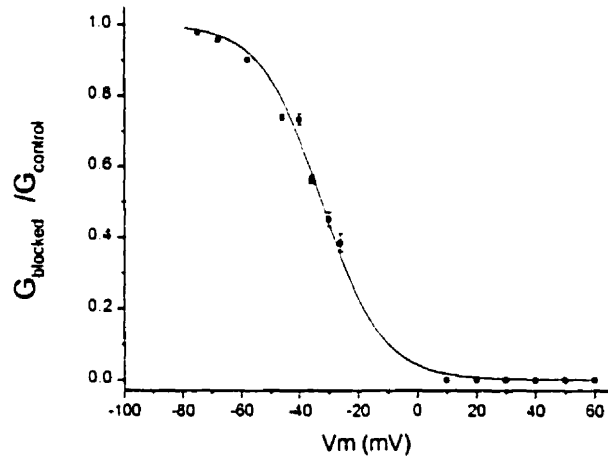
Figure 2.7. Intracellular spermine blocks native SCG nAChRs at the single channel level. A. This figure shows single channel recordings obtained from an SCG neuron in an outside-out patch; native SCG nAChRs show both inward and outward currents in response to 20 μ M ACh. Dotted lines mark the zero current and the first open state. B. Outside-out single channel recordings from another SCG neuron with 100 μ M spermine added to the recording electrode. 100 μ M spermine completely blocked the outward single channel openings and reduced the amplitude of the inward openings ([ACh]=20 μ M). At positive potentials, dotted lines mark the base-line; and at negative potentials dotted lines mark the base line and the first open state. C. This figure shows ACh-evoked single channel I-V curves obtained from outside-out patches of SCG neurons. The control I-V curve (open circles, n=7) exhibits slight outward rectification, similar to recombinant neuronal nAChRs (Fig. 3B, D and F). In the presence of 100 μ M spermine in the recording electrode (solid circles, n=4), however, the I-V relationship exhibits strong inward rectification. Single channel amplitudes were measured in both steady-state and ramp experiments, and points represent mean \pm SE. Solid lines are polynomial fits. D. This figure shows the current in response to 20 μ M ACh recorded from an outside-out macro-patch of an SCG neuron in the presence of 100 μ M spermine in the recording electrode. The current was recorded while V_m was ramped from -60 to +50mV (at 1V/s). The solid line is a polynomial fit.

curve in the presence of 100 μ M spermine exhibits a strong inward-rectification, similar to that seen at the macroscopic level (compare with Fig. 1B). We also measured ACh-evoked currents in outside-out macropatches. As shown in figure 7D, in the presence of spermine (100 μ M) the ACh-evoked current from a macropatch shows strong inward rectification.

Figure 8A shows the G-V plot obtained from 4 outside-out patches of SCG neurons with 100 μ M spermine added to the recording electrode. Similar to our results for $\alpha_4\beta_2$ receptors, the block by spermine of native SCG nAChRs increases as the membrane is depolarized in a sigmoidal manner. Using equation 1, we fit this single channel G-V curve and estimated $K_{d(0)}$ and δ to be $4.27 \pm 0.6 \mu$ M and 65%, respectively (with $z\delta$ being 2.48 ± 0.16). These results suggest that spermine has comparable affinity for $\alpha_4\beta_2$ receptors and native nAChRs expressed on SCG neurons.

Using the parameters obtained from the single channel analysis, we analyzed the macroscopic ACh-evoked currents in SCG neurons. In figure 8B, we transformed a whole-cell ACh-evoked I-V curve into a G-V curve, assuming a reversal potential of -5mV (Haghighi and Cooper, unpublished observations) for ACh-evoked currents in SCG neurons. The macroscopic chord conductance progressively decreases as V_m is depolarized from -65mV (Fig. 8B). We used equation 1 to fit the whole-cell ACh-evoked G-V curves using $K_{d(0)}$ and δ as determined at the single channel level (solid line in 8B). Results from 8 different experiments estimated the intracellular spermine concentration, [S], to be $51 \pm 4 \mu$ M. The exact concentration of free spermine in rat sympathetic neurons has not been determined, but the value predicted from equation 1 is within the range measured for other mammalian cells (Watanabe et al., 1991) and comparable to that estimated in HEK cells using similar analysis for kainate receptors (Bowie and Mayer, 1995).

A



B

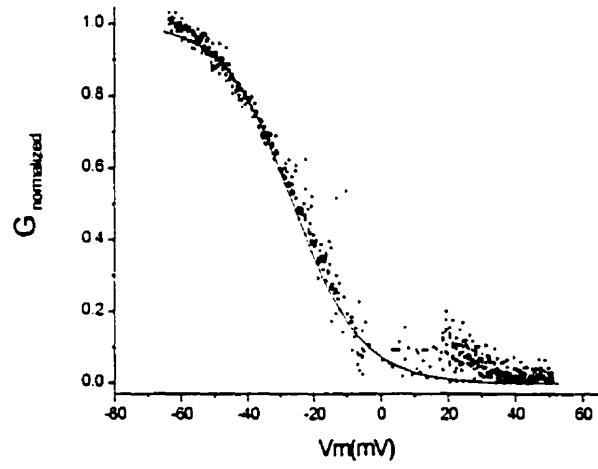


Figure 2.8. Block by intracellular spermine underlies the inward rectification of macroscopic ACh-evoked currents in SCG neurons. A, This figure shows the single channel G-V plot for native SCG nAChR in the presence of 100 μ M spermine. The single channel conductance shows a progressive decrease with depolarization. Points represent the single channel chord conductance (mean \pm SE, n=4) in the presence of spermine as a fraction of the control single channel conductance at every potential; all values were normalized to the conductance at -75mV. The solid line is the fit to the data using equation 1 (see results). B, This is a representative whole-cell G-V plot obtained from an SCG neuron. Similar to the single channel conductance in the presence of spermine, the macroscopic ACh-evoked conductance in SCG neurons shows a progressive decrease with depolarization. The solid line is a fit to these data using equation 1. This fit was performed using values for $K_{d,0}$ and $z\delta$ from single channel analysis (see results).

Extracellular Spermine Blocks Neuronal nAChRs

Extracellular polyamines have been shown to block both native and recombinant AMPA receptors (Robichaud and Boxer, 1993; Washburn and Dingledine, 1996). Therefore, we asked whether extracellular spermine can also block neuronal nAChRs, and whether this effect is similar to the voltage-dependent block produced by intracellular spermine. Extracellular spermine blocked the inward ACh-evoked currents in oocytes expressing $\alpha_4\beta_2$ (Fig. 9A). Co-application of 33 μ M spermine with 1 μ M ACh in the extracellular solution resulted in a ~45% block of the macroscopic ACh-evoked inward current recorded from $\alpha_4\beta_2$ receptors (Fig. 9A).

To examine the voltage-dependence, we measured the block when ramping the membrane potential from -90mV to +50mV. Figure 9B shows the ACh-evoked I-V curves for $\alpha_4\beta_2$ receptors in the absence or presence of 33 μ M extracellular spermine. The form of the typical inward rectification of the I-V curve is not affected by extracellular spermine. We also plotted the changes in macroscopic conductance (as a fraction of the control conductance) of the receptor versus membrane potential in the presence of 33 μ M spermine (Fig 9C). As apparent from this G-V plot, the blocking effect of extracellular spermine shows little voltage-dependence. To test whether extracellular spermine can act as a competitive antagonist, we examined the effect of increasing concentrations of ACh on the block by extracellular spermine. The blocking effect of 50 μ M extracellular spermine on inward currents evoked by either 0.1, 1 or 10 μ M ACh in $\alpha_4\beta_2$ expressing oocytes was not significantly different (n=5).

We tested the effect of 1nM to 1mM extracellular spermine on ACh-evoked currents in oocytes expressing $\alpha_3\beta_4$, $\alpha_4\beta_2$ or $\alpha_4\beta_2$ E260. The inhibition curves for all three receptors were well described by a single binding site isotherm according to the equation: $I = I_{\max} / (1 + [S] / IC_{50})$.

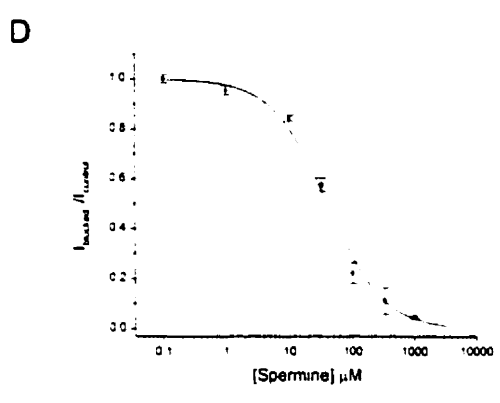
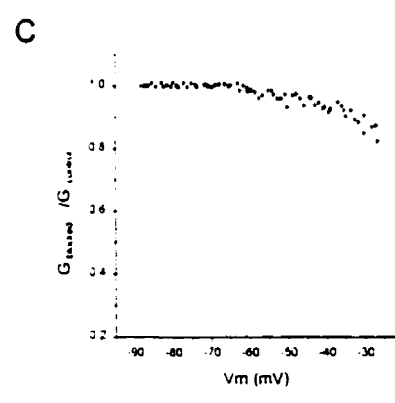
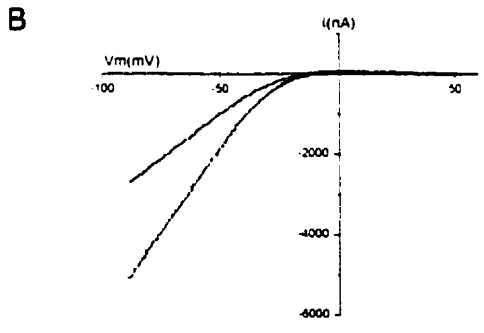
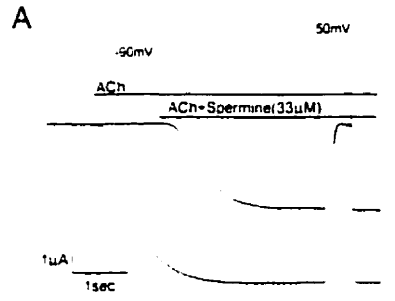


Figure 2.9. Extracellular spermine blocks macroscopic ACh-evoked inward currents. A, This figure shows inward ACh-evoked currents recorded from an oocyte expressing $\alpha_4\beta_2$ in the absence and the presence of extracellular spermine. At -90mV , $33\mu\text{M}$ extracellular spermine blocks the current in response to $1\mu\text{M}$ ACh by 45%. B, Macroscopic I-V relationship for the oocyte in A is plotted in the presence and absence of $33\mu\text{M}$ extracellular spermine. Macroscopic inward-rectification is not affected by extracellular spermine. C, This figure shows the change in the macroscopic conductance versus the membrane potential in the presence of $33\mu\text{M}$ extracellular spermine. The macroscopic conductance in the presence of spermine is presented as a fraction of the control conductance at every membrane potential and then normalized to the conductance at -90mV . The macroscopic conductance in the presence of extracellular spermine shows little change with depolarization. D, This figure shows the inhibition curve for $\alpha_4\beta_2$ receptors with increasing concentrations of extracellular spermine. Extracellular spermine blocks the ACh-evoked current in $\alpha_4\beta_2$ expressing oocytes in a concentration-dependent manner. Data points were obtained using current measurements from 7 oocytes per spermine concentration (mean \pm SE). Solid line is a fit for single binding site isotherm (see results).

Where I is the current measured at any V_m in the presence of spermine; I_{\max} is the current at the same V_m in the absence of spermine; $[S]$ is the concentration of extracellular spermine; and IC_{50} is the concentration of spermine for half-maximal inhibition. The extracellular block by spermine was concentration-dependent with an IC_{50} of $40.3 \pm 3.8 \mu\text{M}$ ($n=7$) (fig. 9D) for $\alpha_4\beta_2$ receptors. We obtained similar results for $\alpha_3\beta_4$ ($42.3 \pm 4.3 \mu\text{M}$, $n=5$) and $\alpha_4\beta_2\text{E260}$ ($39.5 \pm 2.7 \mu\text{M}$, $n=6$) expressed in oocytes (data not shown).

DISCUSSION

In this study, we investigated mechanisms involved in the strong inward rectification of neuronal nAChRs. Our results demonstrate that spermine blocks neuronal nAChRs with high affinity at depolarized membrane potentials when acting on the cytoplasmic side of the channel. Given the high concentration of free spermine in neurons, the voltage-dependent block by intracellular spermine likely underlies inward rectification of neuronal nAChRs.

We examined the effects of spermine on 3 different subtypes of neuronal nAChRs: recombinant $\alpha_3\beta_4$ and $\alpha_4\beta_2$ receptors expressed in *Xenopus* oocytes, and native receptors expressed by SCG neurons. At the whole-cell level, we demonstrated that the ACh-evoked currents for all 3 receptors exhibit strong inward rectification, consistent with previously published reports (Bertrand et al., 1990; Mathie et al., 1990; Ifune and Steinbach, 1992; Sands and Barish, 1992). Furthermore, at the single channel level, we showed that this inward rectification is abolished in cell-free outside-out patches, as shown for neuronal nAChRs expressed on SCG neurons and PC12 cells (Mathie et al., 1990; Ifune and Steinbach, 1992; Sands and Barish, 1992; Neuhaus and Cachelin, 1990).

Intracellular spermine has been shown to underlie inward rectification of glutamate receptors (Bowie and Mayer, 1995) and inward-rectifying K^+ channels (Fakler et al., 1995); therefore, we examined the effects of intracellular spermine on neuronal nAChRs. In outside-out recordings, we found that the addition of spermine (0.1-100 μ M) to the recording pipette produced a voltage-dependent block of neuronal nAChRs in a concentration-dependent manner. To analyze the spermine block, we fit the single channel G-V curves to a derivation of the Woodhull model (Woodhull, 1973). According to this model, spermine enters the open receptor and binds to a site within the membrane electrical field. Spermine at this site interferes with the

movement of small cations through the channel pore, and the occupancy of this site by spermine is affected by changes in membrane potential. This analysis gave a $K_{d(0)}$ of $3.6\mu\text{M}$ and a $z\delta$ of 1.9 for $\alpha_4\beta_2$ receptors and a $K_{d(0)}$ of $4.3\mu\text{M}$ and a $z\delta$ of 2.5 for nAChRs on SCG neurons, suggesting that the spermine binding site is located at 51% or 65% of the membrane electrical field, respectively. These values are comparable to those measured for kainate receptors ($K_{d(0)}=5.5\mu\text{M}$ and $z\delta=2.5$) and AMPA receptors ($K_{d(0)}=1.5\mu\text{M}$) (Bowie and Mayer, 1995).

Using the Woodhull model with the above parameters, we were able to describe the G-V relationships for whole-cell ACh-evoked currents and estimate the free intracellular spermine in oocytes ($82\mu\text{M}$) and SCG neurons ($51\mu\text{M}$). These values are well within the range ($50\text{-}200\mu\text{M}$) of physiological free spermine concentrations (Watanabe et al., 1991; Traynelis et al., 1995; Bowie and Mayer, 1995). Although our analysis suggests that spermine alone is capable of conferring rectification to ACh-evoked currents in neurons, it is possible that other polyamines such as spermidine and putrescine contribute to the action of spermine.

The model also assumes that spermine does not pass through the channel (Woodhull, 1973). This model describes our data well for membrane potentials from -100mV to $+50\text{mV}$. However, at membrane potentials greater than $+50\text{mV}$ (or $+20\text{mV}$ for spermine $<3.3\mu\text{M}$), the ACh-evoked conductance increased, suggesting a relief of spermine block. One interpretation for such a relief of block is that at strongly depolarized potentials spermine permeates the pore; this unblocking allows small cations to flow out and gives rise to an outward current. A similar interpretation has also been suggested for AMPA and kainate receptors (Bowie and Mayer, 1995).

Previous work on native nAChRs on PC12 cells indicated that it was possible to reduce rectification of the whole-cell ACh-evoked current if the cells were dialyzed with $5\text{-}10\text{mM}$ Na_2ATP for up to 20min (Sands and Barish, 1992; Ifune and Steinbach, 1993); Mg^{++} chelators alone had little effect on rectification (Neuhaus and Cachelin,

1990; Ifune and Steinbach, 1993). This partial removal of rectification is likely due to the chelation of polyamines by Na_2ATP (Watanabe et al., 1991; Fakler et al., 1995; Bowie and Mayer 1995). Our results are in agreement with this interpretation. Lowering spermine concentrations inside cells is technically difficult, however, because intracellular spermine is present at high concentrations and effectively buffered (Watanabe et al., 1991; Swärd et al., 1997). The high concentration of intracellular bound spermine is in equilibrium with the intracellular free spermine (Watanabe, 1991; Gilad and Gilad, 1991); reduction in the concentration of intracellular free spermine, thus, will cause the release of more spermine from the large pool of bound spermine. We attempted to chelate spermine in SCG neurons using whole-cell recordings with 10mM Na_2ATP in the pipette, but our results were variable: in the best cases, we observed only a 10-20% reduction of inward rectification after 15-20 minutes. One possibility for not observing a greater reduction is that spermine is effectively buffered in SCG neurons.

AMPA/kainate receptors, neuronal nAChRs and inwardly-rectifying K^+ channels are thought to have different membrane topologies (Hollman et al., 1994; Karlin and Akabas, 1995; Nichols and Lopatin, 1997), yet they appear to use a common mechanism for inward rectification. In the case of the glutamate receptors, inward rectification and spermine sensitivity are unique properties of Ca^{++} -permeable receptor subtypes (Bowie and Mayer, 1995; Koh et al., 1995; Kamboj et al., 1995). By comparison, neuronal nAChRs, including the α -bungarotoxin-sensitive homomeric α_7 receptors, are highly permeable to Ca^{++} and exhibit strong inward rectification. For glutamate receptors, both Ca^{++} -permeability and inward rectification have been attributed to a glutamine (Q) residue in the M2 hydrophobic domain; substitution of this residue to a positively charged arginine (R) renders the receptor Ca^{++} -impermeable, and outwardly rectifying (Hume et al., 1991). There is evidence to

suggest that a comparable site may exist in the neuronal nAChRs (Bertrand et al. 1993).

Inwardly rectifying AMPA and kainate receptors are blocked also by extracellular spermine (Washburn and Dingledine, 1996); therefore, we tested the effects of extracellular spermine on neuronal nAChRs. We demonstrated that extracellular spermine blocks ACh-evoked current for both $\alpha_3\beta_4$ and $\alpha_4\beta_2$ in a concentration-dependent manner, with an IC_{50} of 40-42 μ M for both receptors. The degree of block was largely independent of ACh concentration (100nM-10 μ M) and, unlike the block by intracellular spermine, weakly voltage-dependent. To determine whether this block was sensitive to charges at the extracellular mouth of the pore, we investigated the effects of extracellular spermine on $\alpha_4\beta_2$ E260 receptors. We obtained a similar IC_{50} for $\alpha_4\beta_2$ E260 (39.5 μ M) compared to wild-type $\alpha_4\beta_2$, indicating that increasing negative charges in the extracellular ring of the channel does not affect the block. Our results suggest that extracellular spermine acts as a non-competitive open channel blocker.

Neuronal nAChRs are more sensitive to block by extracellular spermine compared to AMPA and kainate receptors. Extracellular spermine blocks AMPA receptors with an IC_{50} of 120 μ M for GluR3 and an IC_{50} of 1000 μ M for GluR1 and GluR4 with little voltage-dependence (Washburn and Dingledine, 1996). The effects of extracellular spermine on NMDA receptors are more complex: 1-30 μ M extracellular spermine enhances the response of NMDA receptors (Williams et al., 1990; Rock and MacDonald, 1992; Benveniste and Mayer, 1993), whereas at higher concentrations (IC_{50} =344 μ M at -60mV), extracellular spermine inhibits NMDA receptors in a voltage-dependent manner with a $K_{d(0)}$ of 22.8mM (Benveniste and Mayer, 1993).

Although normally the metabolism and excretion of polyamines are tightly regulated, extracellular levels of polyamines can vary in diseased states (Marton and

Pegg, 1995; Williams, 1997) and likely increase upon cell lysis. In such circumstances, micromolar changes in local extracellular spermine concentrations would affect neuronal nAChRs more than glutamate receptors. Recent studies have provided strong evidence that presynaptic nicotinic transmission modulates the release of neurotransmitters including dopamine, GABA and glutamate (McGehee and Role, 1995). Small changes in extracellular spermine could, therefore, selectively block this modulation.

The voltage-dependent block of neuronal nAChRs by intracellular spermine plays important physiological roles. In the CNS, many nAChRs are thought to be located at presynaptic terminals (Role and Berg, 1996). When activated, these receptors depolarize the nerve terminal to modulate transmitter release. In the absence of inward rectification, the conductance increase produced by these receptors would reduce the amplitude of the nerve terminal action potential. The high affinity block of nAChRs by intracellular spermine rapidly abolishes the conductance increase at positive membrane potentials, thereby allowing an effective depolarization of the terminal. The block by intracellular spermine also affects postsynaptic nAChRs on dendrites and cell bodies. The non-linear ACh-evoked G-V curves show a decrease in conductance even at membrane potentials near rest; therefore, changes in the membrane potential of the postsynaptic neuron can affect the conductance of the nAChRs and alter synaptic efficacy.

CHAPTER 3

A Molecular Link between Inward Rectification and Calcium Permeability of Neuronal Nicotinic Acetylcholine $\alpha 3\beta 4$ and $\alpha 4\beta 2$ receptors

ABSTRACT

Many nicotinic acetylcholine receptors (nAChRs) expressed by central neurons are located at presynaptic nerve terminals. These receptors have high calcium permeability and exhibit strong inward rectification, two important physiological features that enable them to facilitate transmitter release. Previously, we showed that intracellular polyamines act as gating molecules to block neuronal nAChRs in a voltage-dependent manner, leading to inward rectification. Our goal is to identify the structural determinants that underlie the block by intracellular polyamines and govern calcium permeability of neuronal nAChRs. We hypothesize that two ring-like collections of negatively charged amino acids (cytoplasmic and intermediate rings) near the intracellular mouth of the pore mediate the interaction with intracellular polyamines and also influence calcium permeability. Using site-directed mutagenesis and electrophysiology on $\alpha_4\beta_2$ and $\alpha_3\beta_4$ receptors expressed in *Xenopus* oocytes, we observed that removing the five negative charges of the cytoplasmic ring had little effect on either inward rectification or calcium permeability. However, partial removal of negative charges of the intermediate ring diminished the high-affinity, voltage-dependent interaction between intracellular polyamines and the receptor, abolishing inward-rectification. In addition, these non-rectifying mutant receptors showed a drastic reduction in calcium permeability. Our results indicate that negatively charged residues on the intermediate ring form both a high affinity binding-site for intracellular polyamines and a selectivity filter for inflowing calcium ions; that is, a common site links inward rectification and calcium permeability of neuronal nAChRs. Physiologically, this molecular mechanism provides insight into how presynaptic nAChRs act to influence transmitter release.

INTRODUCTION

A number of studies implicate cholinergic nicotinic receptors in a wide variety of cognitive functions, including visual and auditory processing, nociception, and attention and memory mechanisms (Picotto et al., 1995; Bannon et al., 1998; Xiang et al., 1998; Marubio et al., 1999; Vetter et al., 1999). Many neurons express nAChRs at synapses; at some, nAChRs are located postsynaptically and mediate fast excitatory synaptic transmission, while at many others, nAChRs are located presynaptically and facilitate neurotransmitter release (Clarke, 1993; MacDermott et al., 1999). Functionally, neuronal nAChRs have two properties that make them suitable to influence transmitter release: they have high calcium permeability (McGehee and Role, 1995), and they inwardly rectify, that is, they conduct inward currents at negative potentials but do not conduct outward currents at positive potentials (Mathie et al., 1990; Sands and Barish, 1992; Ifune and Steinbach, 1993). Inward rectification provides an important mechanism to ensure that the receptors do not short circuit the action potential in the nerve terminal and reduce transmitter release.

That muscle nAChRs have relatively low permeability to calcium (Lewis, 1979; Adams et al., 1980) and do not show inward rectification suggest that calcium permeability and inward rectification go hand in hand for nAChRs. Interestingly, this relationship also holds for subtypes of glutamate receptors: AMPA/kainate receptors that have low calcium permeability show little inward rectification, whereas those that have high calcium permeability show strong inward rectification (Verdoorn et al., 1991; Hume et al., 1991; Dingledine et al., 1999). It is not fortuitous that these two properties correlate for AMPA/kainate receptors, as the same structural determinant affects both properties. The purpose of this study is to determine the structural element(s) of neuronal nAChRs that influence calcium permeability and inward rectification.

nAChRs have three ring-like collections of charged residues on either side of the pore (extracellular, cytoplasmic and intermediate rings) that influence ion conduction through the pore; the intermediate ring is located at the narrowest region, or gate, of the pore and affects ion selectivity (Imoto et al., 1988; Konno et al., 1991; Cooper et al., 1991; Galzi et al., 1992; Bertrand et al., 1993; Wilson and Karlin, 1998). Previously, we demonstrated that inward rectification of neuronal nAChRs, like glutamate receptors, results from a voltage-dependent block of the receptor pore by intracellular polyamines (Haghighi and Cooper, 1998). Our hypothesis is that the cytoplasmic and intermediate rings form the site of interaction for intracellular polyamines.

To test this hypothesis, we use a combined approach of site directed mutagenesis of neuronal nAChR subunit genes and two-electrode voltage clamp and patch clamp techniques on recombinant receptors expressed in *Xenopus* oocytes. Our results indicate that the negatively charged residues at the intermediate ring are essential for interaction of polyamines with $\alpha 4\beta 2$ and $\alpha 3\beta 4$ neuronal nAChRs. Furthermore, we show that these negatively charged residues influence the calcium selectivity of the pore, indicating that a common structural element governs both inward rectification and calcium permeability of neuronal nAChRs. Part of these results have been reported (Haghighi and Cooper, 1998a).

METHODS and MATERIALS

Site-directed mutagenesis

We designed two complementary oligonucleotide primers containing the substituted nucleotide(s) corresponding to amino acids at the cytoplasmic or intermediate ring of $\alpha 3$, $\alpha 4$, and $\beta 4$ nAChR subunits, and used the Quick-Change Site-Directed Mutagenesis Kit (Stratagene, La Jolla, USA) to mutate each subunit. Rat $\alpha 3$ and $\beta 4$ cDNAs (gifts from Dr. P. Seguela) were cloned into the pCDNA1 expression vector (Invitrogen, San Diego, CA), and chick $\alpha 4$ and $\beta 2$ (gifts from Dr. M. Ballivet) were cloned into derivatives of pSV2.cat expression vectors (Cooper et al., 1991). For each reaction, we mixed 5-50 ng of the wild-type plasmid and 125 ng of each of the two primers in a solution containing 5 μ l of 10x reaction buffer (Stratagene), 1 μ l dNTP mix (Stratagene) and 1 μ l Pfu DNA polymerase (2.5 U/ml, Stratagene), diluted with double-distilled water to a final volume of 50 μ l. The reaction mixture was then cycled in a PCR apparatus (PTC-100, MJ Research Inc., MA, USA) according to the following protocol: 1 cycle at 95°C for 30 s followed by 12-18 cycles at 95°C for 30 s, 55°C for 1 min and 68°C for 2 min. The following amino acids were mutated: $\alpha 3$: aspartic acid (D) at position 237 to alanine (A) ($\alpha 3_{D237A}$), glutamic acid (E) at position 240 to alanine ($\alpha 3_{E240A}$) or glutamine (Q) ($\alpha 3_{E240Q}$); $\alpha 4$: glutamic acid (E) at position 242 to alanine ($\alpha 4_{E242A}$), glutamic acid at position 245 to alanine ($\alpha 4_{E245A}$); $\beta 4$: aspartic acid at position 236 to alanine ($\beta 4_{D236A}$), glutamic acid at position 239 to alanine ($\beta 4_{E239A}$). All mutations were verified by sequencing.

Expression of nAChR subunit cDNAs in Oocytes

Xenopus oocytes were defolliculated and prepared as described by Bertrand et al. (1991). We injected 1-3 ng of pairwise combinations of cDNAs coding for neuronal

nAChR subunits or 3-6 ng of pairwise mutant $\alpha 4$ and $\beta 2$ or $\alpha 3$ and $\beta 4$ into the nucleus of oocytes. This difference in the amount of cDNA injection was to achieve sufficient levels of expression for the mutant receptors. Oocytes were incubated at 19°C for 2-7 days before recording. For single channel experiments, the vitelline membrane surrounding the oocytes was removed.

Injection of BAPTA and Spermine into the oocytes

In order to avoid the activation of the endogenous Ca^{2+} -activated Cl^- currents in the presence of extracellular Ca^{2+} , we injected oocytes 2-10 min before recording with BAPTA. The injection solution contained 100 mM BAPTA with 85 mM Na^+ , 2.5 mM K^+ and 10 mM HEPES adjusted to pH 7.4 with NaOH. We injected between 30 to 60 nl of this solution into oocytes which corresponds to a concentration of approximately 5-7 mM in the oocytes.

In order to examine the effect of the increase in the intracellular concentration of spermine on the wild type and mutant neuronal nAChRs, we injected oocytes with 60 nl of a solution containing 100 mM spermine, 100 mM BAPTA, 85 mM Na^+ , 2.5 mM K^+ and 10 mM HEPES adjusted to pH 7.4. In some recordings a third electrode was used to inject spermine into the oocytes while under two-electrode clamp. In all spermine injection experiments, removal of Ca-activated Cl^- currents was used as an indication of successful injection.

Neuronal and myotube cultures

SCG ganglia were dissected from neonatal Sprague-Dawley rats (Charles River, Canada) and dissociated mechanically and enzymatically as previously described (McFarlane and Cooper, 1992). Briefly, the ganglia were dissected under sterile conditions from animals sacrificed by cervical dislocation. The ganglia were

dissociated at 37°C in collagenase (1 mg/ml, type I, Sigma, St. Louis, MO) for 15min followed by dispase (2.4 mg/ml, grade II, Boehringer-Mannheim, Indianapolis, IN) for 2-3 hr. Dissociated neurons were washed with L-15 medium supplemented with 10% horse serum and plated onto laminin-coated (40 µg/ml, overnight at 4°C; gift of Dr. S. Carbonetto) Aclar coverslips (Allied Chemicals, Clifton, NJ) in modified petri dishes. The neurons were incubated in 1.5 ml of L-15 medium supplemented with 5% rat serum, vitamins, cofactors, penicillin, streptomycin, and sodium bicarbonate as described previously (Hawrot and Patterson, 1979). The media was supplemented with nerve growth factor.

We used a similar method to isolate neonatal rat myoblasts. Briefly, we dissected strips of pectoral muscles from neonatal rats and dissociated them in collagenase (1 mg/ml) for 15 min at 37 C. Myoblasts were incubated in 1.5 ml of L-15 medium supplemented with 10% fetal calf serum. Myoblasts fused to form multinucleated myotubes in 2-4 days after plating. All cultures were maintained at 37°C in a humidified incubator with an atmosphere of 5% CO₂ and 95% air.

Electrophysiology

Whole-cell recordings from oocytes: In order to measure the macroscopic ACh-evoked currents in oocytes, we used the two-electrode voltage clamp technique (Bertrand et al., 1991). These experiments were performed at room temperature (22-24°C) using a standard voltage-clamp amplifier (built by Mr. A. Sherman, McGill University). During the recordings, oocytes were superfused with control perfusion solution or agonist solutions at 10-20 ml/min; switching from one solution to another was done manually. Recording electrodes had tip diameters of 10-15 µm and were filled with 3M KCl. All mutant receptors, α_3 _{D237A} β_4 , $\alpha_3\beta_4$ _{D236A}, α_3 _{D237A} β_4 _{D236A}, α_3 _{E240A} β_4 , α_3 _{E240Q} β_4 , $\alpha_3\beta_4$ _{E239A}, α_4 _{E242A} β_2 and α_4 _{E245A} β_2 , produced ACh-evoked

currents when expressed in *Xenopus* oocytes. For equimolar injections of cDNAs, inward currents at -90 mV were on average 8-12 times smaller for the intermediate mutant receptors or 2-3 times smaller for the cytoplasmic mutant receptors compared to those for the wild type receptors. The half-maximal concentration (EC_{50}) for ACh was not significantly different among the mutant and wild type receptors.

To measure the current voltage (I-V) relationships, we used a voltage ramp protocol applied within 2-4 seconds after the inward current had reached its maximum amplitude; the speed of the ramp was 333 mV/s. Voltage ramps were applied for 360-600 ms (corresponding to 120-200 mV), during which time no significant desensitization was observed. I-V curves were also obtained by measuring the ACh-evoked currents at different membrane potentials (steady-state I-V curves). Both current and voltage traces were monitored and stored for analysis. Currents were sampled at 100-350 Hz on-line with a Pentium PC computer (running at 60 MHz and an A/D card: Omega, Stamford, CT). The program PATCHKIT (Alembic Software, Montreal) was used for stimulation and data acquisition.

External perfusion solution contained 96 mM NaCl, 2 mM KCl, 1 mM $Na_2H_2PO_4$, 1 mM $BaCl_2$, 10 mM HEPES and 1 μ M atropine; pH was adjusted with NaOH to 7.4-7.5. For Ca^{2+} permeability measurements, we used a control solution containing 1 mM $CaCl_2$ instead of $BaCl_2$ and compared the reversal potential change when we switched to a solution of either 100 mM $CaCl_2$; 10 mM $CaCl_2$ and 90 mM NaCl; 25 mM $CaCl_2$ and 75 mM NaCl; or 50 mM $CaCl_2$ and 50 mM NaCl. All solutions were buffered by 10 mM HEPES and NaOH to a pH of 7.4-7.5 and contained 1 μ M atropine. Spermine (Sigma) was added to the control solution containing 1 mM $BaCl_2$ where indicated. Spermine was dissolved in sterile water and aliquots were kept frozen at $-20^\circ C$.

Single channel recordings from oocytes: Only oocytes that gave rise to large inward currents ($>1\mu A$ in response to 1 μ M ACh for $\alpha 4\beta 2$ expressing oocytes or in response

10 μ M ACh for α 3 β 4 expressing oocytes when voltage clamped at -40 mV) were used for single channel recordings. Outside-out recordings were carried out using a List EPC-7 amplifier at room temperature (22-24°C) (Hamill et al., 1981). Pipette resistance ranged from 5-10 M Ω for outside-out recordings, and electrodes were coated with Sylgard (Dow Corning). Recordings were obtained in the continuous presence of ACh (0.1-0.2 μ M for α 4 β 2 receptors and 1-10 μ M for α 3 β 4) in the recording bath. ACh-evoked single channel activity gradually diminished after excision of the patch (in 2-5 min). Signals were digitized with a PCM (501, Sony) and stored on VCR tapes. For off-line analysis, stored signals were filtered at 1.5-2kHz with an eight-pole Bessel filter (Frequency Devices Inc.) and sampled at 10 kHz using a Pentium-60 PC computer. The program PATCHKIT was used for stimulation and data acquisition.

External solution contained 100 mM KCl, 1 mM CaCl₂, 10 HEPES and 1 μ M atropine, and pH was 7.4 adjusted with KOH. Recording electrodes contained 80 mM KF, 20 mM potassium acetate, 10 mM HEPES and 10 mM EGTA and pH was adjusted to 7.4 with KOH. Spermine was added to the intracellular solution where indicated.

Whole-cell recordings from rat SCG neurons and cultured myotubes: Whole-cell patch-clamp recordings were performed at room temperature (22-24°C) using a List EPC-7 amplifier (Hamill et al., 1981). Throughout the recordings cells were perfused with the external solution at a rate of 1 ml/min. ACh was applied by pressure ejection from pipettes with tip diameters of 20-30 μ m (Mandelzys et al., 1995). The resistance of patch pipettes ranged from 2-6 M Ω , and 50-80% of the series resistance was compensated. For experiments with muscle nAChRs, we chose small multinucleated myotubes that had grown for 2-4 days in culture.

Both steady state and ramp I-V curves were obtained for ACh-evoked macroscopic currents recorded from myotubes and SCG neurons. The speed of the

voltage ramp protocol was 200-1000 mV/s; voltage ramps were applied 600 ms following the application of ACh and lasted for 120-600 ms, during which time no significant desensitization was observed. Both current and voltage were monitored during the recordings and stored for analysis. Currents were filtered at 1.5 kHz with an eight-pole Bessel filter, sampled at 2.5-5kHz, displayed and stored on-line with a Pentium-60 PC computer. The program PATCHKIT was used for stimulation and data acquisition.

External perfusion solution contained 140 mM NaCl, 5.4 mM KCl, 0.33 mM NaH₂PO₄, 0.44 mM KH₂PO₄, 2.8 mM CaCl₂, 10 mM HEPES, 5.6 mM glucose, 2 mM glutamine, 0.5-1 μM TTX (Sigma) and 1μM atropine; pH was adjusted to 7.4. ACh (acetylcholine iodide, Sigma) was dissolved in the same external perfusion solution (100 μM for SCG neurons and 20 μM for myotubes). Recording electrodes were filled with intracellular solution containing 70 mM KF, 65 mM potassium acetate, 5 mM NaCl, 1 mM MgCl₂, 10 mM EGTA and 10 mM HEPES; pH was 7.4, adjusted with KOH.

Analysis

Whole-cell ACh-evoked I-V curves were obtained by subtracting the current in response to a ramp voltage change in the absence of agonist from that in the presence of agonist (see Haghghi and Cooper, 1998). The G-V curves were obtained by plotting the cord conductance against voltage. The cord conductance was calculated according to the following equation:

$$G=I / (V_m-E_{rev}) \quad (1)$$

where G is the cord conductance corresponding to each membrane potential (V_m), I is the ACh-evoked current at the corresponding V_m and E_{rev} is the reversal potential.

To measure the amplitude of single channel currents, we used either all-points histograms of open and closed distributions, or measured the amplitude of the channel openings individually using PATCHKIT. Histograms were fit by Gaussian curves using Origin 4.1 graphics software (MICROCAL™ Software, Inc.).

To quantify the voltage-dependent block by intracellular spermine, we fit the single channel G-V relationships to a derivation of the Woodhull (1973) equation (Johnson and Ascher, 1990; Haghghi and Cooper, 1998):

$$G/G_{\max} = 1/\{1 + [S]/K_d\} \quad (2)$$

where

$$K_d = K_{d(0)} \exp(-Vmz\delta F/RT)$$

and G is the conductance in the presence of spermine at any given V_m , G_{\max} is the maximum unblocked conductance, $[S]$ is the internal concentration of spermine, K_d is the dissociation constant at a given V_m , $K_{d(0)}$ is the dissociation constant at 0 mV, z is the valence of spermine, δ is the fraction of the membrane electric field sensed by spermine, and F , R and T have their usual meanings. In order to estimate the intracellular concentration of spermine, we fit the macroscopic G-V curves to equation (2) using the $K_{d(0)}$ and δ measured from the single channel experiments.

To measure the effect of increasing intracellular spermine, we fit the macroscopic G-V curves to the Boltzman equation:

$$G/G_{\max} = 1/\{1 + (\exp(V - V_{1/2})/k)\} \quad (3)$$

where $V_{1/2}$ is the membrane potential at which conductance (G) has reduced to half of the maximum conductance (G_{\max}) and k is a slope factor corresponding to the amount of depolarization needed to change the conductance e-fold.

Dose response curves for the effect of extracellular spermine were fit to a derivation of the logistic equation:

$$I/I_{\max} = 1/\{1 + (IC_{50}/[S])\} \quad (4)$$

where IC_{50} is the half maximal inhibition dose, and $[S]$ is the external concentration of spermine.

In order to calculate P_{Ca}/P_{Na} , we measured the reversal potential of the I-V curves in external solutions containing different amounts of Ca^{++} and used these values in a derivation of the Goldman, Hodgkin and Katz constant field voltage equation as presented by Lewis (1979):

$$E_{rev(Ca)} - E_{rev(Na)} = RT/F \ln \left\{ \frac{([Na]_o + P_K/P_{Na} [K]_o + 4P'_{Ca}/P_{Na} [Ca]_o)}{([Na]_i + P_K/P_{Na} [K]_i + 4P'_{Ca}/P_{Na} [Ca]_i)} \right\} \quad (5)$$

where

$$P'_{Ca} = P_{Ca} / (1 + \exp(E_{rev(Ca)} F/RT))$$

and P_X is the permeability coefficient of ion X . $[X]_o$ is the extracellular concentration of ionic specie X , and R , T and F have their usual meanings. Concentration of each ion was multiplied by its corresponding activity coefficient (Robinson and Stokes, 1960; Butler, 1968) and P_K/P_{Na} was 1.2 (Haghighi and Cooper, unpublished data). IV-curves were fit to a 9th order polynomial function and reversal potentials were measured by eye. We compensated for junction potentials caused by switching between different solutions.

The best fit to the data was achieved by minimizing χ^2 using a routine from Origin 4.1 graphics software that is based on a Levenberg-Marquardt algorithm. All data points are presented as mean \pm standard error of the mean. Statistical significance between values was examined using a paired Student's t test.

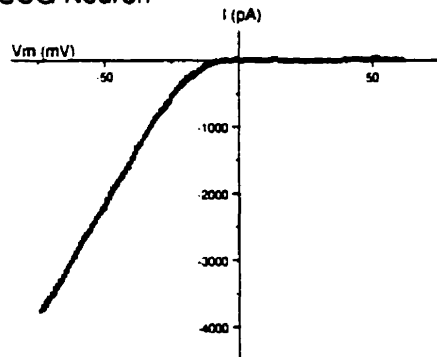
RESULTS

Figure 1 highlights the difference in inward rectification among nAChR subtypes. Figure 1A shows the ACh-evoked whole-cell current-voltage (I-V) relationship for native nAChRs expressed by neonatal rat sympathetic neurons from the superior cervical ganglion (SCG); these receptors showed strong inward rectification. Figure 1B shows the corresponding ACh-evoked I-V curve for native nAChRs expressed by neonatal rat myotubes. In contrast to nAChRs on SCG neurons, these muscle nAChRs showed little inward rectification.

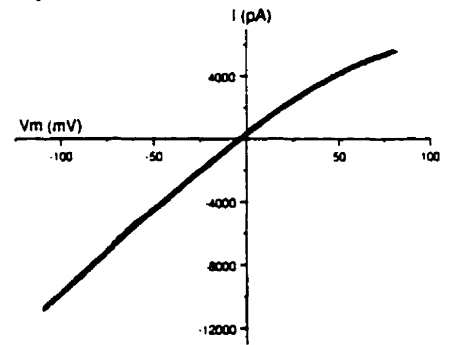
To further investigate the inward rectification of neuronal nAChRs, we studied recombinant receptors in *Xenopus* oocytes. Figures 1C and 1D show I-V curves for two neuronal nAChR subtypes: $\alpha 4\beta 2$ receptors (Fig.1C), made up of 2 subunits widely expressed in the CNS (Wada et al., 1989; Sargent, 1993; McGehee and Role, 1995), and $\alpha 3\beta 4$ receptors (Fig.1D), made up of 2 subunits highly expressed in peripheral autonomic neurons (Boyd et al., 1988; Couturier et al., 1990; Mandelzys et al., 1994). Similar to nAChRs on SCG neurons, the ACh-evoked I-V curves for both $\alpha 4\beta 2$ and $\alpha 3\beta 4$ receptor exhibited strong inward rectification.

Previously, we demonstrated that the strong inward rectification of $\alpha 4\beta 2$ receptors results from a voltage-dependent block of the receptor pore by intracellular polyamines (Haghighi and Cooper, 1998). A similar mechanism holds true for $\alpha 3\beta 4$ receptors. Figures 1E and 1F show examples from single channel experiments on $\alpha 4\beta 2$ and $\alpha 3\beta 4$ measured in outside-out patches; at positive potentials (V_m), spermine blocked the outward current from both these receptors when applied from the intracellular side. To determine the affinity of $\alpha 3\beta 4$ receptors for polyamines, we repeated these single channel experiments with 4 different spermine concentrations ranging from 0.1 μM to 100 μM on at least 3 different patches for each concentration and used a Woodhull model (Woodhull, 1973) (see methods and Haghighi and Cooper, 1998) to analyze this voltage-dependent block (data not shown). From these

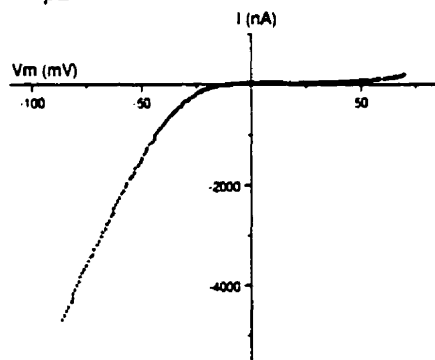
A SCG Neuron



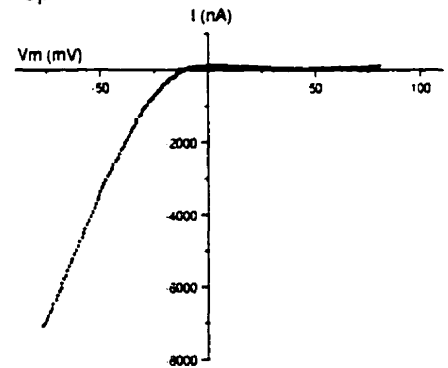
B Myotube



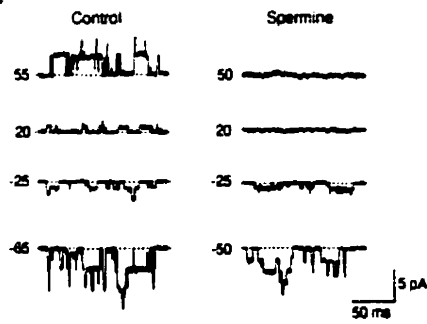
C $\alpha 4\beta 2$



D $\alpha 3\beta 4$



E $\alpha 4\beta 2$



F $\alpha 3\beta 4$

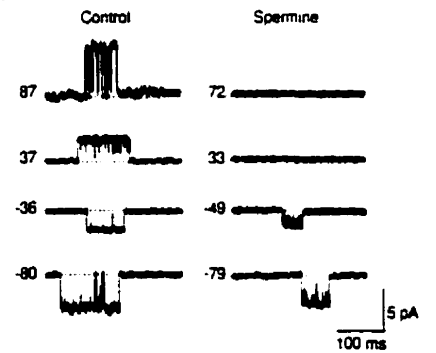


Figure 3.1. Inward rectification of neuronal nAChRs. A, This figure shows the ACh-evoked macroscopic current-voltage relationship (I-V curve) recorded from a neonatal rat SCG neuron. Whole-cell currents were recorded while the membrane potential was ramped from -80 to $+60$ mV (333 mV/sec). The IV-curve was obtained by subtracting the control current from the current evoked by 100 μ M ACh. The I-V curve is fitted to a 9th order polynomial function and shows strong inward rectification. B, This figure shows the ACh-evoked macroscopic I-V curve recorded from a rat myotube (ACh = 20 μ M). In contrast to A, this I-V curve shows no inward rectification. C shows a macroscopic ACh-evoked I-V curve for $\alpha 4\beta 2$ neuronal nAChR, and D shows a macroscopic ACh-evoked I-V curve for $\alpha 3\beta 4$ neuronal nAChR expressed in *Xenopus* oocytes. Similar to native nAChRs on SCG neurons, these recombinant receptors exhibit strong inward rectification. E and F show single channel records obtained from outside-out patches expressing $\alpha 4\beta 2$ or $\alpha 3\beta 4$ receptors, respectively. In control patches, inward rectification of these receptors is lost. Addition of spermine (20 μ M for $\alpha 4\beta 2$ and 50 μ M for $\alpha 3\beta 4$) to the patch electrode blocks outward currents at positive potentials and reduces the amplitude of inward currents.

experiments, we determined that the affinity of $\alpha 3\beta 4$ receptors for spermine at 0mV ($K_{d(0)}$) was $6.7 \pm 0.5 \mu\text{M}$, approximately 2-fold higher than $K_{d(0)}$ for $\alpha 4\beta 2$ receptors ($3.6 \mu\text{M}$) (Haghighi and Cooper, 1998); however, the proportion of the membrane field sensed by spermine ($\delta=50-55\%$) was the same for both receptor types.

We were interested to determine the site of interaction between intracellular polyamines and neuronal nAChRs. Since polyamines are highly positively charged, a likely site for the interaction between neuronal nAChRs and intracellular polyamines is the negatively charged region at the cytoplasmic side of the channel pore between M1 and M2. Figure 2 shows an amino acid alignment of this region for the 4 neuronal nAChR subunits: $\alpha 3$, $\alpha 4$, $\beta 2$ and $\beta 4$. The region between M1 and M2 contains 5 amino acids, 2 of which are negatively charged and are in homologous positions for each subunit. The location of the five glutamic acids (E), corresponding to position 240 for $\alpha 3$, has been referred to as the intermediate ring, and the site of the negatively charged aspartic acid residues (D) ($\alpha 3$, $\beta 2$ and $\beta 4$) or E ($\alpha 4$) closer to M1 has been referred to as the cytoplasmic ring (Imoto et al., 1988; Galzi et al., 1991; Karlin and Akabas, 1995). We hypothesized that these negatively charged residues form the site of interaction for the positively charged polyamines. To test this, we mutated these residues to neutral amino acids, using site-directed mutagenesis, and examined the functional properties of these mutant receptors expressed in *Xenopus* oocytes.

Cytoplasmic ring mutations have little effect on inward rectification

First, we investigated the role of the cytoplasmic ring on the rectification of $\alpha 3\beta 4$ receptors by mutating the D at this site to alanine (A) for both $\alpha 3$ and $\beta 4$ subunits; we refer to these mutant subunits as $\alpha 3_{D237A}$ and $\beta 4_{D236A}$, respectively. We co-expressed pairwise combinations of mutant and wild-type $\alpha 3$ and $\beta 4$ cDNAs in *Xenopus* oocytes to produce 3 different receptors: $\alpha 3_{D237A}\beta 4$, $\alpha 3\beta 4_{D236A}$ and $\alpha 3_{D237A}\beta 4_{D236A}$.

	<u>M1</u>	Intracellular	<u>M2</u>	Extracellular
α_3	VFYLP	217DCGK	VTLCISVLLSLTVFLLVIT	ETIP
α_4	VFYLP	218ECGK	ITLCISVLLSLTVFLLIT	ETIP
β_2	VFYLP	216DCGK	MTLCISVLLALTVFLLIS	KIVP
β_4	VFYLP	216DCGK	MTLCISVLLALTFLLIS	KIVP

Figure 3.2. Charged amino acids flanking the pore region are conserved in neuronal nAChRs subunits. This figure shows the amino acid sequence alignment of neuronal nAChR subunits $\alpha 3$, $\alpha 4$, $\beta 2$ and $\beta 4$ for the cytoplasmic end of M1, M1-M2 loop, M2 segment and part of the M2-M3 loop. This alignment shows the presence of three ring-like accumulations of charged residues flanking M2: the cytoplasmic ring (corresponding to $\alpha 3$ D237), the intermediate ring (corresponding to $\alpha 3$ D240) and the extracellular ring (corresponding to $\alpha 3$ E261).

For each receptor, we obtained the macroscopic ACh-evoked I-V curve. To quantify the rectification, we measured the relative conductance at 4 membrane potentials, -40mV, +20mV, +40mV and +80mV to that at -90 mV. For $\alpha 3_{D237A}\beta 4$ or $\alpha 3\beta 4_{D236A}$ receptors, we observed no significant difference in rectification compared to that for wild-type $\alpha 3\beta 4$ receptors (Fig. 3A & Table 1). The I-V curves for $\alpha 3_{D237A}\beta 4_{D236A}$ receptors also showed strong inward rectification up to +20 mV (Fig. 3B); however, at V_m greater than +25mV, we observed significantly more outward current compared to wild-type $\alpha 3\beta 4$ receptors. The conductance at +40mV and that at +80mV for $\alpha 3_{D237A}\beta 4_{D236A}$ receptors were approximately 12 times greater than those for wild-type $\alpha 3\beta 4$ receptors at these potentials.

In addition to $\alpha 3\beta 4$ receptors, we investigated the role of the cytoplasmic ring on the rectification of $\alpha 4\beta 2$ receptors. We mutated the E at 240 to A for $\alpha 4$ ($\alpha 4_{E242A}$) and co-expressed $\alpha 4_{E242A}$ with wild-type $\beta 2$ in *Xenopus* oocytes. We observed no significant difference in the ACh-evoked I-V curves for $\alpha 4_{E242A}\beta 2$ receptor compared to that for wild-type $\alpha 4\beta 2$ receptors (Table 1).

Intermediate Ring mutations abolish inward rectification

Next, we investigated the role of the intermediate ring on the rectification of $\alpha 3\beta 4$ receptors by mutating the E to A for both $\alpha 3$ and $\beta 4$ subunits; we refer to these mutant subunits as $\alpha 3_{E240A}$ and $\beta 4_{E239A}$, respectively. We co-expressed these mutant subunits with wild-type $\alpha 3$ and $\beta 4$ in *Xenopus* oocytes to produce either $\alpha 3\beta 4_{E239A}$ or $\alpha 3_{E240A}\beta 4$ receptors.

These mutations in the intermediate ring had a dramatic effect on inward rectification. Figure 3C shows a result from an oocyte expressing $\alpha 3\beta 4_{E239A}$ receptors. In contrast to wild-type $\alpha 3\beta 4$ receptors, the ACh-evoked I-V curve for $\alpha 3\beta 4_{E239A}$ receptors was virtually linear (Fig. 3C); the ACh-evoked current reversed

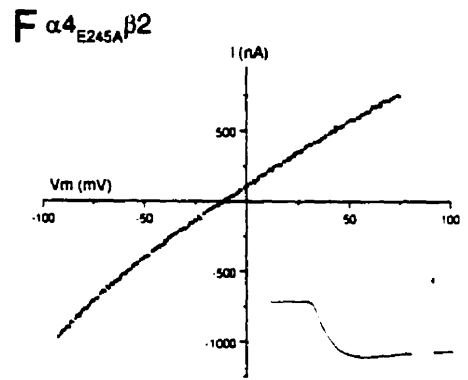
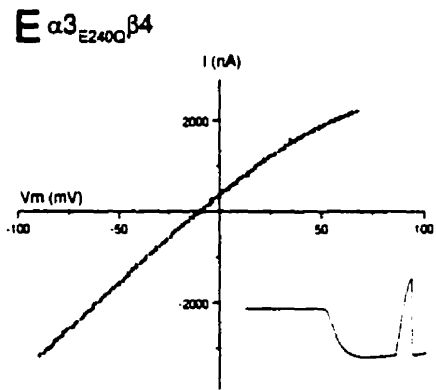
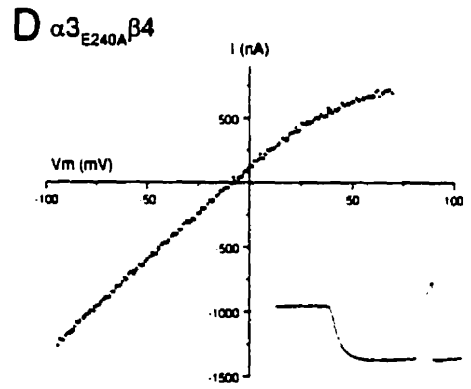
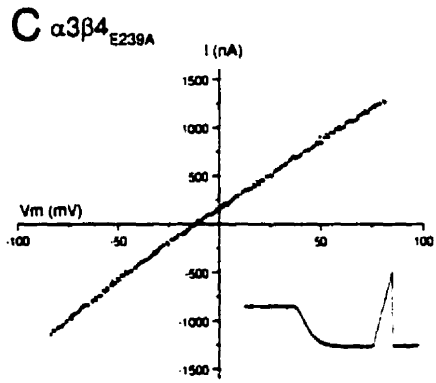
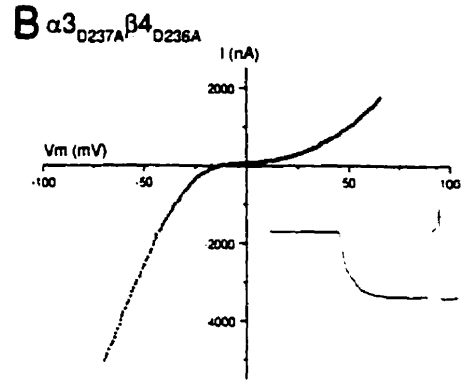
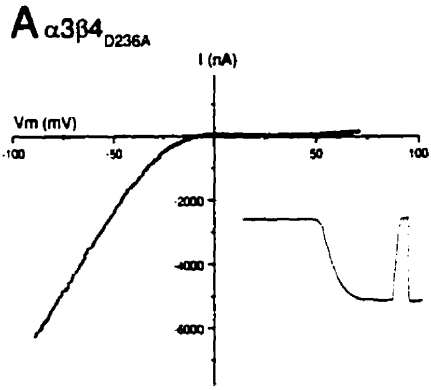


Figure 3.3. Substitution of negatively charged residues of the intermediate ring abolishes inward-rectification of neuronal nAChRs. A shows an ACh-evoked macroscopic I-V curve obtained from an oocyte expressing the cytoplasmic ring mutant receptor $\alpha\beta 4_{D236A}$. This mutant receptor exhibits inward rectification similar to the wild type $\alpha\beta 4$ receptor. The inset shows the ACh-evoked current recorded from this oocyte before and during a voltage ramp. B shows an ACh-evoked macroscopic I-V curve obtained from an oocyte expressing the cytoplasmic ring mutant receptor $\alpha 3_{D237A}\beta 4_{D236A}$. The inset shows the ACh-evoked current from this oocyte in response to a voltage ramp. C, D, E and F show ACh-evoked macroscopic I-V curves obtained from oocytes expressing $\alpha\beta 4_{E239A}$, $\alpha 3_{E240A}\beta 4$, $\alpha 3_{E240Q}\beta 4$ or $\alpha 4_{E245A}\beta 2$ intermediate ring mutant receptors, respectively. All four mutant receptors show a nearly linear ACh-evoked IV-relationship from -90 to $+80$ mV. Insets in each figure show ACh-evoked currents in response to a voltage ramp and demonstrate that the ACh-evoked currents do not show any significant desensitization. For all insets the length of the trace is 6 s.

Table 1. The effect of mutations in the cytoplasmic and the intermediate ring on the macroscopic inward rectification and Ca^{++} permeability of $\alpha 4\beta 2$ and $\alpha 3\beta 4$ nAChRs.

nAChR subtype	G_{-40}/G_{-90}	G_{-20}/G_{-90}	G_{-40}/G_{-90}	G_{-80}/G_{-90}	$P_{\text{Ca}^{++}}/P_{\text{Na}^{+}}$	ΔE_{rev} (mV) [†]
$\alpha 4\beta 2$	31.52 ± 1.10 (n=35)	0.42 ± 0.15 (n=35)	0.88 ± 0.22 (n=35)	2.78 ± 0.5 (n=33)	1.65 ± 0.15 (n=8)	15.5 ± 1.7 (n=8)
$\alpha 4_{\text{E242A}}\beta 2$	32.40 ± 2.10 (n=6)	0.50 ± 0.20 (n=6)	1.0 ± 0.40 (n=6)	2.50 ± 0.6 (n=6)	-	-
$\alpha 4_{\text{E245A}}\beta 2$	91.6 ± 1.20* (n=17)	81.92 ± 2.4* (n=17)	78.7 ± 2.60* (n=17)	73.23 ± 2.9* (n=17)	0.06 ± 0.005* (n=6)	-40.75 ± 1.95* (n=6)
$\alpha 3\beta 4$	44.66 ± 1.9 (n=35)	1.75 ± 0.5 (n=35)	0.94 ± 0.2 (n=35)	2.06 ± 0.4 (n=32)	0.78 ± 0.02 (n=8)	3.6 ± 0.5 (n=8)
$\alpha 3_{\text{D237A}}\beta 4$	45.8 ± 3.0 (n=6)	1.9 ± 0.4 (n=6)	0.64 ± 0.3 (n=6)	2.7 ± 0.35 (n=6)	-	-
$\alpha 3\beta 4_{\text{D236A}}$	45.3 ± 2.0 (n=8)	1.76 ± 0.2 (n=8)	0.76 ± 0.2 (n=8)	3.76 ± 0.4 (n=8)	-	-
$\alpha 3_{\text{D237A}}\beta 4_{\text{D236A}}$	49.28 ± 4.0 (n=12)	5.75 ± 2.2 (n=12)	11.51 ± 1.3* (n=12)	24.42 ± 2.4* (n=12)	0.77 ± 0.03 (n=6)	3.30 ± 0.60 (n=6)
$\alpha 3_{\text{E240Q}}\beta 4$	93.17 ± 1.7* (n=16)	84.11 ± 2.7* (n=16)	79.66 ± 2.7* (n=16)	72.13 ± 3.2* (n=16)	0.55 ± 0.007* (n=6)	-44.2 ± 2.2* (n=6)
$\alpha 3_{\text{E240A}}\beta 4$	93.78 ± 1.2* (n=21)	82.358 ± 2.6* (n=21)	79.30 ± 2.9* (n=21)	75.0 ± 2.8* (n=21)	0.62 ± 0.001* (n=8)	-42.6 ± 2.5* (n=8)
$\alpha 3\beta 4_{\text{E239A}}$	96.0 ± 1.6* (n=31)	94.42 ± 2.6* (n=31)	93.14 ± 2.5* (n=31)	92.28 ± 2.6* (n=31)	0.45 ± 0.005* (n=6)	-47.8 ± 1.9* (n=6)

* These values for mutant receptors are significantly different from those for the corresponding wild-type receptors ($P < 0.01$).

[†] These reversal potential shifts were measured when switching from the control solution (1 mM Ca^{++}) to one containing 100 mM Ca^{++} .

at approximately -10 mV (Fig. 3C), and our ion substitution experiments indicated that this current was carried exclusively by cations (data not shown). We obtained similar results from over 30 oocytes expressing $\alpha 3\beta 4_{E239A}$ receptors. We measured the relative conductance at -40 mV, +20 mV, +40 mV and +80mV to that at -90 mV (Table 1); we observed no significant difference in conductance at each potential (Table 1). The conductance at +40 mV was 93% of that at -90 mV, approximately 100 times greater than that of wild-type $\alpha 3\beta 4$ receptors.

Our results with $\alpha 3\beta 4_{E239A}$ receptors indicate that removal of the negative charge in the intermediate ring of $\beta 4$ abolishes the strong inward rectification of $\alpha 3\beta 4$ receptors. To determine the effect of a similar mutation in the $\alpha 3$ subunit, we examined the rectification properties of $\alpha 3_{E240A}\beta 4$ receptors. The ACh-evoked I-V curve for $\alpha 3_{E240A}\beta 4$ receptors was almost linear, and the current reversed at approximately -10 mV (Fig.3D). The conductance at +40mV was 79% of that at -90 mV, roughly 85 times greater than that of wild-type $\alpha 3\beta 4$ receptors (Table 1). These results indicate that removal of the negative charge in the intermediate ring of the α subunit is sufficient to abolish the strong inward rectification of $\alpha 3\beta 4$ receptors.

To test the effect of different amino acid side chains at the intermediate ring on rectification, we mutated E at 240 to glutamine (Q) in $\alpha 3$ and co-expressed it with wild-type $\beta 4$ in *Xenopus* oocytes. These $\alpha 3_{E240Q}\beta 4$ receptors had essentially linear ACh-evoked I-V curves, reversing at around -10 mV (Fig.3E); the relative conductances at -40mV, +20mV, +40mV and +80mV were not significantly different from those of $\alpha 3_{E240A}\beta 4$ receptors (Table 1). This indicates that the negative charge at this position, not the size or polarity of the side chain, is crucial for the strong inward rectification of neuronal nAChRs.

In addition, to test whether this effect on the rectification was specific to $\alpha 3\beta 4$ receptors, we mutated E at the intermediate ring to A in the $\alpha 4$ subunit and co-expressed it with wild-type $\beta 2$ in *Xenopus* oocytes. As shown in figure 3F, these

$\alpha_{4E245A}\beta_2$ receptors had almost linear I-V curves reversing at about -10 mV. The conductance at +40mV was 79% of that at -90 mV, and approximately 90 times greater than that of wild-type $\alpha\beta_2$ receptors (Table 1). These results demonstrate that partial removal of negatively charged residues in the intermediate ring abolishes strong inward rectification of $\alpha\beta_2$ receptors.

Elevated intracellular spermine increased inward rectification of $\alpha\beta_2$ and $\alpha\beta_4$ receptors, but had no effect on non-rectifying $\alpha_{4E245A}\beta_2$ and $\alpha_{3E240A}\beta_4$ receptors

Our results on intermediate ring mutations suggest that a decrease in the net negative charge of the intermediate ring abolishes the interaction of intracellular polyamines with neuronal nAChRs. To further investigate this possibility, we examined the effects of increasing the intracellular spermine concentration in *Xenopus* oocytes expressing either $\alpha\beta_2$, $\alpha\beta_4$, $\alpha_{4E245A}\beta_2$ or $\alpha_{3E240A}\beta_4$ receptors. For most experiments, first we recorded the ACh-evoked I-V curve, then injected the oocytes with spermine, and repeated the I-V measurements at 2-3 minute intervals. To verify that our injections worked, we included BAPTA along with spermine; in all injected oocytes, BAPTA abolished calcium activated chloride currents when we recorded the ACh-evoked current with 1 mM Ca^{++} as the only divalent cation in the extracellular solution (see methods). Alone, BAPTA had no effect on inward rectification of wild-type or mutant receptors.

For ACh-evoked currents from *Xenopus* oocytes expressing wild-type $\alpha\beta_2$ or $\alpha\beta_4$ receptors, we observed that intracellular injections of spermine caused a progressive increase in rectification, producing its maximal effect in approximately 10 min. Figure 4 shows example I-V curves from $\alpha\beta_2$ (4A) and $\alpha\beta_4$ (4D) receptors before and after spermine injection. Increasing intracellular spermine caused a significant leftward shift in the ACh-evoked I-V and G-V curves, without affecting the ACh-evoked current amplitude at -90 mV or the reversal potential (Fig. 4). To

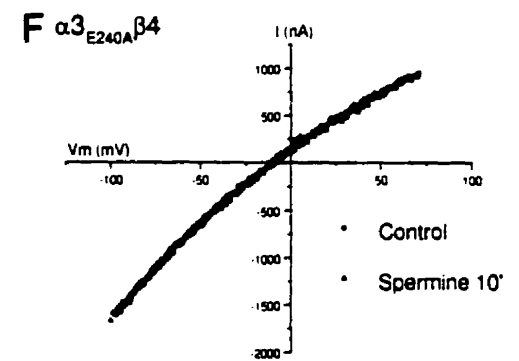
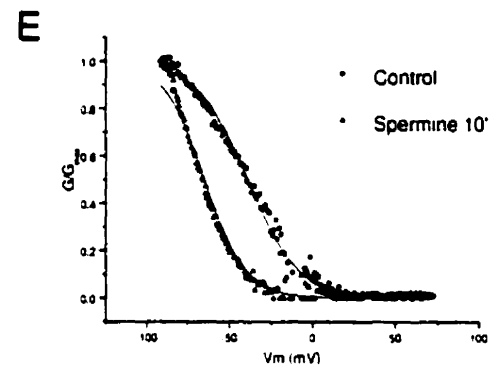
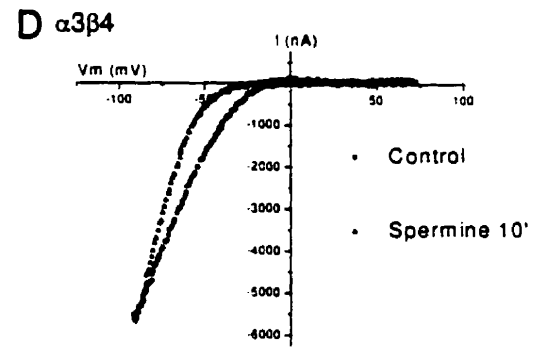
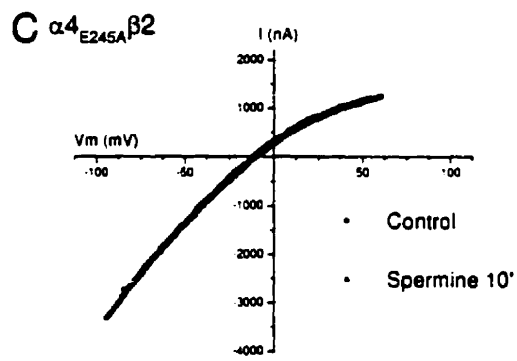
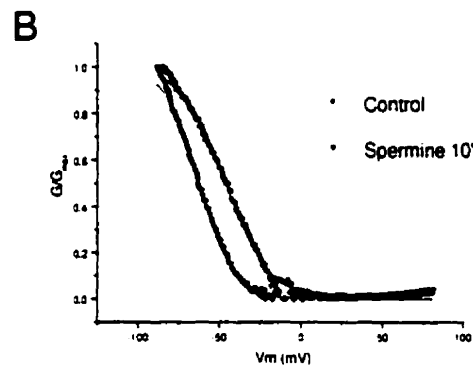
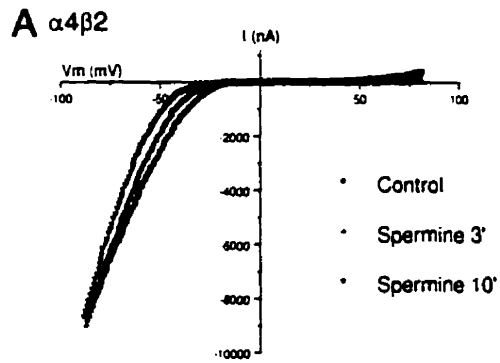


Figure 3.4. Effect of increasing intracellular spermine. A shows macroscopic ACh-evoked I-V curves obtained from $\alpha 4\beta 2$ receptors expressed in *Xenopus* oocytes. IV-curves were obtained before and 3 and 10 min after injecting 60 nl of a solution containing 100 mM spermine into the oocytes. B, This figure shows the G-V curves corresponding to the I-V curves in A. Solid lines are fits to the G-V curves using the Woodhull equation. The leftward shift in the G-V curve corresponds to an approximately 10 fold increase in intracellular spermine concentration. C. This figure shows the macroscopic ACh-evoked IV-curves before and after injection of spermine recorded from an oocyte expressing $\alpha 4_{E245A}\beta 2$ receptors. There was no significant difference between the IV-curves before and after injection of spermine. D and E show the I-V and G-V curves from an oocyte expressing $\alpha 3\beta 4$ receptors before and after injection with 60 nl of a solution containing 100 mM spermine. The solid lines are fits to the G-V curves using the Woodhull equation. The leftward shift in the G-V curve corresponds to an approximately 15 fold increase in intracellular spermine concentration. F shows the I-V curves for $\alpha 3_{E240A}\beta 4$ receptors before and after spermine injection. Similar to $\alpha 4_{E245A}\beta 2$ receptors, there was no significant difference between the IV-curves before and after injection of spermine

quantify the effect of increasing intracellular spermine, we fit the G-V curves to a Boltzmann equation (Eq. 3, see methods) and determined $V_{1/2}$, the V_m where G was reduced to 50% of G_{max} , and k, the amount of depolarization needed to change the conductance e-fold. For $\alpha 4\beta 2$, $V_{1/2}$ was shifted to left by 16 ± 1.3 mV after spermine injection and for $\alpha 3\beta 4$, $V_{1/2}$ was shifted to the left by 19 ± 2.4 mV; k decreased from 14.5 ± 1.2 to 12 ± 1.5 mV for both $\alpha 4\beta 2$ and $\alpha 3\beta 4$.

To estimate the concentration of free spermine in oocytes after injection, we used the Woodhull equation (Eq. 1, see methods). Using values for k_{d0} , and δ for $\alpha 4\beta 2$ (Haghighi and Cooper, 1998) and $\alpha 3\beta 4$ (Fig. 1), we solved the Woodhull equation to estimate the free intracellular spermine concentrations [S] that best described the macroscopic G-V curves. The solid lines in figure 4B & 4E represent the best fits to the Woodhull equation. Before spermine injections, [S] ranged from 70-80 μ M in different oocytes (75.6 ± 1.6 μ M, $n=37$). For the oocyte expressing $\alpha 4\beta 2$ receptors shown in 4B, injecting spermine increased [S] roughly 10 fold; for the oocyte expressing of $\alpha 3\beta 4$ receptors shown in 4E, spermine injection increased [S] by approximately 15 fold. On average, spermine injection increased [S] by 10.1 ± 1.7 fold ($n=19$). These results indicate that raising free intracellular spermine levels leads to stronger inward rectification of $\alpha 4\beta 2$ and $\alpha 3\beta 4$ receptors, providing further evidence that inward rectification of neuronal nAChRs results from a voltage-dependent block by intracellular spermine (Haghighi and Cooper, 1998).

Next, we investigated whether increased intracellular free spermine would be sufficient to confer inward rectification to ACh-evoked currents for the intermediate ring mutant receptors. Figure 4 shows example I-V curves for $\alpha 4_{E245A}\beta 2$ (4C) and $\alpha 3_{E240A}\beta 4$ (4F) receptors before and after spermine injection. Increasing intracellular spermine caused no significant shift in the ACh-evoked I-V or G-V curves for either receptor. Furthermore, increasing intracellular spermine had no effect on the ACh-evoked current amplitudes or the reversal potential (Fig. 4C&4F). We observed

similar results from 26 out of 26 oocytes. These results suggest that the reduction in the net negative charge at the intermediate ring dramatically decreases the affinity of intracellular polyamines for the receptor.

Extracellular spermine blocks non-rectifying mutant receptors

To determine whether the intermediate ring mutations affected polyamine permeability, we carried out ion substitution experiments. We expressed $\alpha_{4E245A}\beta_2$ receptors in *Xenopus* oocytes and then measured ACh-evoked currents in the extracellular solution containing different concentrations of spermine. With spermine as the only conducting ion in the extracellular solution, this mutant receptor failed to produce detectable ACh-evoked currents, even at -120 mV holding potential (data not shown). With an extracellular solution containing 90 mM Na⁺ and 10 mM spermine, we found that spermine blocked over 95% of the ACh-evoked current without affecting the reversal potential. We found that the block by extracellular spermine had little voltage-dependence and reversed relatively slowly (~80% in 3-5 min). These results suggest that spermine has negligible permeability through $\alpha_{4E245A}\beta_2$ receptors. To examine the block by extracellular spermine, we measured ACh-evoked currents at 3 minute intervals upon co-application of 1 μ M ACh with increasing concentrations of spermine. Figure 5A shows the spermine inhibition curves for $\alpha_4\beta_2$ and $\alpha_{4E245A}\beta_2$ receptors; by first approximation, these curves can be described by a logistic equation (Eq. 4). From the spermine inhibition curves, we obtained the IC₅₀ for mutant $\alpha_{4E245A}\beta_2$ receptors (62.3 ± 13.3 μ M, n=6) and wild-type $\alpha_4\beta_2$ receptors (42.8 ± 5.7 μ M, n=8), which were not significantly different ($P > 0.05$).

We repeated these measurements on wild-type $\alpha_3\beta_4$ receptors and mutant $\alpha_{3E240A}\beta_4$ (Figure 5B). We observed no significant difference in the spermine inhibition curves between wild-type $\alpha_3\beta_4$ (IC₅₀ = 45.1 ± 7.2 μ M, n=5) and mutant $\alpha_{3E240A}\beta_4$ receptors (IC₅₀ = 65.4 ± 12.3 μ M, n=5) (Figure 5B). We observed similar

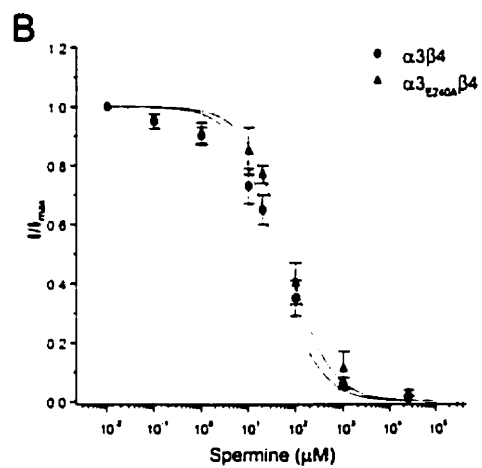
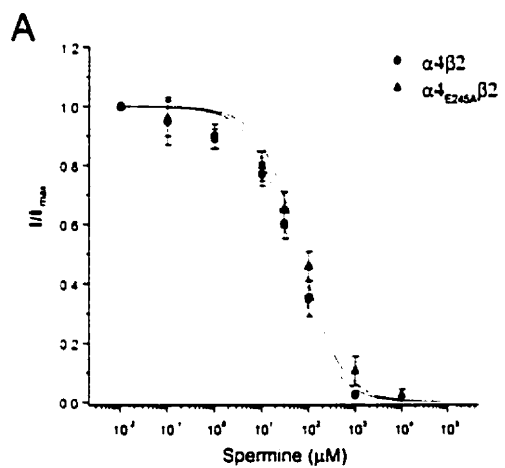


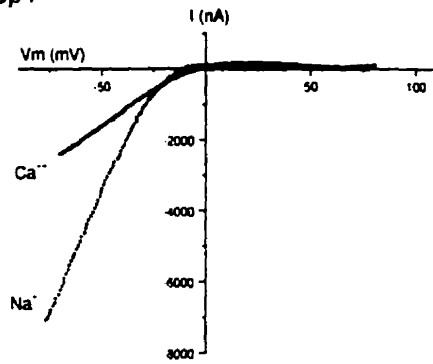
Figure 3.5. Extracellular spermine blocks non-rectifying mutant receptors. A shows the dose-inhibition curves for the effect of extracellular spermine on $\alpha 4\beta 2$ and $\alpha 4_{E245A}\beta 2$, and B shows the dose-inhibition curves for $\alpha 3\beta 4$ and $\alpha 3_{E240A}\beta 4$. Data points were fitted to a logistic equation (see methods). There is no significant difference in the block by extracellular spermine for all four receptors.

block by extracellular spermine for $\alpha 3_{E240Q}\beta 4$ and $\alpha 3\beta 4_{E239A}$ (data not shown). The cytoplasmic ring mutant, $\alpha 3_{D237A}\beta 4_{D236A}$, was also blocked by extracellular spermine in a similar manner ($IC_{50} = 43.8 \pm 4.9 \mu M$, $n=5$; data not shown). These results indicate that mutations in the intermediate ring that abolish inward rectification have little effect on the block by extracellular spermine.

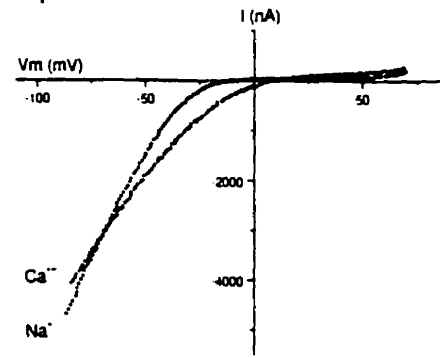
Relative calcium permeability

The Ca^{++} to Na^{+} permeability ratios (P_{Ca}/P_{Na}) for neuronal nAChRs have been reported to range from 0.7 to 10 depending on the subunit composition of the receptors (Sands and Barish, 1991; Adams and Nutter, 1992; Trouslard et al., 1993; Bertrand et al., 1993). As the intermediate ring has been shown to influence permeability of cations (Konno et al., 1991; Galzi et al., 1992; Corringer et al. 1999), we compared P_{Ca}/P_{Na} among wild-type and mutant $\alpha 4\beta 2$ and $\alpha 3\beta 4$ receptors expressed in *Xenopus* oocytes. To avoid contaminating ACh-evoked currents with the endogenous Ca^{++} -activated chloride currents in these cells (Miledi and Parker, 1984), we injected oocytes with BAPTA prior to our electrophysiological measurements (see methods). In figure 6A, we recorded the ACh-evoked I-V curve from $\alpha 3\beta 4$ receptors in control external solution (98 mM Na^{+} , 2 mM K^{+} and 1 mM Ca^{++}) and repeated the measurement in a solution containing equimolar Ca^{++} . In 100 mM Ca^{++} , we observed a rightward shift in the reversal potential of 3.6 mV. From the modified GHK equation (Eq. 5; Lewis et al., 1979; see methods), we obtained an average P_{Ca}/P_{Na} of 0.78 ± 0.02 for $\alpha 3\beta 4$ receptors ($n=8$)(see table 1). We observed that the macroscopic ACh-evoked current from $\alpha 3\beta 4$ receptors was reduced by 60-70% when we switched to 100 mM external Ca^{++} ; this observation is consistent with the decrease in single channel conductance for neuronal nAChRs when Ca^{++} is the main charge carrier (Adams and Nutter, 1992; Mulle et al., 1992; Vernino et al., 1992). We repeated these experiments with external solutions of either 10 mM Ca^{++} and 90 mM Na^{+} , 25 mM

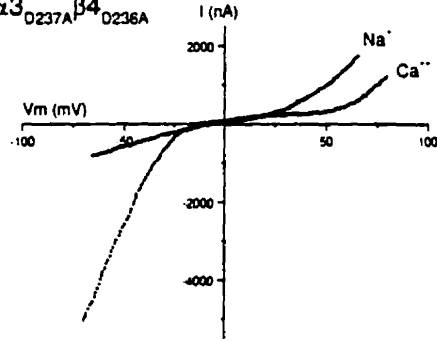
A $\alpha 3\beta 4$



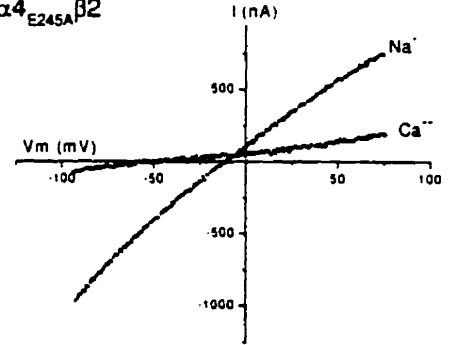
B $\alpha 4\beta 2$



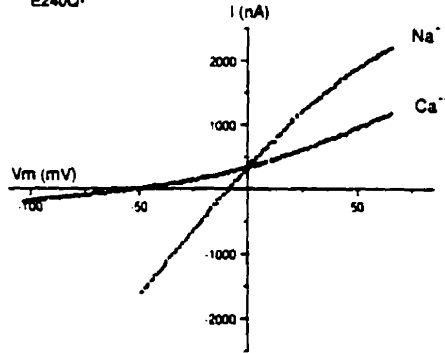
C $\alpha 3_{D237A}\beta 4_{D236A}$



D $\alpha 4_{E245A}\beta 2$



E $\alpha 3_{E240Q}\beta 4$



F $\alpha 3\beta 4_{E239A}$

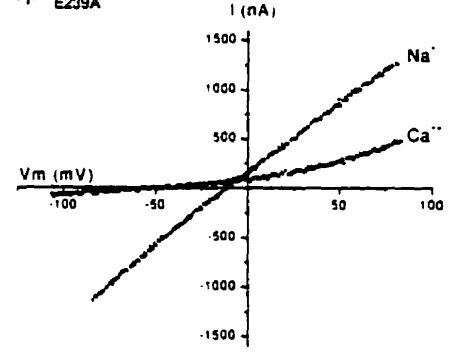


Figure 3.6. Substitution of the negatively charged residues of the intermediate ring with neutral amino acids drastically reduces Ca^{++} permeability of $\alpha 4\beta 2$ and $\alpha 3\beta 4$ receptors. A and B show I-V curves for $\alpha 4\beta 2$ and $\alpha 3\beta 4$ receptors expressed in *Xenopus* oocytes, respectively. Switching from the control solution to one containing 100 mM Ca^{++} causes a rightward shift of the reversal potential for both receptors. C shows ACh-evoked I-V curves for the mutant $\alpha 3_{D237A}\beta 4_{D236A}$ receptor in the presence of the control solution and one containing 100 mM Ca^{++} . Switching to 100 mM Ca^{++} causes a rightward shift of the reversal potential, similar to that observed for $\alpha 3\beta 4$ wild type receptor. D, E and F show I-V curves for $\alpha 4_{E245A}\beta 2$, $\alpha 3_{E240Q}\beta 4$ and $\alpha 3\beta 4_{E239A}$, respectively. Switching to 100 mM Ca^{++} causes a significant leftward shift in the reversal potential for all three receptors, indicating low relative Ca^{++} permeability for these receptors.

Ca^{++} and 75 mM Na^+ , or 50 mM Ca^{++} and 50 mM Na^+ . We found that $P_{\text{Ca}}/P_{\text{Na}}$ for $\alpha 3\beta 4$ in all 3 solutions ($n=4$ at each concentration) was not significantly different from that when we made equimolar substitutions of Na^+ and K^+ with Ca^{++} ; however, we only observed a significant reduction of ACh-evoked currents when Ca^{++} in the external solutions was greater than 25 mM (data not shown).

We also measured $P_{\text{Ca}}/P_{\text{Na}}$ for $\alpha 4\beta 2$ receptors (Fig. 6B). Upon switching the control external solution to 100 mM Ca^{++} , we observed an average rightward shift in the reversal potential of 15.5 ± 0.28 mV ($n=8$); from the GHK equation we calculated an average $P_{\text{Ca}}/P_{\text{Na}}$ of 1.65 ± 0.15 for $\alpha 4\beta 2$ receptors ($n=8$), roughly twice that for $\alpha 3\beta 4$ receptors (Table 1). We repeated these experiments with an external solution of 10 mM Ca^{++} and 90 mM Na^+ and found similar values for $P_{\text{Ca}}/P_{\text{Na}}$ ($n=6$). Consistent with the higher value for $\alpha 4\beta 2$, we found that we needed to pre-inject greater amounts of BAPTA to ensure that we did not activate Ca^{++} -activated chloride currents.

Next, we investigated whether mutations of negatively charged residues at the cytoplasmic and intermediate ring alter the relative calcium permeability of $\alpha 4\beta 2$ and $\alpha 3\beta 4$ receptors. Upon switching the control external solution to 100 mM Ca^{++} , we observed a rightward shift in the reversal potential for $\alpha 3_{\text{D237A}}\beta 4_{\text{D236A}}$ receptors similar to that for $\alpha 3\beta 4$ (Fig. 6C & table 1). We obtained similar results in 6/6 oocytes expressing $\alpha 3_{\text{D237A}}\beta 4_{\text{D236A}}$ receptors (Table 1). These results indicate that the negatively charged residues of the cytoplasmic ring have little influence on calcium permeability.

We tested whether mutations of charged residues at the intermediate ring alter calcium permeability by measuring $P_{\text{Ca}}/P_{\text{Na}}$ for mutant $\alpha 3_{\text{E240A}}\beta 4$, $\alpha 3_{\text{E240Q}}\beta 4$, $\alpha 3\beta 4_{\text{E239A}}$ and $\alpha 4_{\text{E245A}}\beta 2$ receptors. Fig. 6D, E & F show example I-V curves for $\alpha 3_{\text{E240Q}}\beta 4$, $\alpha 3\beta 4_{\text{E239A}}$ and $\alpha 4_{\text{E245A}}\beta 2$ receptors with either Na^+ or Ca^{++} as the main charge carrier. Upon substituting Na^+ and K^+ in the external solution with 100 mM

Ca^{++} , we observed a significant leftward shift in the I-V curves for all 4 intermediate ring mutant receptors (see table 1). Using the GHK equation (Eq. 4), we calculated that these intermediate ring mutations reduced $P_{\text{Ca}}/P_{\text{Na}}$ by 13-18 fold for $\alpha 3\beta 4$ receptors and more than 25 fold for $\alpha 4\beta 2$ receptors (Table 1). Our results indicate that the negatively charged residues of the intermediate ring constitute a common site that governs both inward rectification and Ca^{++} permeability of $\alpha 3\beta 4$ and $\alpha 4\beta 2$ nAChRs.

DISCUSSION

Interaction between polyamines and neuronal nAChRs

Our results add to our previous findings that strong inward rectification of neuronal nAChRs results from a voltage-dependent block by intracellular polyamines (Haghighi and Cooper, 1998). We show that $\alpha 3\beta 4$ receptors have a $K_{d(0)}$ for intracellular spermine of $6.7 \mu\text{M}$, similar to the $K_{d(0)}$ for $\alpha 4\beta 2$ receptors ($3.6 \mu\text{M}$). Normally, vertebrate cells have free intracellular spermine concentrations of $50\text{-}100 \mu\text{M}$ (Seiler and Schmidt-Glenewinkel, 1975; Watanabe et al., 1991; Ficker et al., 1994); this is more than sufficient to block these neuronal nAChRs. Furthermore, we show that increasing free spermine concentrations 10-15 fold increases this rectification by shifting the G-V curves towards more hyperpolarized potentials. These results provide further evidence that inward rectification of neuronal nAChRs results from a voltage-dependent block by intracellular polyamines (Haghighi and Cooper, 1998).

We find that mutating the negatively charged glutamic acid residues of the intermediate ring removes rectification of $\alpha 4\beta 2$ and $\alpha 3\beta 4$ receptors. This is also the case for homomeric $\alpha 7$ receptors (Forster and Bertrand, 1995). The I-V curves of mutant $\alpha 4_{E245A}\beta 2$, $\alpha 3_{E240A}\beta 4$ and $\alpha 3\beta 4_{E239A}$ receptors are essentially linear, showing very little voltage-dependence. Mutating the glutamic acid to either an alanine or glutamine in $\alpha 3$ abolishes inward rectification, indicating that the charge and not the size or polarity of the amino acid side chains determines inward rectification.

As $\alpha 4\beta 2$ and $\alpha 3\beta 4$ receptors have pentameric structures composed of two α subunits and three β subunits (Cooper et al., 1991), we took advantage of this known subunit stoichiometry to investigate the number of negatively charged residues in the intermediate ring necessary for inward rectification. We demonstrate that mutating

the negatively charged glutamic acid at the intermediate ring of either the α or the β subunit removes rectification of $\alpha 4\beta 2$ and $\alpha 3\beta 4$ receptors. Therefore, we conclude that removal of only two negative charges is sufficient to disrupt the interaction of intracellular polyamine.

To explain our results, we propose that the intermediate ring forms a high affinity binding site for intracellular polyamines; polyamines are attracted to this site under the influence of the membrane electrical field and are held there through an electrostatic interaction with the negatively charged glutamic acids. Since the intermediate ring is at the narrowest part of the pore (Wilson and Karlin, 1998), polyamines at this site occlude the pore preventing the flow of ions.

Our model assumes that polyamines have negligible permeation through the pore. Consistent with this, our experiments on the effects of extracellular polyamines indicate that polyamines permeate the channel very poorly. We find that extracellular spermine blocks $\alpha 4_{E245A}\beta 2$, $\alpha 3_{E240A}\beta 4$, $\alpha 3_{E240Q}\beta 4$ and $\alpha 3\beta 4_{E239A}$ receptors in a similar manner to wild-type receptors. At 70-80 μM , concentrations similar to that of the cytoplasm, spermine blocks more than 50% of the ACh-evoked current at all membrane potentials, and at 800-1200 μM spermine blocks 80-90% of the current. This indicates that spermine has difficulty crossing the pore and likely interacts with polar and non-polar amino acid side chains in M2 (Cu et al., 1998). If intracellular spermine could access the pore in the non-rectifying mutant receptors, we would expect it to block the channel, similar to extracellular spermine. However, even increasing intracellular spermine several fold had no effect on ACh-evoked I-V curve for the non-rectifying, intermediate ring mutant receptors. Therefore, it is likely that $\alpha 4_{E245A}\beta 2$, $\alpha 3_{E240A}\beta 4$, $\alpha 3_{E240Q}\beta 4$ and $\alpha 3\beta 4_{E239A}$ receptors do not rectify because the intermediate ring, with a lower net negative charge, no longer forms a high affinity binding site for polyamines.

The region between M1 and M2 has two rings of negatively charged residues; however, the intermediate ring appears to be the major site of interaction between intracellular polyamines and the pore. Removing the negative charges at the cytoplasmic ring of either the α or β subunit has no significant effect on inward rectification. Even receptors with mutations at the cytoplasmic ring of both α and β subunits inwardly rectify, although these receptors do conduct outward current at membrane potentials greater than +25 mV; this suggests that the cytoplasmic ring also interacts with intracellular polyamines. Since spermine is approximately 20 Å long (Araneda et al., 1999) and could span both rings, we speculate that the cytoplasmic ring helps stabilize polyamines at the mouth of the pore; without these five negatively charged residues, intracellular K⁺ ions destabilize the interaction of polyamines with the receptor at large depolarizations and flow out through the channel. This model has similarities to one proposed for polyamine block of AMPA receptors (Washburn, et al. 1997).

Comparison to AMPA/kainate receptors

Inward rectification of calcium permeable AMPA/kainate receptors is mediated by a voltage-dependent block by polyamines with a comparable $K_{d(0)}$ to heteromeric $\alpha 4\beta 2$ and $\alpha 3\beta 4$ nAChR (Bowie and Mayer, 1995), suggesting that the underlying mechanisms are similar. However, there are a few important differences. These AMPA/kainate receptors conduct considerable outward current at depolarized potentials (from +50 to +100 mV) (Bowie and Mayer, 1995; Koh et al., 1995), whereas we observe very little outward current from $\alpha 4\beta 2$ and $\alpha 3\beta 4$ receptors at these potentials. Furthermore, non-rectifying AMPA/kainate receptors, whose subunits have undergone RNA editing substituting a glutamine (Q) to an arginine (R) in the pore region, are not blocked by extracellular spermine (Washburn and

Dingledine, 1996; Washburn et al., 1997; Bähring et al., 1997); in contrast, extracellular spermine blocks non-rectifying mutant $\alpha 4\beta 2$ and $\alpha 3\beta 4$ receptors. These differences may be explained, in part, by differences in the putative location of the high-affinity polyamine binding-site in the pore. For AMPA/kainate receptors, this site appears to be near the middle of the pore (Kuner et al., 1996; Washburn et al., 1997), while for neuronal nAChRs, this site is most likely at the cytoplasmic mouth of the pore (Imoto et al., 1988; Wilson and Karlin, 1998). Equally interesting, substituting two glutamic acid residues with glutamines at the intermediate ring of neuronal nAChRs abolishes inward rectification, whereas glutamine residues make up the high-affinity polyamine site in rectifying AMPA/kainate receptors. If the high-affinity binding of polyamines to the receptor results from electrostatic interactions, this suggests that the geometry of the high-affinity polyamine site in AMPA/kainate receptors and neuronal nAChRs is different.

A common site affects both inward rectification and calcium permeability

For AMPA/kainate receptors, there is a strong correlation between calcium permeability and inward rectification (Verdoorn et al., 1991; Hume et al., 1991; Dingledine et al., 1999). This correlation holds true for nAChRs as well. Muscle nAChRs, which rectify slightly, have low calcium permeability (Adams et al., 1980; Villarroel and Sakmann, 1996), whereas neuronal nAChRs, which show strong inward rectification, have high calcium permeability (McGehee and Role, 1995). Calcium permeability of nAChRs appears to be influenced by residues in the M2 as well as residues in the intermediate ring (Bertrand et al., 1993; Villarroel and Sakmann, 1996). Our results on relative calcium permeability for $\alpha 4\beta 2$ and $\alpha 3\beta 4$ receptors are consistent with this. Our ion substitution experiments indicate that P_{Ca}/P_{Na} is 1.65 for $\alpha 4\beta 2$ receptors and 0.8 for $\alpha 3\beta 4$ receptors; the amino acid

differences in the M2 between these receptors likely underlie the differences in Ca^{++} permeability.

In addition, we show that partial removal of negative charges in the intermediate ring reduces $P_{\text{Ca}}/P_{\text{Na}}$ by approximately 15 fold for $\alpha 3\beta 4$ and 25 fold for $\alpha 4\beta 2$ receptors. We observe similar reduction in $P_{\text{Ca}}/P_{\text{Na}}$ when we substitute glutamic acid residues by either alanine or glutamine residues in the intermediate ring; this indicates that the reduction in calcium permeability is caused by a change in net negative charge of the intermediate ring and not by alteration in the size or polarity of the amino acid side chains. We find that substituting all five negatively charged residues with neutral residues at the cytoplasmic ring has no effect on $P_{\text{Ca}}/P_{\text{Na}}$, further demonstrating the important role of the intermediate ring in determining calcium permeability. Therefore, a common structural element of neuronal nAChRs governs both interaction with intracellular polyamines and high calcium permeability.

Physiological implications

In the CNS, many neuronal nAChRs are located at presynaptic nerve terminals (MacDermott et al., 1999). Given the small size and high input impedance of nerve terminals together with the relatively large single channel conductance of neuronal nAChRs, activation of only a few nAChRs would likely trigger action potentials in the terminal and evoke transmitter release. Support for this idea comes from studies on adrenal chromaffin cells, a model for transmitter release, where activation of a single nAChR is sufficient to evoke action potentials (Fenwick et al., 1982). In the absence of inward rectification, the ACh-evoked conductance in the terminal would act to shunt the action potential, preventing it from reaching its full amplitude. Considering the steep relationship between presynaptic depolarization and transmitter release, a reduction in action potential amplitude in the terminal would severely affect

release. To ensure that the action potential reaches its full amplitude, intracellular polyamines rapidly block neuronal nAChRs by interacting with the intermediate ring in a voltage-dependent manner.

In this study, we provide a molecular understanding of inward rectification of neuronal nAChRs and establish a link between two important physiological properties of these receptors, calcium permeability and inward rectification. By linking these two properties through a common structural element, neuronal nAChRs limit the inflow of calcium into the cell, thereby preventing excitotoxicity. Equally important, small depolarizations from rest can lead to screening of the negative charges at the intermediate ring by intracellular polyamines thereby modulating calcium inflow through these receptors.

CHAPTER 4

**A Phenylalanine In The M2 Of β 4 Neuronal nAChR Subunit
Governs Gating Kinetics And Influences The Block By Extracellular
Polyamine-Related Joro Spider Toxin**

ABSTRACT

Polyamines exert a variety of inhibitory, excitatory and modulatory actions on a number of cation selective ion channels. Previously, we have demonstrated that intracellular polyamines block neuronal nicotinic receptors with high affinity and in a voltage dependent manner, resulting in inward rectification of ACh-evoked currents. Extracellular polyamines also block neuronal nAChRs but with lower affinity and little voltage dependence. Polyamine-like structures are found in a variety of insect toxins including the Joro spider toxin (JSTX) and the digger wasp toxin philanthotoxin (PhTX). These toxins exert potent blocking effects on a number of ionotropic glutamate receptors. Little is known about the mechanism of interaction of extracellular polyamines and polyamine-related toxins with neuronal nAChRs and the structural domain(s) of the receptor involved in this interaction. Our hypothesis is that polyamine-related toxins also block neuronal nAChRs by interacting with residues in the conducting pathway of the receptor. To test this hypothesis we used two recombinant neuronal nAChR subtypes $\alpha 3\beta 4$ and $\alpha 4\beta 2$ expressed in *Xenopus* oocytes. Using the two-electrode voltage-clamp technique, we found that JSTX blocks both receptors with high affinity and in a use-dependent manner. Dose-inhibition curves for $\alpha 3\beta 4$ and $\alpha 4\beta 2$ indicates that JSTX has a higher sensitivity for $\alpha 3\beta 4$ ($IC_{50} = 8.5 \pm 0.25$ nM) than that for $\alpha 4\beta 2$ receptors ($IC_{50} = 45 \pm 2.3$ nM). We further show that a phenylalanine residue (F) in the second transmembrane domain (M2) of $\beta 4$ ($\beta 4F253$) underlies this difference. Mutation of this residue to a valine (V) causes a decrease in sensitivity to JSTX in $\alpha 3\beta 4$ receptors. This change in JSTX sensitivity correlates with a decrease in the single channel burst duration of $\alpha 3\beta 4_{F253V}$ compared to that of $\alpha 3\beta 4$ receptors. Therefore, we propose that longer channel openings allow a more effective block by JSTX, consistent with the use-dependent nature of this block.

INTRODUCTION

A growing body of evidence implicates cation-selective neurotransmitter-gated ion channels as important targets for extracellular polyamines under both physiological and pathophysiological conditions (Scott et al., 1993; Bowie et al., 1998). One of the earliest studies on the physiological action of spermine demonstrated that elevated levels of extracellular spermine have adverse effects on the autonomic nervous system (Dixon, 1900), suggesting a possible action on postganglionic nicotinic acetylcholine receptors (nAChRs). Recently, we have shown that extracellular spermine blocks neuronal nAChRs as an open channel blocker at μM concentrations. Furthermore, polyamine-related toxins, Philanthotoxin and Joro spider toxin (JSTX) block ACh-evoked currents on PC12 cells (Liu et al., 1997). The purpose of this study is to learn more about the structural elements of neuronal nAChRs that determine the block by these toxins.

Nicotinic receptors have a pentameric structure; each subunit has a structural motif consisting of 4 hydrophobic domains (Karlin and Akabas, 1995). The second hydrophobic domain, M2, of each nAChR subunit forms part of the ion channel pore and three ring-like accumulations of charged amino acids (extracellular, cytoplasmic and intermediate rings) neighbouring M2 affect ion transport through the pore (Imoto et al., 1988; Cooper et al., 1991). The intermediate ring is located near the gate of the receptor and is a major determinant of ion selectivity of the receptor (Konno et al., 1991; Wang and Imoto, 1988). Recently, we have demonstrated that the intermediate ring also forms a high-affinity binding-site for intracellular polyamines. Upon depolarization, polyamines, acting as gating molecules, block the pore, leading to inward rectification (Haghighi and Cooper, 1998). Partial removal of the negatively charged residues at the intermediate ring abolishes both inward rectification and calcium permeability of the receptor without affecting the block by extracellular spermine (Haghighi and Cooper, unpublished). This suggests that spermine, like the

non-competitive antagonists QX-222 and CPZ (Charnet et al., 1990; Revah et al., 1990), blocks within the pore of the receptor and does not access the intermediate ring.

We hypothesize that JSTX blocks both rectifying wild type and non-rectifying mutant neuronal nAChRs with high affinity, and that the negatively charged residues of the intermediate ring have no influence on this block. To test this hypothesis, we examined the blocking effect of JSTX on ACh-evoked currents from recombinant $\alpha 4\beta 2$ receptors, composed of two subunits abundantly expressed in the CNS. In addition, we examined $\alpha 3\beta 4$ receptors, composed of two subunits abundantly expressed in the PNS, in part, because $\alpha 3\beta 4$ receptors are different from $\alpha 4\beta 2$ receptors in the M2 region. $\alpha 3$, $\alpha 4$ and $\beta 2$ subunits contain a highly conserved valine (Val) residue ($\alpha 3V254$) in the M2, while $\beta 4$ (for human, mouse, rat, monkey but not chick) contains a phenylalanine (Phe) residue at the corresponding position ($\beta 4F253$). We found that JSTX blocks both $\alpha 3\beta 4$ and $\alpha 4\beta 2$ at nanomolar concentrations, with five fold higher affinity for $\alpha 3\beta 4$. The non-rectifying intermediate ring mutant receptor $\alpha 3_{E239A}\beta 4$ showed similar sensitivity to the block by JSTX, compared to wild-type $\alpha 3\beta 4$ receptors. Moreover, substitution of F253 with Val in $\beta 4$, caused a decrease in the sensitivity of the receptor to JSTX. Our results indicate that neuronal nAChRs are targets for polyamine-related toxins and that this block is mediated by residues in the M2 region.

METHODS and MATERIALS

Site-directed mutagenesis

We used the Quick-Change Site-Directed Mutagenesis Kit (Stratagene, La Jolla, USA) to construct the mutant $\beta 4$ subunit, ($\beta 4_{F254V}$). We designed two complementary oligonucleotide primers containing the substituted nucleotide changing phenylalanine at position 254 of $\beta 4$ to valine ($\beta 4_{F254V}$). For the mutation reaction, we mixed 5-50 ng of the wild-type $\beta 4$ plasmid and 125 ng of each of the two primers in a solution containing 5 μ l of 10x reaction buffer (Stratagene), 1 μ l dNTP mix (Stratagene) and 1 μ l Pfu DNA polymerase (2.5 U/ml, Stratagene), diluted with double-distilled water to a final volume of 50 μ l. The reaction mixture was then cycled in a PCR apparatus (PTC-100, MJ Research Inc., MA, USA) according to the following protocol: 1 cycle at 95°C for 30 s followed by 12-18 cycles at 95°C for 30 s, 55°C for 1 min and 68°C for 2 min. $\alpha 4_{E242A}\beta 2$, $\alpha 3_{E240A}\beta 4$ and $\alpha 3_{E240Q}\beta 4$ were generated as described earlier (Haghighi and Cooper, 1999). All mutations were verified by sequencing.

Expression of nAChR subunit cDNAs in Oocytes

Xenopus oocytes were defolliculated and prepared as described by Bertrand et al. (1991). We injected 1-3 ng of pairwise combinations of cDNAs coding for neuronal nAChR. For intermediate mutant receptors, $\alpha 4_{E242A}\beta 2$, $\alpha 3_{E240A}\beta 4$ and $\alpha 3_{E240Q}\beta 4$, we injected 3-6 ng of each subunit to achieve sufficient levels of expression (Haghighi and Cooper, 1999). Oocytes were incubated at 19°C for 2-7 days before recording. For single channel experiments, the vitelline membrane surrounding the oocytes was removed.

Electrophysiology

Whole-cell recordings from oocytes: In order to measure the macroscopic ACh-evoked currents in oocytes, we used the two-electrode voltage clamp technique (Bertrand et al., 1991). These experiments were performed at room temperature (22-24°C) using a standard voltage-clamp amplifier (built by Mr. A. Sherman, McGill University). During the recordings, oocytes were superfused with control perfusion solution or agonist alone (or agonist plus blocker) solutions at 10-20 ml/min; switching from one solution to another was done manually. Recording electrodes had tip diameters of 10-15 μm and were filled with 3M KCl. All mutant receptors, $\alpha 3_{E240A}\beta 4$, $\alpha 3_{E240Q}\beta 4$, $\alpha 4_{E242A}\beta 2$ and $\alpha 3\beta 4_{F253V}$, produced ACh-evoked currents when expressed in *Xenopus* oocytes.

To measure the current-voltage (I-V) relationships, we used a voltage ramp protocol applied within 2-4 seconds after the inward current had reached its maximum amplitude; the speed of the ramp was 333 mV/s. Voltage ramps were applied for 360-600 ms (corresponding to 120-200 mV), during which time no significant desensitization was observed. I-V curves were also obtained by measuring the ACh-evoked currents at different membrane potentials (steady-state I-V curves). Both current and voltage traces were monitored and stored for analysis. Currents were sampled at 100-350 Hz on-line with a Pentium PC computer (running at 60 MHz and an A/D card; Omega, Stamford, CT). The program PATCHKIT (Alembic Software, Montreal) was used for stimulation and data acquisition.

External perfusion solution contained 96 mM NaCl, 2 mM KCl, 1 mM $\text{Na}_2\text{H}_2\text{PO}_4$, 1 mM BaCl_2 , 10 mM HEPES and 1 μM atropine; pH was adjusted with

NaOH to 7.4-7.5. For ion substitution experiments with monovalent organic cations, we measured ACh-evoked I-V curves in either 100 mM NaCl and 1mM BaCl or in a test solution containing the test cation (at concentrations indicated) and 1mM BaCl. All solutions were buffered by 10 mM HEPES and NaOH to a pH of 7.4-7.5 and contained 1 μ M atropine. Spermidine (Sigma), Putrescine (Sigma), TRIS hydrochloride (ICN, Canada), ethanolamine hydrochloride (Sigma) were freshly prepared and used at concentrations indicated. Jorotoxin (JSTX-3) (RBI) was dissolved in distilled water and kept frozen before use.

Single channel recordings from oocytes: Only oocytes that gave rise to large inward currents ($>1\mu$ A in response to 1μ M ACh for $\alpha 4\beta 2$ expressing oocytes) were used for single channel recordings. Outside-out recordings were carried out using a List EPC-7 amplifier at room temperature (22-24°C) (Hamill et al., 1981). Pipette resistance ranged from 5-10 M Ω for outside-out recordings, and electrodes were coated with Sylgard (Dow Corning). Recordings were obtained in the continuous presence of ACh (0.1-0.2 μ M for $\alpha 4\beta 2$ receptors and 1-10 μ M for $\alpha 3\beta 4$) in the recording bath. ACh-evoked single channel activity gradually diminished after excision of the patch (in 2-5 min). Signals were digitized with a PCM (501, Sony) and stored on VCR tapes. For off-line analysis, stored signals were filtered at 1.5-2kHz with an eight-pole Bessel filter (Frequency Devices Inc.) and sampled at 10 kHz using a Pentium-60 PC computer. The program PATCHKIT was used for stimulation and data acquisition.

External solution contained 85 mM KCl, 1 mM CaCl₂, 10 HEPES and 1 μ M atropine, and pH was 7.4 adjusted with KOH. Recording electrodes contained 65 mM KF, 20 mM potassium acetate, 10 mM HEPES and 10 mM EGTA and pH was adjusted to 7.4 with KOH. CsCl, NH₄Cl, NaCl and TRIS hydrochloride were used in the extracellular solutions as indicated.

Analysis

Whole-cell ACh-evoked I-V curves were obtained by subtracting the current in response to a ramp voltage change in the absence of agonist from that in the presence of agonist (see Haghghi and Cooper, 1998).

To measure the amplitude of single channel currents, we used either all-points histograms of open and closed distributions, or measured the amplitude of the channel openings individually using PATCHKIT. Histograms were fit by Gaussian curves using Origin 4.1 graphics software (MICROCAL™ Software, Inc.). Mean burst durations were calculated by averaging the burst durations from 50-200 bursts. The open time was measured by eye using Patchkit software.

In order to calculate the relative permeability of monovalent cations to that of Na⁺ (P_X/P_{Na}), we measured the reversal potential of the I-V curves in external solutions containing different monovalent cations as the main charge carrier and used a derivative of the Goldman, Hodgkin and Katz constant field voltage equation (Adams et al., 1980):

$$E_{rev(X)} - E_{rev(Na)} = RT/F \ln \{ (P_X [X]_o) / (P_{Na} [Na]_o) \} \quad (1)$$

where P_X is the permeability coefficient of ion X , $[X]_o$ is the extracellular concentration of ionic specie X , and R , T and F have their usual meanings.

To measure the relative permeability of divalent putrescine to that on Na⁺, we used a derivation of the Goldman, Hodgkin and Katz constant field voltage equation for divalent cations as presented by Lewis (1979):

$$E_{rev(Put)} - E_{rev(Na)} = RT/F \ln \{ ([Na]_o + P_K/P_{Na} [K]_o + 4P'_{Put}/P_{Na} [Put]_o) / ([Na]_i + P_K/P_{Na} [K]_i + 4P'_{Put}/P_{Na} [Put]_i) \} \quad (2)$$

where

$$P'_{Put} = P_{Put} / (1 + \exp(E_{rev(Put)} F/RT))$$

and P_{Put} is the permeability coefficient of putrescine, $[Put]_o$ is the extracellular concentration of putrescine; R , T and F have their usual meanings. P_K/P_{Na} was obtained from single channel measurements (Fig. 1A, see above).

Single channel IV-curves were fit to a 3rd order polynomial function and reversal potentials were measured by eye. We compensated for junction potentials caused by switching between different solutions.

To measure the effect of putrescine on the voltage-dependence of inward rectification, we fit the macroscopic G-V curves to the Boltzman equation:

$$G/G_{max} = 1 / \{ 1 + (\exp((V - V_{1/2})/k)) \} \quad (3)$$

where $V_{1/2}$ is the membrane potential at which conductance (G) is reduced to half of the maximum conductance (G_{max}) and k is a slope factor corresponding to the amount of depolarization needed to change the conductance e-fold.

Dose response curves for the blocking effect of JSTX were fit to a derivation of the logistic equation:

$$I/I_{max} = 1 / \{ 1 + (IC_{50}/[J]) \} \quad (4)$$

where IC_{50} is the half maximal inhibition dose, and $[J]$ is the concentration of JSTX.

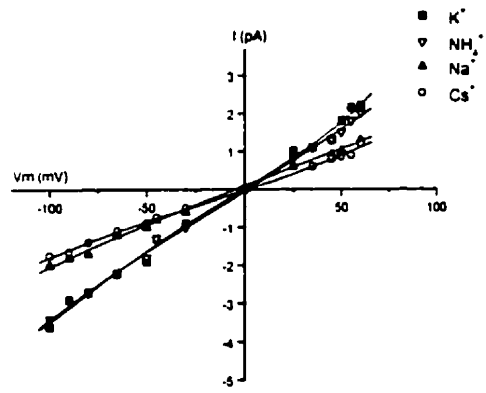
The best fit to the data was achieved by minimizing χ^2 using a routine from Origin 4.1 graphics software that is based on a Levenberg-Marquardt algorithm. All data points are presented as mean \pm standard error of the mean. Statistical significance between values was examined using the Student t test.

RESULTS

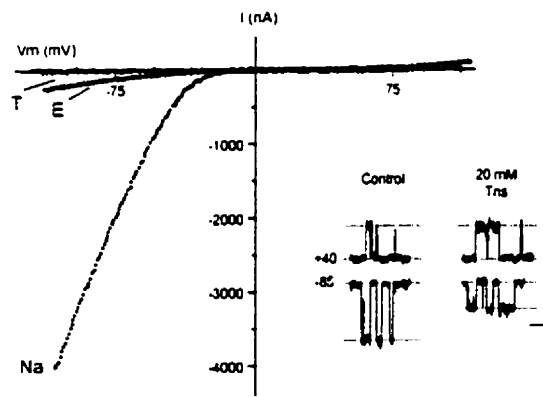
To examine the permeability of recombinant $\alpha 4\beta 2$ receptors for different organic cations, we conducted ion substitution experiments. We measured current-voltage relationships for ACh-evoked currents in different test solutions containing small monovalent cations. Like muscle nAChRs and native nAChRs on parasympathetic neurons, $\alpha 4\beta 2$ and $\alpha 3\beta 4$ receptors show little selectivity among small monovalent cations, Na^+ , K^+ , Cs^+ and NH_4^+ . Figure 1A shows single-channel I-V curves from $\alpha 4\beta 2$ receptors expressed in *Xenopus* oocytes measured in outside-out patches. The inward single channel conductance was largest with K^+ as the main charge carrier in the extracellular solution and smallest for Cs^+ according to the following sequence: K^+ (39pS) > NH_4^+ (34pS) > Na^+ (22pS) > Cs^+ (18pS). From the shift in the reversal potential, we calculated the relative permeability for these cations from the GHK equation (Adams et al. 1980; methods, Eq. 1): $P_{\text{Cs}}/P_{\text{Na}}$ (1.32 ± 0.12) \geq $P_{\text{NH}_4}/P_{\text{Na}}$ (1.3 ± 0.09) > $P_{\text{K}}/P_{\text{Na}}$ (1.2 ± 0.13). These values are consistent with those from native nAChRs on parasympathetic neurons (Nutter and Adams, 1995).

Next, we measured the relative permeability of $\alpha 4\beta 2$ to monovalent organic cations. Figure 1B shows the macroscopic ACh-evoked I-V curves for $\alpha 4\beta 2$ receptors expressed in an oocyte with TRIS, ethanolamine (etham) or Na^+ as the main charge carrier in the external solution. The ACh-evoked current measured in ethanolamine at -80 mV was less than 10% of the current in equimolar Na^+ , and the I-V curve was shifted 12.5 mV to the left. From the GHK equation, we calculated that $P_{\text{Etham}}/P_{\text{Na}}$ was 0.58 (± 0.04 , n=8). We obtained similar $P_{\text{Etham}}/P_{\text{Na}}$ when the external solution contained 40 mM ethanolamine and 60 mM Na^+ . This suggests that ethanolamine conducts slowly through the channel. Upon switching back to the external solution containing Na^+ , we found that the ACh-evoked current took 2-3 minutes to reverse the blocking effect of ethanolamine and return to control levels (data not shown). At the macroscopic level, we observed no detectable current upon

A



B



C

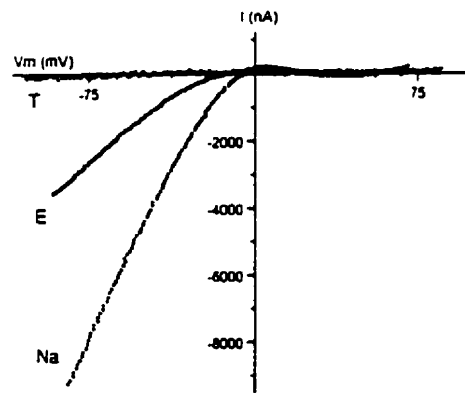


Figure 4.1. Permeability of neuronal nAChRs to monovalent alkali metals and organic cations. A, This figure shows single channel ACh-evoked I-V curves for $\alpha 4\beta 2$ neuronal nAChRs expressed in *Xenopus* oocytes recorded from outside out patches. I-V curves were measured in the presence of 85 mM Na^+ , K^+ , Cs^+ or NH_4^+ in the external solution (see methods) and 85 mM K^+ in the recording pipette. Compared to Na^+ all other cations caused a rightward shift of the I-V curve. Single channel conductance was highest for K^+ followed by NH_4^+ , Na^+ and Cs^+ . B, This figure shows macroscopic ACh-evoked I-V curves recorded from an oocyte expressing $\alpha 4\beta 2$ receptors. I-V curves were measured in the presence of control solution (Na), 100 mM TRIS (T) or 100 mM ethanolamine (E). Switching to ethanolamine caused a leftward shift in the I-V curve. Inward currents in the presence of ethanolamine as the main charge carrier were approximately 10% of those in the presence of Na^+ . No detectable currents were measured in the presence of TRIS as the main charge carrier. The inset shows single channel recordings from $\alpha 4\beta 2$ receptors in outside out patches. Switching from the control external solution (85 mM K^+) to one containing 85 mM K^+ and 20 mM TRIS caused a 50 % reduction in the single channel amplitude at -85 mV, without affecting the amplitude of the outward currents significantly. C, This figure shows macroscopic ACh-evoked I-V curves recorded from an oocyte expressing $\alpha 3\beta 4$ receptors. I-V curves were measured in the presence of control solution (Na), 100 mM TRIS (T) or 100 mM ethanolamine (E). Inward currents in the presence of ethanolamine as the main charge carrier were approximately 40% of those in the presence of Na^+ . Negligible inward currents were measured in the presence of TRIS as the main charge carrier.

switching to equimolar TRIS (Fig. 1B), suggesting that TRIS has negligible permeability through the receptor. To ensure that TRIS was not having an adverse effect on the receptor, we measured ACh-evoked single channel currents in outside-out patches in the presence 20 mM TRIS and 85 mM K⁺. Under these conditions we observed inward currents that were reduced 2-3 fold in amplitude compared to those in control solution with 85 mM K⁺; the outward currents appeared unaffected (Fig. 1B, inset). We observed no significant shift in the single channel I-V curve when 20 mM TRIS was added to the control solution (n=5).

Previously, we observed differences in the permeability for calcium between $\alpha 4\beta 2$ and $\alpha 3\beta 4$ receptors, therefore we tested the permeability of organic cations through $\alpha 3\beta 4$ receptors. Figure 1C shows the macroscopic ACh-evoked I-V curves for $\alpha 3\beta 4$ receptors expressed in an oocyte with TRIS, ethanolamine or Na⁺ as the main charge carrier in the external solution. We observed that the ACh-evoked current in ethanolamine at -80 mV was approximately 40% of the current in equimolar Na⁺, and the I-V curve was shifted 7.1 mV to the left. From the GHK equation (equation 1), we calculated that $P_{\text{Etham}}/P_{\text{Na}}$ was 0.78 (± 0.06 , n=11), 1.4 fold greater than that for $\alpha 4\beta 2$ receptors. Upon switching to equimolar TRIS (Fig. 1C), we observed that the ACh-evoked current at -80 mV was less than 1% of the current in equimolar Na⁺, and the I-V curve was shifted approximately 80 mV to the left, corresponding to a relative permeability of approximately 0.05 (± 0.01 , n=8). This indicates that $\alpha 3\beta 4$ receptors have a higher permeability to monovalent organic cations compared to $\alpha 4\beta 2$ receptors (P<0.05).

The intermediate ring of M2 affects the permeability of organic cations through muscle nAChRs (Konno et al., 1991; Wang and Imoto, 1992). Previously, we showed that negatively charged residues of the intermediate ring determine both inward rectification and calcium permeability of $\alpha 4\beta 2$ and $\alpha 3\beta 4$ receptors (Haghighi and Cooper, 1999). Therefore, we investigated the effects of the intermediate ring of

$\alpha 4\beta 2$ and $\alpha 3\beta 4$ receptors on TRIS and ethanolamine permeability. For these experiments, we examined 4 receptors in which the negatively charged glutamic acid residue (Glu, E) of the intermediate ring of the α subunit had been substituted with the neutral amino acids alanine (Ala, A) or glutamine (Gln, Q): $\alpha 3_{E240A}\beta 4$, $\alpha 3_{E240Q}\beta 4$ and $\alpha 4_{E245A}\beta 2$ (Haghighi and Cooper, 1999; see methods).

Figure 2A shows the macroscopic ACh-evoked I-V curves for $\alpha 3_{E240A}\beta 4$ receptors expressed in an oocyte with TRIS, ethanolamine or Na^+ as the main charge carrier in the external solution. Since $\alpha 3_{E240A}\beta 4$ receptors are non-rectifying, we could readily measure the outward current. This mutation increased the relative permeability of TRIS and ethanolamine through the receptor. Upon switching to an ethanolamine-containing solution, we observed a rightward shift in the ACh-evoked I-V curve of 4 mV, indicating a relative permeability of 1.17 (± 0.9 , $n=6$). Upon switching to a TRIS-containing solution, we observed a leftward shift in the ACh-evoked I-V curve of 40 mV, indicating a relative permeability of 0.20 (± 0.05 , $n=5$).

We also examined $\alpha 4_{E245A}\beta 2$ receptors. Figure 2C shows the macroscopic ACh-evoked I-V curves for $\alpha 4_{E245A}\beta 2$ receptors with TRIS, ethanolamine or Na^+ as the main charge carrier. Similar to $\alpha 3_{E240A}\beta 4$ receptors, switching to an ethanolamine-containing solution caused a rightward shift in the ACh-evoked I-V curve of 1 mV, indicating a relative permeability of 1.0 (± 0.02 , $n=5$). Upon switching to a TRIS-containing solution, we observed a leftward shift in the ACh-evoked I-V curve of 50 mV, indicating a relative permeability of 0.14 (± 0.04 , $n=5$). These results indicated that the intermediate ring plays a role in determining monovalent organic cation permeability for both $\alpha 3\beta 4$ and $\alpha 4\beta 2$ receptors.

Since both TRIS and ethanolamine are larger than Na^+ , the increase in $P_{\text{Etham}}/P_{\text{Na}}$ and $P_{\text{TRIS}}/P_{\text{Na}}$ is most likely due to the size of the amino acid side chain at the intermediate ring. Similar results have been reported for muscle nAChRs (Wang and Imoto, 1992). Since E and Q have side chains of similar size, we substituted E

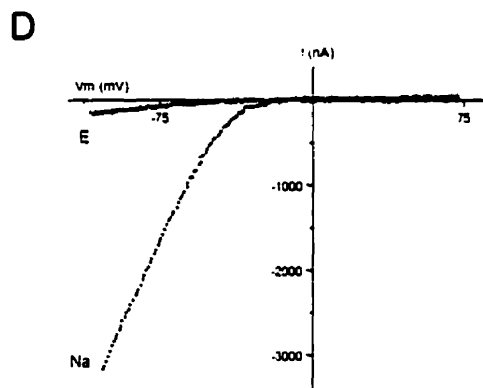
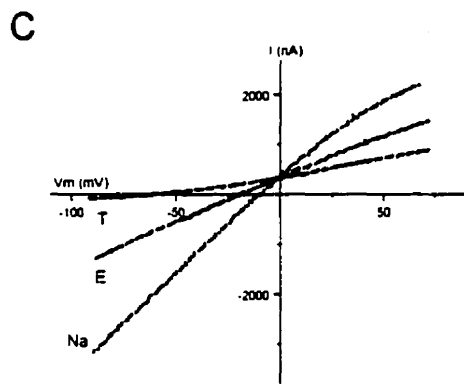
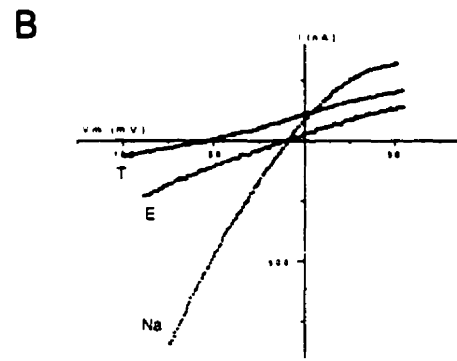
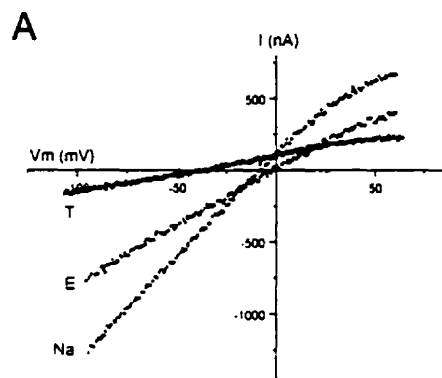


Figure 4.2. Amino acid side-chain at the intermediate ring influences the permeability of organic cations. A and B show macroscopic ACh-evoked I-V curves recorded in the presence of control solution (Na), 100 mM TRIS (T) or 100 mM ethanolamine (E) from $\alpha 3_{E240A}\beta 4$ and $\alpha 4_{E245A}\beta 2$ receptors, respectively. These mutations lead to removal of strong inward rectification (Haghighi and Cooper, 1999). Compared to wild type receptors, these mutant receptors showed larger conductance and higher permeability for ethanolamine and TRIS. C shows macroscopic ACh-evoked I-V curves recorded in the presence of control solution (Na), 100 mM TRIS (T) or 100 mM ethanolamine (E) for $\alpha 3_{E240Q}\beta 4$. In the presence of ethanolamine or TRIS, this receptor showed similar permeability and conductance to those for wild type $\alpha 3\beta 4$ receptors, suggesting that the side chain size at the intermediate ring affects the permeability of the receptor to organic cations. D, This figure shows macroscopic ACh-evoked I-V curves recorded in the presence of control solution (Na) or 100 mM ethanolamine (E) for $\alpha 3\beta 4_{F253V}$ mutant receptor. Switching from sodium to ethanolamine caused a decrease in inward conductance of about 90%, similar to the effect of ethanolamine on $\alpha 4\beta 2$ receptors. This suggests that F253 in the M2 of $\beta 4$ likely underlies the differences in permeability to organic cations between $\alpha 3\beta 4$ and $\alpha 4\beta 2$.

with Q in the intermediate of the $\alpha 3$ subunit and examined $P_{\text{Etham}}/P_{\text{Na}}$ and $P_{\text{TRIS}}/P_{\text{Na}}$ for $\alpha 3_{\text{E240Q}}\beta 4$ receptors. Figure 2B shows the ACh-evoked I-V curves for TRIS, ethanolamine or Na^+ as the main charge carrier in the external solution. We observed that both $P_{\text{Etham}}/P_{\text{Na}}$ ($.72 \pm .09$, $n=5$) and $P_{\text{TRIS}}/P_{\text{Na}}$ ($.078 \pm .013$, $n=4$) were smaller than those for $\alpha 3_{\text{E240A}}\beta 4$ receptors, and not significantly different from wild-type $\alpha 3\beta 4$ receptors. Unlike wild-type $\alpha 3\beta 4$ and $\alpha 4\beta 2$ receptors, $\alpha 3_{\text{E240A}}\beta 4$, $\alpha 3_{\text{E240Q}}\beta 4$ and $\alpha 4_{\text{E245A}}\beta 2$ receptors do not rectify and give rise to readily measurable outward ACh-evoked currents. We observed that the outward conductance of these receptors in both TRIS and ethanolamine was approximately 50% of the conductance measured in control external solution.

Our results indicate that when ethanolamine is the main charge carrier, $\alpha 3\beta 4$ receptors give rise to significantly larger conductance compared to $\alpha 4\beta 2$ receptors (Fig. 1A&B). The major difference in M2 between $\alpha 3\beta 4$ and $\alpha 4\beta 2$ receptors is at the position 254 where the $\beta 4$ subunit has a phenylalanine (Phe, F) and all other subunits have a valine (Val, V). To test whether the F253 in the M2 of $\beta 4$ underlies this difference, we mutated the F to V in $\beta 4$ and expressed $\alpha 3\beta 4_{\text{F253V}}$ receptors in *Xenopus* oocytes. Figure 2D shows the ACh-evoked I-V curve in control and upon switching to a solution with ethanolamine as the main charge carrier. The $P_{\text{Etham}}/P_{\text{Na}}$ for $\alpha 3\beta 4_{\text{F253V}}$ receptors ($.61 \pm .04$, $n=3$) was smaller than that for $\alpha 3\beta 4$ and similar to $\alpha 4\beta 2$ receptors: similarly, the relative $G_{\text{Etham}}/G_{\text{Na}}$ at -80 mV for $\alpha 3\beta 4_{\text{F253V}}$ receptors was 4 fold less than that for $\alpha 3\beta 4$ and not significantly different from $\alpha 4\beta 2$ receptors. This indicates that F₂₅₃ influences both the permeability and the rate of transport of ethanolamine through M2.

Differential permeability of divalent organic cations through $\alpha 3\beta 4$ and $\alpha 4\beta 2$ receptors

Next, we examined the relative permeability of putrescine, a ubiquitous divalent organic cation that is present at high concentrations in vertebrate cells and is a precursor to the formation of the polyamines, spermidine and spermine. Figure 3A shows the macroscopic ACh-evoked I-V curves for $\alpha 4\beta 2$ receptors expressed in an oocyte with putrescine or Na^+ as the main charge carrier. We observed small inward currents upon substitution to equimolar putrescine (Fig. 3A), suggesting that putrescine has negligible permeability through the receptor.

Since substituting E to A at the intermediate ring increased monovalent organic cation permeability, we investigated the effects of this mutation on putrescine permeability. Figure 3B shows the ACh-evoked I-V curves for non-rectifying $\alpha 4_{\text{E245A}}\beta 2$ receptors in the presence of either putrescine or Na^+ as the main charge carrier. In the presence of putrescine, we observed larger inward currents from $\alpha 4_{\text{E245A}}\beta 2$ receptors compared to those from wild-type $\alpha 4\beta 2$ receptors. Putrescine shifted the reversal potential by 60 mV to the left. From this shift, we calculated the $P_{\text{Put}}/P_{\text{Na}}$ for $\alpha 4_{\text{E245A}}\beta 2$ receptors using equation (2) (0.05 ± 0.02 , $n=6$).

We observed greater putrescine permeability for $\alpha 3\beta 4$ receptors. Figure 3C shows the ACh-evoked I-V curves with putrescine or Na^+ as the main charge carrier. In contrast, to $\alpha 4\beta 2$ receptors, $\alpha 3\beta 4$ has high permeability to putrescine: from the shift in the reversal potential of the I-V curves, we calculated that $P_{\text{Put}}/P_{\text{Na}}$ was 2.3 (± 0.2 , $n=5$). Putrescine also affected the voltage-dependence of inward rectification of $\alpha 3\beta 4$ receptors. To quantify this effect, we fit the macroscopic G-V curves to a Boltzmann equation (Eq. 3, methods); we found that in the presence of putrescine the amount of depolarization needed for an e-fold change in conductance was increased by 2 fold ($k=28 \pm 1.3$ ($n=5$) for putrescine vs $k=13 \pm 1.2$ ($n=26$) for Na^+). This indicates

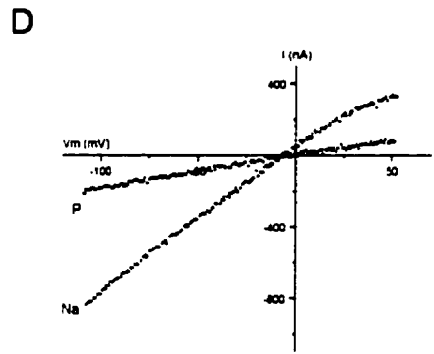
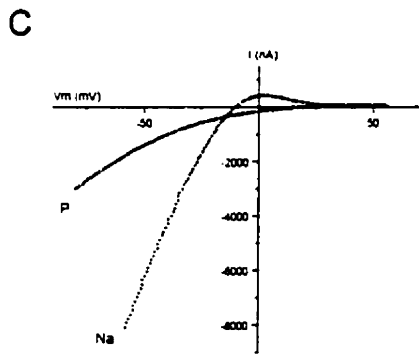
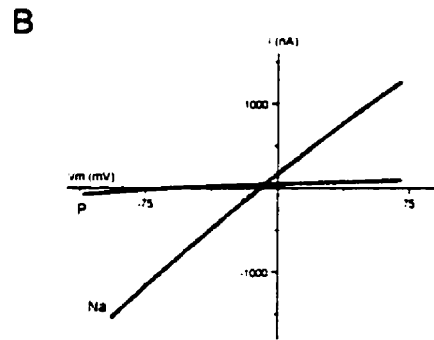
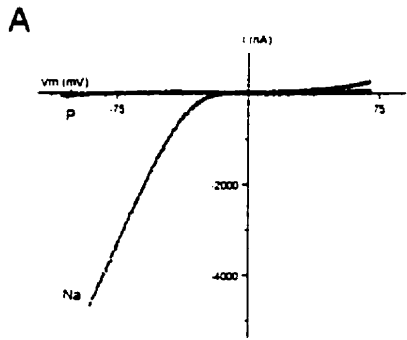


Figure 4.3. Putrescine has differential permeability through $\alpha 3\beta 4$ and $\alpha 4\beta 2$ receptors. A shows macroscopic ACh-evoked I-V curves recorded in the presence of control solution (Na) or 100 mM putrescine (P) for $\alpha 4\beta 2$ receptors. Putrescine has negligible permeability through this receptor. B shows macroscopic ACh-evoked I-V curves recorded in the presence of control solution (Na) or 100 mM putrescine (P) for $\alpha 4_{E245}\beta 2$ receptors. This receptor does permeate putrescine detectably; however, the inward currents were over 90% smaller in the presence of putrescine as compared to those in the presence of Na, suggesting a blocking effect by putrescine. C. This figure shows ACh-evoked I-V curves recorded in the presence of control solution (Na) or 100 mM putrescine (P) for $\alpha 3\beta 4$ receptors. These receptors readily permeate putrescine; the right ward shift in the I-V curve upon switching from Na^+ to putrescine indicates a high permeability to putrescine. D. This figure shows ACh-evoked I-V curves recorded in the presence of control solution (Na) or 100 mM putrescine (P) for $\alpha 3_{E240A}\beta 4$ receptors. These receptors also readily permeate putrescine; however, the shifts in the I-V curve in the presence of putrescine is less than that for $\alpha 3\beta 4$ receptors, suggesting less permeability for putrescine for this receptor compared to that for the wild type $\alpha 3\beta 4$ receptor.

that the inflow of putrescine affects the interaction of intracellular polyamines with the intermediate ring.

Extracellular polyamines block $\alpha 3\beta 4$ and $\alpha 4\beta 2$ receptors

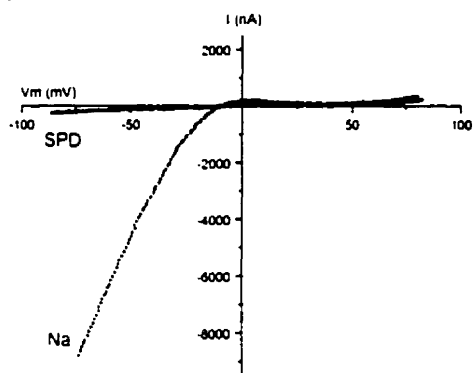
Since putrescine, the divalent precursor to spermidine and spermine, had differential permeability through $\alpha 3\beta 4$ and $\alpha 4\beta 2$ receptors, we investigated the permeability of the multivalent intermediate precursor, spermidine. When spermidine was used as the only charge carrier, we did not observe a detectable ACh-evoked inward current through $\alpha 3\beta 4$ and $\alpha 4\beta 2$ receptors at hyperpolarized potentials up to -120 mV (data not shown). Figure 4A shows the macroscopic ACh-evoked I-V curves for $\alpha 3\beta 4$ receptors in the presence of either the control solution or the control solution plus 10 mM spermidine. Addition of spermidine to the external solution caused a significant block (>90%) of the inward current at -80 mV without affecting the reversal potential of the ACh-evoked currents (Fig. 4A). These results indicate that spermidine has little permeability through the receptor, comparable to what we showed previously for spermine (Haghighi and Cooper, 1998 & 1999). We observed similar effects for spermidine on $\alpha 4\beta 2$ receptors (data not shown).

The mutations in the intermediate ring did not increase the permeability of spermidine through $\alpha 3\beta 4$ and $\alpha 4\beta 2$ receptors. Figure 4B shows the ACh-evoked I-V curves for $\alpha 3_{E240A}\beta 4$ receptors in the presence of either the control solution or the control solution plus 10 mM spermidine. Spermidine did not affect the reversal potential of the I-V curve, indicating that it does not permeate through these receptors. We observed similar results for $\alpha 4_{E245A}\beta 2$ receptors (data not shown).

Joro spider toxin blocks $\alpha 3\beta 4$ and $\alpha 4\beta 2$ receptors in a use dependent manner

Since we found that extracellular polyamines blocked neuronal nAChRs, we tested the effects of Joro toxin (JSTX), a polyamine-related toxin (Fig. 5E). Figure 5A shows the ACh-evoked currents from $\alpha 3\beta 4$ receptors in response to co-applications

A



B

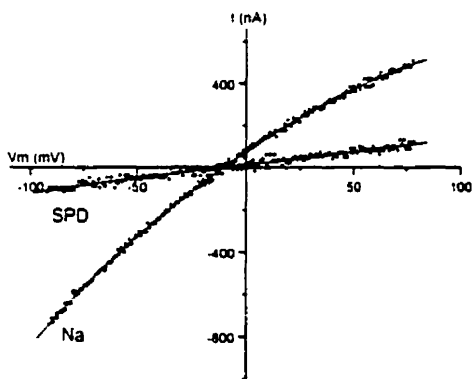


Figure 4.4. Spermidine has negligible permeability through neuronal nAChRs. A shows ACh-evoked I-V curves recorded in the presence of control solution (Na) or the control solution plus 10 mM spermidine (SPD) for $\alpha 3\beta 4$ receptors. Spermidine blocks the inward currents (>95%) without affecting the reversal potential, suggesting negligible permeability for spermidine through these receptors. B shows similar recordings from $\alpha 3_{E240A}\beta 4$ receptors. Spermidine also blocks the inward currents through these receptors without affecting the reversal potential of the ACh-evoked currents, suggesting that the intermediate ring does not influence the permeability of spermidine through the receptor.

Figure 4.5. JSTX blocks $\alpha 3\beta 4$ and $\alpha 4\beta 2$ receptors with high affinity and in a use-dependent manner. A, this figure shows macroscopic ACh-evoked currents recorded from an oocyte expressing $\alpha 3\beta 4$ receptors at -90 mV. Repeated coapplication of 50 nM JSTX with ACh (100 μ M) caused an increasing reduction of the inward currents recorded from these receptors. After three coapplications, the current was blocked over 90%. The horizontal and vertical bars correspond to 5 s and 200 nA, respectively. B, This figure shows similar recordings from $\alpha 3\beta 4$ receptors in response to coapplication of 100 nM JSTX with ACh (100 μ M). One coapplication caused a nearly complete block of the inward current. The horizontal and vertical bars correspond to 5 s and 200 nA, respectively. C, This figure shows macroscopic ACh-evoked currents recorded from an oocyte expressing $\alpha 4\beta 2$ receptors at -90 mV. Traces from bottom to top correspond to a control ACh (1 μ M) application and the 2nd, 6th and 10th coapplication with 100 nM JSTX and ACh 2 min apart. The horizontal and vertical bars correspond to 5 s and 200 nA, respectively. D shows the dose-inhibition curves for the blocking effect of JSTX on $\alpha 3\beta 4$ and $\alpha 4\beta 2$ receptors. We fit the data points ($n=4-6$ for each point) to a logistic equation (Eq. 4.) to estimate the half maximal inhibition dose (IC_{50}). The IC_{50} of JSTX was 8.5 ± 0.25 nM for $\alpha 3\beta 4$ and 45 ± 2.3 nM for $\alpha 4\beta 2$ receptors. 5E shows the structure of putrescine, spermidine, spermine and JSTX.

of ACh and 50 nM JSTX. The block developed during the co-application and increased with use: after 3 co-applications, JSTX blocked the ACh-evoked current by over 90%. The degree of block was increased with increasing concentration of ACh from 1 to 100 μ M (data not shown). This suggests that JSTX acts as an open channel blocker. Figure 5B shows the blocking effect of 100 nM JSTX when coapplied with ACh. A 10 s coapplication was enough to completely block the ACh-evoked currents in α 3 β 4. Figure 5C shows the ACh-evoked currents from α 4 β 2 receptors in response to co-applications of ACh and 100 nM JSTX. After 10 co-applications (figure shows the 2nd, 6th and 10th applications), JSTX blocked approximately 75% of the ACh-evoked current, suggesting that JSTX is more effective on α 3 β 4 receptors. Figure 5D shows JSTX-inhibition curves for α 3 β 4 and α 4 β 2 receptors. We fit the data to a logistic equation (Eq. 4, methods) and estimated the IC₅₀. The IC₅₀ for JSTX on α 3 β 4 (8.5 \pm 0.25 nM) was 5 fold less than that for α 4 β 2 receptors (45 \pm 2.3 nM). This high-affinity block reversed slowly (50% recovery after 10 min), and using voltage ramps, we found that it had little voltage-dependence (data not shown).

For AMPA/kainate receptors the site that undergoes RNA editing within the pore (Q/R) underlies inward rectification, calcium permeability and block by JSTX (Blaschke et al., 1993; Tsubokawa et al., 1995; Dingledine et al., 1999). Therefore, we tested whether JSTX blocks the non-rectifying intermediate ring mutant receptors, α 3_{E240A} β 4. Figure 6A shows the ACh-evoked currents from an oocyte expressing α 3_{E240A} β 4 receptors in response to co-applications of ACh and 50 nM JSTX at -90 mV. After 4 co-applications, JSTX blocked the ACh-evoked current by over 90%, similar to the block on wild-type α 3 β 4 receptors. These results indicate that JSTX does not interact with the intermediate ring, and that for neuronal nAChRs, unlike AMPA/kainate receptors, JSTX block and inward rectification do not go hand in hand.

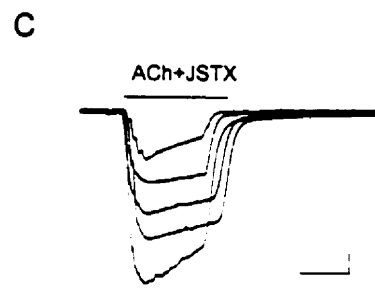
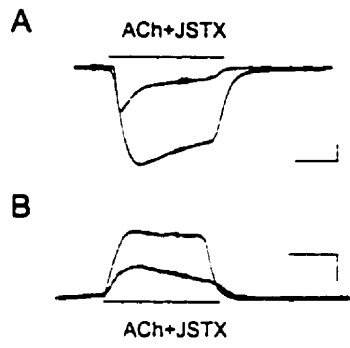


Figure 4.6. The block by JSTX has little voltage dependence and is influenced by F253 in the M2 of $\beta 4$. A and B show macroscopic ACh-evoked currents recorded from an oocyte expressing $\alpha 3_{E240A}\beta 4$ receptors at -90 mV and $+50$ mV, respectively. Each figure shows a control trace in response to ACh (100 μ M) alone or a trace corresponding to the 4th coapplication of (50 nM) JSTX together with ACh. JSTX blocked the ACh currents at both positive and negative membrane potentials in a similar manner, indicating a weak voltage dependence for this block. C. This figure shows macroscopic ACh-evoked currents recorded from an oocyte expressing $\alpha 3\beta 4_{F240V}$ receptors at -90 mV. Traces from bottom to top correspond to a control ACh (100 μ M) application and the 2nd, 4th, 6th and 10th coapplication with 100 nM JSTX and ACh in 2 min intervals. 100 nM JSTX blocked these receptors by approximately 80%.

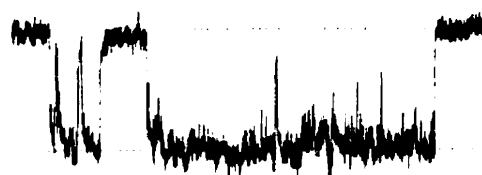
In addition, we used these non-rectifying $\alpha 3_{E240A}\beta 4$ receptors to investigate the voltage-dependence of the block by JSTX. Figure 6B shows the ACh-evoked currents from the oocyte in figure 6A at +50 mV. We observed a similar block by JSTX of the ACh-evoked currents at +50 mV compared to -90 mV. These results suggest that the block by JSTX has little voltage-dependence.

$\alpha 3\beta 4$ receptors are 5 fold more sensitive to block by JSTX compared to $\alpha 4\beta 2$ receptors. Since JSTX appears to act as an open channel blocker, it is likely that the M2 region of the receptor underlies the differential sensitivity to JSTX. To test whether $\beta 4_{F253V}$ underlies the increased JSTX sensitivity of $\alpha 3\beta 4$, we examined block by JSTX of $\alpha 3\beta 4_{F253V}$ receptors. Figure 6C shows the ACh-evoked currents from $\alpha 3\beta 4_{F253V}$ receptors in response to co-applications of ACh and 100 nM JSTX. After 10 co-applications, JSTX blocked approximately 80% of the ACh-evoked current, less effective than that for $\alpha 3\beta 4$ receptors ($P < 0.05$) and similar to what we observed for $\alpha 4\beta 2$ receptors.

Phenylalanine at 253 in $\beta 4$ affects single channel burst duration of $\alpha 3\beta 4$ receptors

Our results indicate that JSTX blocks open receptors. The difference in JSTX sensitivity between $\alpha 3\beta 4$ and $\alpha 4\beta 2$ correlates with the difference in single channel burst duration. Single channel burst duration for $\alpha 3\beta 4$ receptors are approximately 10 times longer than those for $\alpha 4\beta 2$ receptors (Papke, 1993; Haghghi and Cooper, 1998). Since $\alpha 3\beta 4_{F253V}$ receptors are less sensitive to JSTX compared to wild-type $\alpha 3\beta 4$, we tested whether this mutation also affected the single channel burst duration. Figure 7 shows examples of single channel bursts for $\alpha 3\beta 4$, $\alpha 4\beta 2$ and $\alpha 3\beta 4_{F253V}$ receptors measured in outside-out patches. The mean burst duration for $\alpha 3\beta 4_{F253V}$ receptors (12.3 ± 1.6 ms; $n=52$) was about 10 times shorter than that for $\alpha 3\beta 4$ receptors (98.9 ± 6.7 ms; $n=207$) and not significantly different from that for $\alpha 4\beta 2$

$\alpha 3\beta 4$



$\alpha 4\beta 2$



$\alpha 3\beta 4_{F253V}$



2 pA

Figure 4.7. F253 in the M2 of $\beta 4$ determines the long single channel burst duration in $\alpha 3\beta 4$ receptors. This figure shows single channel bursts for $\alpha 3\beta 4$, $\alpha 4\beta 2$ and $\alpha 3\beta 4_{F240V}$ recorded from outside out patches. The mean burst duration for $\alpha 3\beta 4$, $\alpha 4\beta 2$ and $\alpha 3\beta 4_{F240V}$ were 98.9 ± 6.7 ms (n =207), 10.5 ± 1.1 ms (n=187) and 12.3 ± 1.6 ms (n=52), respectively.

receptors (10.5 ± 1.1 ms; n=187). These results indicate that F253 in the M2 of β_4 influences the single channel gating of $\alpha_3\beta_4$ receptors.

DISCUSSION

In this paper, we demonstrate that neuronal nAChRs are targets for extracellular polyamines and polyamine-related toxins. We show that JSTX blocks neuronal nAChRs in a use-dependent manner with nanomolar affinity. This block is similar to the block of Ca⁺⁺ permeable AMPA/kainate receptors by JSTX (Blaschke et al., 1993; Tsubokawa et al., 1995; Washburn and Dingledine, 1996). For AMPA receptors, high calcium permeability, strong inward rectification and the block by JSTX go hand in hand. We show that this is not the case for neuronal nAChRs: Ca⁺⁺ impermeable, non rectifying mutant receptors are blocked by JSTX as effectively as wild-type receptors are. This suggests that the negatively charged residues in the intermediate ring, which govern both calcium permeability and strong inward rectification of the receptor, are not involved in the block by JSTX. It is likely that JSTX blocks the receptor by interacting with polar and non-polar residues in M2 that line the conductive pathway, as has been shown for the block of muscle nAChRs by the local anaesthetic, QX-222 (Charnet et al., 1990).

A phenylalanine in the M2 of $\beta 4$ ($\beta 4F253$) influences gating and toxin sensitivity of $\alpha 3\beta 4$ nAChR

We show that $\alpha 3\beta 4$ and $\alpha 4\beta 2$ differ in their sensitivity to JSTX. In the M2 domain, there is one striking amino acid difference among nAChR subunits: all known vertebrate nAChR subunits have a LLxxxVF motif in M2, except for $\beta 4$ in rat, monkey and human in which the motif is LLxxxFF. Our results demonstrate that this amino acid difference underlies the long single channel burst duration of $\alpha 3\beta 4$ receptors. Since JSTX interacts with the open receptor, long bursts of $\alpha 3\beta 4$ increase the likelihood of JSTX entering the channel and blocking the pore, giving rise to increased JSTX sensitivity.

In the past decade, by combining genetic analysis and patch-clamp electrophysiology, several mutations in the muscle nAChR subunits have been identified that lead to an increased single channel burst duration and are linked to slow-channel myasthenic syndrome (Engel et al., 1998). Of particular interest are two mutations that incorporate a Phe residue in the M2 (α V249F; ϵ L269F); both these mutations cause a lengthening of the single channel burst duration of muscle nAChRs (Engel et al., 1996; Milone et al., 1997). This is consistent with our findings that mutation of Phe254 to Val in β 4 causes a significant decrease in single channel burst duration of α 3 β 4 receptors. It is possible that the bulky aromatic side chain of Phe in the pore interferes with the movement of the M2 α -helices that is thought to underlie the proposed conformational switch between open and closed states (Unwin, 1993).

Both the M2 and the intermediate ring influence permeability through neuronal nAChRs

By examining the relative permeability of various organic cations, we demonstrate that two structural loci in the channel of neuronal nAChRs differentially affect the permeability of organic cations based on their cross-sectional diameter, length and charge. For short chain (less than $(\text{CH})_2$) monovalent organic cations, such as TRIS and ethanolamine, the permeability is governed by the size at the intermediate ring. Substituting Glu with Ala at the intermediate ring of α 3 β 4 and α 4 β 2 increased permeability for both TRIS and ethanolamine, whereas Glu with Gln had little effect. At the other extreme, long chain multivalent spermine and spermidine block in the M2 and do not appear to have access to the intermediate ring when applied from

outside, in contrast to intracellular polyamines that tightly interact with the intermediate ring (Haghighi and Cooper, 1999). Interestingly, divalent, intermediate-length organic cations appear to interact with both the M2 and the intermediate ring: putrescine is poorly permeable through $\alpha 4\beta 2$, whereas $\alpha 3\beta 4$ readily permeates putrescine, suggesting a role for M2 in determining putrescine permeability. In addition, the intermediate ring mutant receptor $\alpha 3_{E240A}\beta 4$ has a lower permeability to putrescine than the wild type $\alpha 3\beta 4$, indicating that the intermediate ring influences the permeability of putrescine. These results indicate that two structural domains, the M2 and the intermediate ring, differentially influence the permeability through neuronal nAChRs.

It is outside the scope of this study to identify individual residues along the M2 that influence permeability of organic cations; however, we have identified one such residue. Our results suggest that the Phe253 residue of $\beta 4$ is partly responsible for the differences between the permeability of organic cations through $\alpha 3\beta 4$ and $\alpha 4\beta 2$. The aromatic residues are thought to have a stabilizing effect on cations through an interaction known as cation- π interaction (Dougherty and Stauffer, 1990; Kumpf and Dougherty, 1993). This interaction is thought to underlie the selectivity of potassium channels (Kumpf and Dougherty, 1993). It is therefore conceivable that the presence of the aromatic Phe in the M2 of $\beta 4$ underlies the differences in permeability of monovalent organic cations and the divalent putrescine between $\alpha 3\beta 4$ and $\alpha 4\beta 2$.

CHAPTER 5

General Discussion and Conclusion

DISCUSSION

Physiological role of neuronal nAChRs

The function of neuronal nAChRs in the peripheral nervous system (PNS) is well understood. Neuronal nAChRs on postsynaptic autonomic neurons give rise to excitatory postsynaptic currents in response to ACh released from the preganglionic cholinergic nerve terminals. The importance of neuronal nAChRs in the peripheral nervous system has been recently highlighted in a study on mutant mice lacking the nAChR $\alpha 3$ gene (Xu et al., 1999). These mice have a fatality rate of about 40% one week after birth and over 90% eight weeks after weaning and show severe post natal growth deficiencies with 60% less weight on average compared to wild type mice. They also show severe defects in bladder contractility and pupillary contraction (Xu et al., 1999). The SCG neurons of these mice show a great reduction in their ACh-evoked response, consistent with the rate limiting role of $\alpha 3$ gene expression for the normal development of ACh-currents in these neurons (Mandelzys et al., 1994). Therefore, the lack of bladder and pupillary contractility is most likely due to the lack of $\alpha 3$ -containing nAChR receptors in the parasympathetic intramural ganglia of the bladder and the lack of parasympathetic input to the ciliary ganglion of the eye. These results further stress the important role of neuronal nAChRs for the normal physiology of the PNS. The function of neuronal nAChRs in the central nervous system (CNS), however, is still unclear.

The physiological role of central nicotinic receptors has been explored in mutant mice that lack either $\alpha 4$ or $\beta 2$, the two most abundant nAChR subunits in the

brain (Picciotto et al., 1995; Marubio et al., 1999). Surprisingly, both mutant mice live to adulthood, mate normally, show no obvious physical abnormalities and are no different from their wild-type littermates in any behavioral tests. The only differences between these mutant mice and wild-type littermates are a reduction of nicotine induced avoidance learning (Picciotto et al., 1995) and reinforcing effects (Picciotto et al., 1998) in the $\beta 2^{-/-}$ mice and reduced nicotine induced antinociception in $\alpha 4^{-/-}$ mice (Marubio et al., 1999). Indeed, $\beta 2^{-/-}$ mice show better avoidance learning (non-nicotine induced) than their wild type littermates (Picciotto et al., 1995). From these studies, it appears that these subunits that comprise the majority of high affinity nicotine binding sites in the brain are not essential for the normal physiology of the nervous system in animal models. However, an argument can be raised that a compensatory mechanism may be involved. This mechanism is not likely through an over expression of other nAChR subunit genes in the brain, since in either mutant mice mRNA levels for the other subunits appeared to be identical to those in their wild type littermates (Picciotto et al., 1995; Marubio et al., 1999). An alternative interpretation is that the nicotinic transmission in the brain may be involved in higher cognitive functions that are not easily measurable in animal models.

In humans, neuronal nAChRs have been implicated in neurological diseases including Alzheimer's disease and epilepsy. Recent genetic analysis of patients with autosomal nocturnal frontal lobe epilepsy has demonstrated a linkage between this disease and two mutations in the $\alpha 4$ nAChR subunit gene (Steinlein et al., 1995; Steinlein et al., 1997). Recombinant mutant $\alpha 4$ subunits expressed with $\beta 2$ subunit in heterologous systems give rise to functional $\alpha 4\beta 2$ receptors that show abnormal

properties. These findings suggest that defects in a neuronal nAChR in the brain are directly involved in causing abnormalities in the nervous system, revealing the importance of these receptors for the normal physiology of the nervous system.

Central nAChRs are mainly presynaptic and influence neurotransmitter release

Although nAChRs are widespread in the CNS, excitatory nicotinic transmission is not prominent in the brain. Evidence accumulating in the past two decades strongly suggests that most central nAChRs are located presynaptically (Clarke, 1993; McGehee and Role, 1996; MacDermott et al., 1999). Binding studies have demonstrated the presence of high affinity binding sites for radio-labeled nAChR agonists and antagonists in many regions of the CNS that receive cholinergic inputs, including the cerebral cortex, medial habenula, interpeduncular nucleus, substantia nigra, ventral tegmental area and thalamus (Schwarz et al., 1984; Clarke and Pert, 1985; Clarke et al., 1986; Clarke, 1993; Anderson and Arneric, 1994). Lesioning of presynaptic inputs to several nAChR rich regions of the brain has been demonstrated to abolish high affinity nicotine and α -BTX binding sites in the terminals and in the terminal fields (Clarke and Pert, 1985; Clarke et al., 1986), suggesting that many nAChRs are located presynaptically.

Additional studies have provided more support for a presynaptic role for central nAChRs by demonstrating that nAChR activation can trigger the release of a variety of neurotransmitters including dopamine, noradrenaline, GABA and glutamate (Rappier et al., 1990; McGehee et al., 1995; Lena and Changeux, 1997). In both synaptosome and slice preparations of striatum, nicotine application leads to a

significant increase in dopamine release (Rappier et al., 1988, 1990; Rowell, 1995). Similarly, nanomolar concentrations of nicotine enhance the presynaptic intracellular Ca^{++} concentration and cause a significant increase in the frequency of miniature excitatory glutamergic postsynaptic potentials at synapses between the medial habenula nucleus (MHN) neurons and the interpeduncular nucleus (IPN) neurons of chick both in the presence and absence of TTX (McGehee et al., 1995). Moreover, activation of presynaptic nAChRs by dimethylphenylpiperazinium (DMPP, a nicotinic agonist) in slices of thalamus sensory nuclei in mouse leads to enhancement of GABAergic miniature inhibitory postsynaptic potentials (Lena and Changeux, 1997). All these studies together suggest that neuronal nAChRs most likely function as presynaptic receptors in the brain and are involved in modulation of neurotransmitter release.

Presynaptic nAChRs can modulate synaptic transmission

One mechanism by which presynaptic neuronal nAChRs can modulate synaptic transmission is by directly triggering an action potential in a nerve terminal. It has been demonstrated in chromaffin cells that the opening of a single nAChR can cause enough depolarization to trigger an action potential (Fenwick et al., 1982). Considering the small size and high impedance of the nerve terminal and the relatively large single channel conductance of nAChRs, the opening of a few (or even one) neuronal nAChRs can trigger action potentials in the terminal and lead to neurotransmitter release, independent of the up stream activity in the cell body. The ACh-triggered action potential can also propagate retrogradely and create a barrier for

the incoming signals from the cell body, rendering the nerve terminal an independent signaling component controlled by the activity of local presynaptic neuronal nAChRs.

Physiological significance of the interaction of polyamines with neuronal nAChRs

The goal of my work has been to gain insight into the mechanisms that influence the function of presynaptic nAChRs. As direct electrophysiological examination of these receptors at the nerve terminals is technically difficult, I have used recombinant neuronal nAChRs for my experiments. Inward rectification and Ca^{++} permeability are two essential properties that enable these receptors to carry out their function.

The major contribution of my work is the characterization of the mechanism underlying the strong inward rectification of neuronal nAChRs and identification of a molecular link between inward rectification and Ca^{++} permeability. My findings on the interaction of intracellular polyamines with neuronal nAChRs provides insight into the mechanism by which the function of presynaptic nAChRs is modulated. In the absence of inward rectification due to the voltage-dependent block by intracellular spermine, the conductance increase upon activation of nAChRs at positive membrane potentials would short circuit (shunt out) the action potential and reduce the amplitude of the depolarization in the nerve terminal and decrease neurotransmitter release. However, intracellular polyamines prevent this conductance increase by blocking the receptors at positive membrane potentials.

Examination of the effect of intracellular spermine in outside out patches and macroscopic ACh-evoked G-V curves from neurons indicate that intracellular

polyamines can block the conductance of the receptor at membrane potentials near rest. Since both intracellular polyamines and the conducting Ca^{++} ions through the pore interact with the receptor at the same site, polyamines can compete for this site with Ca^{++} , thereby affecting the inflow of Ca^{++} . This process provides a modulatory mechanism for the action of nAChRs at nerve terminals.

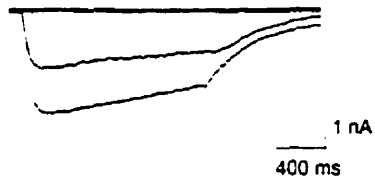
Removal of spermine removes rectification in intact neurons: the use of an animal model

My experiments indicate that polyamines are sufficient for conferring inward rectification to neuronal nAChRs; however, they do not directly show that removal of polyamines from neurons leads to a reduction or removal of inward rectification. Removal of inward rectification in neurons is difficult, in part because polyamines are present at high concentrations inside cells and are highly compartmentalized and tightly buffered (Swärd et al., 1997). Removing free polyamines leads to more release from cytosolic stores such as from those bound to phospholipids, ATP and nucleotides (Nakai and Glinsmann, 1977; Watanabe et al., 1991; Meksuriyen et al., 1998), making it difficult to effectively lower the levels. Since only μM concentrations of free polyamines are enough to block the receptors (Haghighi and Cooper, 1998), little removal of rectification can be achieved by dialysis. One possible approach to lower the levels of polyamines in vivo is the use of animal models where enzymes in the biosynthesis pathway of polyamines are genetically mutated.

Recently, a mutant mouse (Gy) that has served as a model for X-linked hypophosphatemia (Lyon et al., 1986) has been identified to bear a large deletion in the spermine synthase gene, the enzyme that converts spermidine to spermine (Meyer et al., 1998; Lorenz et al., 1998). Examination of the levels of polyamines in the Gy animals indicates that the levels of spermine in these animals are extremely low or non-detectable, whereas spermidine levels are significantly elevated.

I hypothesized that the inward rectification of ACh-evoked currents in these mice would be affected. I tested this hypothesis by measuring the ACh-evoked I-V curves in SCG neurons from these animals using the whole-cell patch-clamp technique. Initially, the I-V curves showed inward rectification, likely due to the presence of high concentrations of spermidine in these neurons. However, after 5-20 minutes dialysis with an intracellular recording solution containing 5-10 mM Na_2ATP , ACh-evoked currents showed a nearly linear I-V curve (Figure 5.1). These results indicate that polyamines are necessary and sufficient to confer inward rectification to neuronal nAChRs and present the Gy mice as a model to study the function of presynaptic nAChRs.

Wild-type SCG



Gy SCG

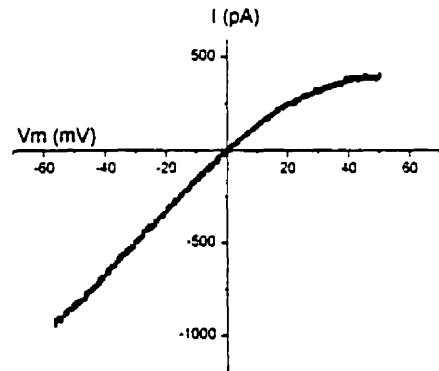
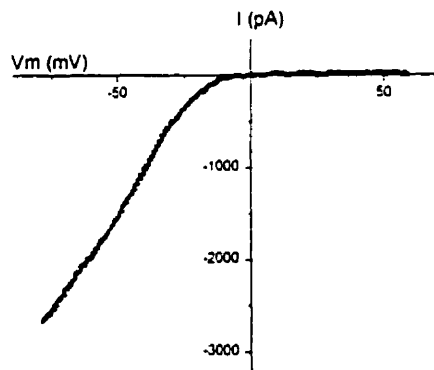
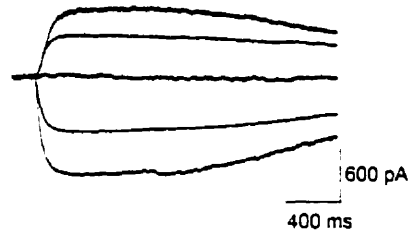


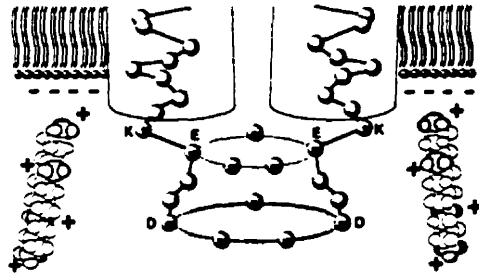
Figure 5.1. This figure shows a comparison between ACh-evoked currents recorded from a normal SCG neuron and a mutant Gy SCG neuron. The upper two panels show steady state macroscopic currents at -40 (-60 for wild type), -20 , $+20$ and $+40$ mV holding potentials. These records were obtained 5 minutes after breakthrough into the whole-cell configuration in the presence of 5 mM Na_2ATP in the recording electrode. Large outward ACh-evoked currents were recorded from the Gy neuron at positive membrane potentials; in contrast, the wild type neuron produced no detectable outward currents. The lower panels show the macroscopic ACh-evoked I-V curves recorded from a normal SCG neuron and a mutant Gy SCG neuron. The I-V curve for the normal neuron shows strong inward rectification; this rectification is significantly reduced for the Gy neuron.

CONCLUSION

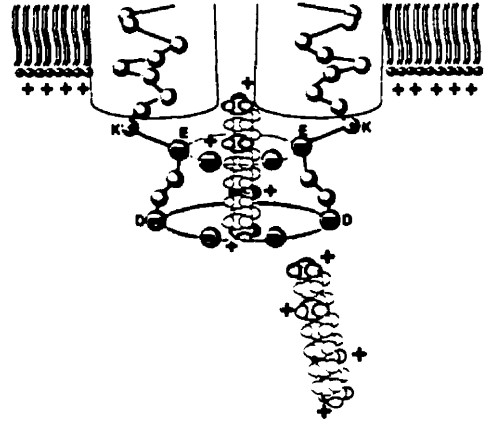
Our model suggests that an electrostatic interaction between positively charged polyamines and the densely negatively charged intermediate ring underlies the blocking effect of polyamines. Under the electrostatic influence of the intermediate ring, polyamine molecules become immobilized at the intermediate ring, and, since this region forms a narrow part, they occlude the pore (Fig. 5.2). At negative membrane potentials both the inward movement of cations through the receptor and the undesirable membrane electrical field oppose the interaction of polyamines with the intermediate ring. In addition, at hyperpolarized membrane potentials, positively charged polyamine molecules more readily interact with negatively charged phospholipids, decreasing the local polyamine concentration in the vicinity of the receptor. On the other hand, depolarization allows accumulation of polyamines near the mouth of the pore and favours their interaction with the densely negatively charged intermediate ring, leading to occlusion of the pore (Fig. 5.2). Since the intermediate ring of negative charges that forms the site of interaction of polyamines also determines Ca^{++} permeability of the receptor, block by polyamines can affect Ca^{++} entry through neuronal nAChRs at the nerve terminals.

In conclusion, my findings introduce a novel mechanism by which the function of neuronal nAChRs is modulated at synapses through the voltage-dependent interaction of polyamines with the intermediate ring of negatively charged residues. Intracellular polyamines interact with several other ion channels including subtypes of AMPA/kainate receptors and inward-rectifier potassium channels in a similar manner (Lopatin et al., 1994; Bowie and Mayer, 1995). It appears that evolutionary

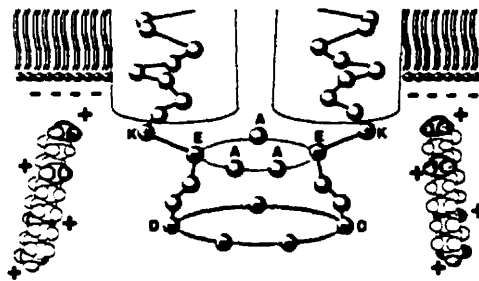
-60 mV



+40 mV



-60 mV



+40 mV

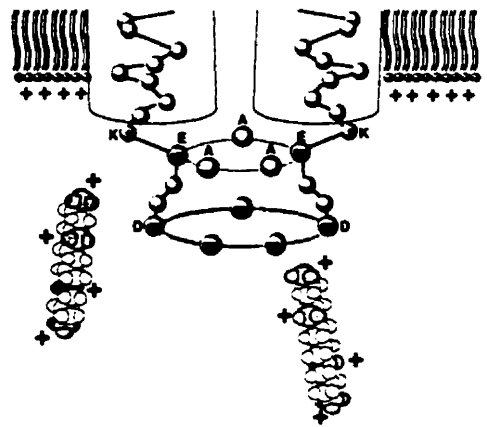


Figure 5.2. Cartoon of the interaction of polyamines with the intermediate ring at the cytoplasmic end of M2. The upper panels show the wild type receptor with five negatively charged glutamic acid (E) residues at the intermediate ring. At negative membrane potentials (top left), polyamines (rod-shaped positively charged molecules) are not attracted to the pore and likely interact with negatively charged phospholipids; thus the receptor can readily conduct inward currents. In contrast, at positive membrane potentials (top right), polyamines are attracted to the intermediate ring and tightly interact with the negative charges at this site. Polyamines then become immobilized at this site through an electrostatic interaction with these negative charges and block the outward ACh-evoked currents. The lower panels show the same cartoon for a mutant receptor, where three negatively charged residues at the intermediate ring have been substituted with neutral alanine (A) residues. At negative membrane potentials these receptors readily give rise to inward currents, similar to wild type receptors. At positive membrane potentials (bottom right), polyamines are no longer attracted to the pore, since the presence of neutral residues interferes with the electrostatic interaction of polyamines and the intermediate ring. Therefore, polyamines no longer block the receptor and ACh evokes outward currents through the receptor.

these ion channels have adopted an alternative mechanism for gating by using ubiquitous polyamines as gating molecules; this is in contrast to voltage-gated sodium and potassium channels, where voltage-dependent gating is mediated by a specialized structural motif. It is conceivable that local fluctuations in the levels of intracellular polyamines under physiological and pathophysiological conditions modulate the function of these ion channels at synapses.

BIBLIOGRAPHY

Ackerman M. Clapham DE (1997) Ion channels – Basic science and clinical disease. *New Engl J Med* 336:1575-1600.

Adams DJ, Dwyer TM, Hille B (1980) The permeability of endplate channels in monovalent and divalent metal cations. *J Gen Physiol* 75: 493-510.

Adams DJ, Nutter TJ (1992) Calcium permeability and modulation of nicotinic acetylcholine receptor-channels in rat parasympathetic neurons. (Lond) *J Physiol* 86:67-76.

Akabas MH, Kaufmann C, Archdeacon P, Karlin A (1994) Identification of acetylcholine receptor channel-lining residues in the entire M2 segment of the α subunit. *Neuron* 13: 919-927.

Akabas MH, Stauffer DA, Xu M, Karlin A (1992) Acetylcholine receptor channel structure probed in cysteine-substitution mutants. *Science* 258:307-310.

Anand R, Conroy WG, Schoepfer R, Whiting P, Lindstrom J (1991) Neuronal nicotinic acetylcholine receptors expressed in *Xenopus* oocytes have a pentameric quaternary structure. *J Biol Chem* 226:11192-11198.

Anderson DJ, Arneric SP (1994) Nicotinic receptor binding of [3 H]cystine, [3 H]nicotine and [3 H]methylcarbamylcholine in rat brain. *Eur J Pharmacol* 253:261-267.

Araneda R, Lan JY, Zheng X, Zukin S, Bennett VL (1999) Spermine and arcaine block and permeate N-methyl-D-aspartate receptor channels. *Biophys J* 76:2899-2911.

Ascher P, Large WA, Rang HP (1979) Studies on the mechanism of action of acetylcholine antagonists on rat parasympathetic ganglion cells. *J Physiol* 295:139-170.

Bähring R, Bowie D, Benveniste M, Mayer ML (1997) Permeation and block of rat GluR6 glutamate receptor channels by internal and external polyamines. (*Lond*) *J Physiol* 502:575-589.

Ballivet M, Nef P, Couturier S, Rungger D, Bader CR, Bertrand D, Cooper E (1988). Electrophysiology of a chick neuronal nicotinic acetylcholine receptor expressed in *Xenopus* oocytes after cDNA injection. *Neuron* 1:847-852.

Bannon AW, Decker MW, Holladay MW, Curzon P, Donnelly-Roberts D, Puttfracken PS, Bitner RS, Diaz A, Dickenson AH, Porsolt RD, Williams M, Arneric SP (1998) Broad-spectrum, non-opioid analgesic activity by selective modulation of neuronal nicotinic acetylcholine receptors. *Science* 279:77-81.

Bennett JA, Dingledine R (1995) Topology profile for a glutamate receptor three transmembrane domains and a channel-lining reentrant membrane loop. *Neuron* 14:373-384.

Benveniste M, Mayer ML (1993) Multiple effects of spermine on *N*-methyl-D-aspartic acid receptor responses of rat cultured hippocampal neurons. *J Physiol* 464:131-163.

Bertrand D, Ballivet M, Rungger D (1990), Activation and blocking of neuronal nicotinic acetylcholine receptor reconstituted in *Xenopus* oocytes. *Proc Natl Acad Sci USA* 87:1993-1997.

Bertrand D, Cooper E, Valera S, Rungger D, Ballivet M (1991) Electrophysiology of neuronal nicotinic acetylcholine receptors expressed in *Xenopus* oocytes following nuclear injection of genes or cDNAs. *Methods Neurosci* 4:174-193.

Bertrand D, Galzi JL, Devillers-Thiéry A, Bertrand S, Changeux JP (1993) Mutations at two distinct sites within the channel domain M2 alter calcium permeability of neuronal $\alpha 7$ nicotinic receptor. *Proc Natl Acad Sci USA* 90:6971-6975.

Blaschke M, Keller BU, Rivosecchi R, Hollmann M, Heinemann S, Konnerth A (1993) A single amino acid determines the subunit-specific spider toxin block of α -amino-3-hydroxy-5-methylisoxazole-4-propionate/kainate receptor channels. *Proc Natl Acad Sci USA* 90:6528-6532.

Boonyapisit K, Kaminski HJ, Ruff RL (1999) Disorders of neuromuscular junction ion channels. *Am J Med* 106:97-113.

Bowie D, Bähring R, Mayer ML (1999) Block of AMPA and kainate receptors by polyamines and arthropod toxins in *Handbook of experimental Pharmacology: Ionotropic Glutamate receptors in the CNS* (Jonas P and Monyer H eds) Springer Verlag, Berlin.

Bowie D, Mayer ML (1995) Inward rectification of both AMPA and kainate subtype glutamate receptors generated by polyamine-mediated ion channel block. *Neuron* 15:453-462.

Boyd RT, Jacob MH, Couturier S, Ballivet M, Berg DK (1988) Expression and regulation of neuronal acetylcholine receptor mRNA in chick ciliary ganglia. *Neuron* 1:495-502.

Brown DA, Fumagalli L (1977) Dissociation of α -bungarotoxin binding and receptor block in the rat superior cervical ganglion. *Brain Res* 129:165-168.

Buisson B, Bertrand D (1998) Open-channel blockers at the human $\alpha 4\beta 2$ neuronal nicotinic acetylcholine receptor. *Mol Pharmacol* 53:555-563.

Buisson B, Gopalakrishnan M, Armeric SP, Sullivan JP, Bertrand D (1996) Human $\alpha 4\beta 2$ neuronal nicotinic acetylcholine receptor in HEK 293 cells: a patch-clamp study. *J Neurosci* 16:7880-7891.

Butler JN (1968) The thermodynamic activity of calcium ion in sodium chloride-calcium chloride electrolytes. *Biophys J* 8:1426-1433.

Carbonetto ST, Fambrough DM, Muller KJ (1978) Nonequivalence of α -bungarotoxin receptors and acetylcholine receptors in chick sympathetic neurons. *Proc Natl Acad sci USA* 75:1016-1020.

Changeux JP (1980) The acetylcholine receptor: an "allosteric" membrane protein. *Harvey Lect Ser* 75:85-254

Charnet P, Labarca C, Leonard RJ, Vogelaar NJ, Czyzyk L, Gouin A, Davidson N, Lester HA (1990) An open-channel blocker interacts with adjacent turns of alpha-helices in the nicotinic acetylcholine receptor. *Neuron* 2:87-95.

Choe S, Stevens CF, Sullivan JM (1995) Three distinct structural environments of a transmembrane domain in the inwardly rectifying potassium channel ROMK1 defined by perturbation. *Proc Natl Acad Sci USA* 92:12046-12049.

Clarke PBS (1993) Nicotinic receptors in mammalian brain: localization and relation to cholinergic innervation. *Prog Brain Res* 98:77-83.

Clarke PBS, Hamill GS, Nadi NS, Jacobowitz DM, Pert A (1986) ^3H -nicotine- and ^{125}I -alpha-bungarotoxin-labeled nicotinic receptors in the interpeduncular nucleus of rats. II. Effects of habenular deafferentation. *J Comp Neurol* 251:407-413.

Clarke PBS, Pert A (1985) Autoradiographic evidences for nicotinic receptors on nigrostriatal and mesolimbic dopaminergic neurons. *Brain Res* 348:355-358.

Claudio T, Ballivet M, Patrick J, Heinemann S (1983) Nucleotide and deduced amino acid sequences of *Torpedo californica* acetylcholine receptor gamma subunit. *Proc Natl Acad Sci USA* 80:1111-5.

Colquhoun D, Cachelin AB, Marshall CG, Mathie A, Ogden DC (1990) Function of nicotinic synapses. *Prog Brain Res* 84: 43-50.

Cooper E, Couturier S, Ballivet M (1991) Pentameric structure and subunit stoichiometry of a neuronal nicotinic acetylcholine receptor. *Nature* 350: 235-238.

Corrigal WA, Franklin KBJ, Coen KM, Clarke PBS (1992) The mesolimbic dopaminergic system is implicated in the reinforcing effects of nicotine. *Psychopharmacol* 107:285-289.

Corringer PJ, Bertrand S, Galzi JL, Devillers-Thiery A, Changeux JP, Bertrand D (1999) Mutational analysis of the charge selectivity filter of the $\alpha 7$ nicotinic acetylcholine receptor. *Neuron* 22:831-843.

Costa ACS, Patrick JW, Dani JA (1993) Improved technique for studying ion channels expressed in *Xenopus* oocytes, including fast superfusion. *Biophys J* 67:395-401.

Couturier S, Erkman L, Valera S, Rungger D, Bertrand S, Boulter J, Ballivet M, Bertrand D (1990) α_5 , α_3 and non- α_3 : three clustered avian genes encoding neuronal nicotinic acetylcholine receptor-related subunits. *J Bio Chem* 265:17560-17567.

Cu C, Bähring R, Mayer ML (1998) The role of hydrophobic interactions in binding of polyamines to non NMDA receptor ion channels. *Neuropharmacol* 37:1381-1391.

Dale HH, Feldberg W, Vogt, M (1936) Release of acetylcholine at voluntary motor nerve endings. *J Physiol (Lond)* 86:353-380.

Dani JA (1989) Site-directed mutagenesis and single-channel currents define the ionic channel of the nicotinic acetylcholine receptor. *TINS* 12:125-128.

Dani JA, Eisenman G (1987) Monovalent and divalent cation permeation in acetylcholine receptor channels. Ion transport related to structure. *J Gen Physiol* 89:959-83.

Davis RH (1990) Management of polyamine pools and the regulation of ornithine decarboxylase. *J Cell Biochem* 44:199-205.

Decker ER, Dani JA (1990) Calcium permeability of the nicotinic acetylcholine receptors: the single channel calcium influx is significant. *J Neurosci* 10:3413-3420.

Dingledine, R, Hume, RI, Heinemann, SF (1992). Structural determinants of barium permeation and rectification in non-NMDA glutamate receptor channels. *J Neurosci* 12:4080-4087.

Dingledine R, Borges K, Bowie D, Traynelis SF (1999) The glutamate receptor ion channels. *Pharmacol Rev* 51:7-61.

DiPaola M, Kao P, Karlin A (1990) Mapping the α -subunit site photolabeled by the noncompetitive inhibitor [^3H]quinacrine azide in the active state of the nicotinic acetylcholine receptor. *J Biol Chem* 265:11017-11029.

Dixon WE (1900) Note on the physiological action of Poehl's spermine. *J Physiol XXV*: 356-363.

Dougherty DA, Stauffer DA (1990) Acetylcholine binding by a synthetic receptor: implications for biological recognition. *Science* 250:1558-60.

Duclert A, Changeux JP (1995) Acetylcholine receptor gene expression at the developing neuromuscular junction. *Physiol Rev* 75:339-68.

Dwyer TM, Adams DJ, Hille B (1980) The permeability of the endplate channel to organic cations in frog muscle. *J Gen Physiol* 75:469-492.

Eccles JC, Schmidt R, Willis WD (1963) Pharmacological studies on presynaptic inhibition. *J Physiol (Lond)* 168:500-530.

Egebjerg J, Heinemann SF (1993) Ca^{2+} permeability of unedited and edited versions of the kainate selective glutamate receptor GluR6. *Proc Natl Acad Sci USA*. 90:755-759.

Eisele JL, Bertrand S, Galzi JL, Devillers-Thiéry A, Changeux JP, Bertrand D (1993) Chimaeric nicotinic-serotonergic receptor combines distinct ligand binding and channel specificities. *Nature* 366:479-483.

Engel AG, Ohno K, Milone M, Sine SM (1998) Congenital myasthenic syndromes. New insights from molecular genetic and patch-clamp studies. *Ann N Y Acad Sci* 841:140-56.

Engel AG, Ohno K, Milone M, Wang H-L, Nakano S, Bouzat C, Pruitt JN, Hutchison DO, Brengman JM, Bren N (1996) New mutations in acetylcholine receptor subunit genes reveal heterogeneity in the slow-channel congenital myasthenic syndrome. *Hum Mol Genet* 5:1217-1227.

Fage D, Voltz C, Scatton B, Carter C (1992) Selective release of spermine and spermidine from the rat striatum by N-methyl-D-aspartate receptor activation *in vivo*. *J Neurochem* 58:2170-2175.

Falker B, Brändle U, Bond C, Glowatzki E, König C, Adelman JP, Zenner HP, Ruppertsberg JP (1994) A structural determinant of differential sensitivity of cloned inward rectifier K⁺ channels to intracellular spermine. *FEBS Lett* 356:199-203.

Falker B, Brandle U, Glowatzki E, Weidemann S, Zenner HP, Ruppertsberg JP (1995) Strong voltage-dependent inward rectification of inward rectifier K⁺ channels is caused by intracellular spermine. *Cell* 80:149-154.

Fatt P, Katz B (1951) An analysis of the end-plate potential recorded with an intracellular electrode. *J Physiol* 115:320-370.

Feldberg W, Gaddum JH (1934) The chemical transmitter at synapses in a sympathetic ganglion. *J Physiol (Lond)* 81:305-319.

Fenwick E, Marty A, Neher E (1982) A patch-clamp study of bovine chromaffin cells and of their sensitivity to acetylcholine. (Lond) *J Physiol* 331:577-597.

Ficker E, Tagliatela M, Wible BA, Henley CM, Brown AM (1994) Spermine and spermidine as gating molecules for inward rectifier K⁺ channels. *Science* 266:1068-1072.

Fieber LA, Adams DJ (1991) Acetylcholine-evoked currents in cultured neurones dissociated from rat parasympathetic cardiac ganglia. *J Physiol* 434:215-237.

Figl A, Viseshakul N, Shafae N, Forsayeth J, Cohen BN (1998) Two mutations linked to nocturnal frontal lobe epilepsy cause use-dependent potentiation of the nicotinic ACh response. *J Physiol* 513:655-70.

Flores CM, Rogers SW, Paberza LA, Wolfe BB, Kellar KJ (1992) A subtype of nicotinic cholinergic receptor in rat brain is composed of α_4 and β_2 subunits and is up-regulated by chronic nicotine treatment. *Mol Pharmacol* 41:31-37.

Forster I, Bertrand D (1995) Inward rectification of neuronal nicotinic acetylcholine receptors investigated by using the homomeric α_7 receptor. *Proc R Soc Lond B* 260:139-148.

Fumagalli L, DeRenzi G, Miani N (1976) Acetylcholine receptors: number and distribution in intact and deafferented superior cervical ganglion of the rat. *J Neurochem* 27:47-52.

Galzi JL, Changeux JP (1995) Neuronal nicotinic receptors: molecular organization and regulations. *Neuropharmacol* 34:563-82.

Galzi JL, Devillers-Thiery A, Hussy N, Bertrand S, Changeux JP, Bertrand D (1992) Mutations in the channel domain of a neuronal nicotinic receptor convert ion selectivity from cationic to anionic. *Nature* 359:500-505.

Galzi JL, Revah F, Bessis A, Changeux JP (1991) Functional architecture of the nicotinic acetylcholine receptor: from electric organ to brain. *Annu Rev Pharmacol* 31:37-72.

Galzi JL, Bertrand S, Corringer PJ, Changeux JP, Bertrand D (1996) Identification of calcium binding sites that regulate potentiation of a neuronal nicotinic acetylcholine receptor. *EMBO J* 15:5824-5832.

Geiger JRP, Melcher T, Koh D-S, Sakmann B, Seeburg PH, Jonas P, Monyer H (1995) Relative abundance of subunit mRNAs determines gating and Ca^{2+} permeability of AMPA receptors in principal neurons and interneurons in rat CNS. *Neuron* 15:193-204.

Gerzanich, V, Wang, F, Kuryatov, A, Lindstrom, J (1998). $\alpha 5$ Subunit alters desensitization, pharmacology, Ca^{2+} permeability and Ca^{2+} modulation of human neuronal $\alpha 3$ nicotinic receptors. *J. Pharmacol Exp Ther* 286:311-320.

Gilad GM, Gilad VH (1991) Polyamine uptake, binding and release in rat brain. *Eur J Pharmacol* 193:41-46.

Giraudat J, Dennis M, Heidmann T, Chang JY, Changeux JP (1986) Structure of the high-affinity binding site for noncompetitive blockers of the acetylcholine receptor: serine-262 of the delta subunit is labeled [3H]chlorpromazine. *Proc Natl Acad Sci* 83:2719-2723.

Giraudat J, Dennis M, Heidmann T, Haumont PY, Lederer F, Changeux JP (1987) Structure of the high-affinity binding site for noncompetitive blockers of the acetylcholine receptor: [3H]chlorpromazine labels homologous residues in the beta and delta chains. *Biochem* 26:2410-8.

Glusman S (1989) Electrophysiology of ganglionic transmission in the sympathetic nervous system. *Internat Anesthesiol Clinics* 27:273-282.

Goldman DE (1943) Potential impedance and rectification in membranes. *J Gen Physiol* 27:37-60.

Gray R, Rajan AS, Radcliffe KA, Yakehiro M, Dani JA (1996) Hippocampal synaptic transmission enhanced by low concentrations of nicotine. *Nature* 383:713-716.

Guo JZ, Tredway TL, Chiappinelli VA (1998) Glutamate and GABA release are enhanced by different subtypes of presynaptic nicotinic receptors in the lateral geniculate nucleus. *J Neurosci* 18:1963-1969.

Haghighi AP, Cooper E (1998a) Neuronal nicotinic acetylcholine receptors inwardly rectify through an interaction between intercellular polyamines and negatively charged residues on the cytoplasmic side of the pore. *Society for Neuroscience Abstracts*, V24:530.4

Haghighi A, Cooper E (1997) Intracellular spermine underlies the inward rectification of $\alpha_4\beta_2$ neuronal nicotinic acetylcholine receptors expressed in *Xenopus* oocytes. *Biophys Soc Abstr* 72:A264-W84

Haghighi AP, Cooper E (1998) Neuronal nicotinic acetylcholine receptors are blocked by intracellular spermine in a voltage-dependent manner. *J Neurosci* 18:4050-4062.

Hamill OP, Marty A, Neher E, Sakmann B, Sigworth F (1981) Improved patch-clamp techniques for high resolution current recording from cells and cell-free membrane patches. *Pflügers Arch* 391:85-100.

Harman RJ, Shaw GG (1981) The spontaneous and evoked release of spermine from rat brain *in vitro*. *Brit J Pharmacol* 73:165-174.

Hawrot E, Patterson P (1979) Long-term culture of dissociated sympathetic neurons. *Methods Enzymol* 58:574-584.

Heidmann T, Changeux JP (1984) Time-resolved photolabeling by the noncompetitive blocker chlorpromazine of the acetylcholine receptor in its transiently open and closed ion channel conformations. *Proc Natl Acad Sci USA* 81:1897-1901.

Hille B (1992) *Ionic channels of excitable membranes*. Sunderland, MA:Sinauer.

Hirano, T, Kidokoro, Y, Ohmori, H (1987) Acetylcholine dose-response relation and the effect of cesium ions in the rat adrenal chromaffin cell under voltage clamp. *Pflügers Arch* 408:401-407.

Hodgkin AL, Katz B (1949) The effect of sodium ions on the electrical activity of the giant axon of the squid. *J Physiol* 108:37-77.

Hollmann M, Heinemann S (1994) Cloned glutamate receptors. *Annu Rev Neurosci* 17:31-108.

Hollmann M, Maron C, Heinemann S (1994) N-Glycosylation site tagging suggests a three transmembrane domain topology for the glutamate receptor GluR1. *Neuron* 13:1331-1343.

Huang, L-YM, Catterall, WA, Ehrenstein, G (1978) Sensitivity of cations and nonelectrolytes for acetylcholine-activated channels in cultured muscle cells. *J Gen Physiol* 71:397-410.

Hucho F, Oberthür W, Lottspeich F (1986) The ion channel of the nicotinic acetylcholine receptor is formed by the homologous helices M2 of the receptor subunits. *FEBS* 205: 137-142.

Hume RI, Dingeldine R, Heinemann SF (1991) Identification of a site in glutamate receptor subunits that controls calcium permeability. *Science* 253:1028-1031.

Hsu KS (1994) Modulation of the nicotinic acetylcholine receptor channels by spermine in *Xenopus* muscle cell culture. *Neurosci Lett* 182:99-103.

Ifune CK, Steinbach JH (1990) Rectification of acetylcholine-elicited currents in PC12 pheochromocytoma cells. *Proceedings of the National Academy of Sciences of the United States of America*. 87(12):4794-4798.

Ifune CK, Steinbach JH (1991) Voltage-dependent block by magnesium of neuronal nicotinic acetylcholine receptor channels in rat pheochromocytoma cells. *J Physiol* 443:683-701.

Ifune CK, Steinbach JH (1992) Inward rectification of acetylcholine-elicited currents in rat pheochromocytoma cells. *J Physiol* 457:143-165.

Ifune CK, Steinbach JH (1993) Modulation of acetylcholine-elicited currents in clonal rat pheochromocytoma (PC12) cells by internal polyphosphates. (*Lond*) *J Physiol* 463:431-447.

Imoto K, Busch C, Sakmann B, Mishina M, Konno T, Nakai J, Bujo H, Mori Y, Fukuda K, Numa S (1988) Rings of negatively charged amino acids determine the acetylcholine receptor channel conductance. *Nature* 335:645-648

Imoto K, Methfessel C, Sakmann B, Mishina M, Mori Y, Konno T, Fukuda K, Kurasaki M, Bujo H, Fujita Y, Numa S (1986) Location of a delta-subunit region determining ion transport through the acetylcholine receptor channel. *Nature* 324:670-4.

Isa T, Iino M, Itazawa S, Ozawa S (1995) Spermine mediates inward rectification of Ca^{2+} -permeable AMPA receptor channels. *Neuroreport* 6:2045-8.

Jenkinson DH, Nicholls JG (1961) Contractions and permeability changes produced by acetylcholine receptors in depolarized denervated muscles. *J Physiol* 159:111-127.

Johnson JW, Ascher P (1990) Voltage-dependent block by intracellular Mg^{2+} of N-methyl-D-aspartate-activated channels. *Biophys J* 57:1085-1090.

Kamboj SK, Swanson GT, Cull-Candy SG (1995) Intracellular spermine confers rectification on rat calcium-permeable AMPA and kainate receptors. *J Physiol* 486:297-303.

Karlin A (1991) Explorations of the nicotinic acetylcholine receptor. *Harvey Lect Ser* 85:71-107.

Karlin A, Akabas MH (1995) Toward a structural basis for the function of nicotinic acetylcholine receptors and their cousins. *Neuron* 15:1231-1244.

Katz B, Miledi R (1969) Spontaneous and evoked activity of motor nerve endings in calcium ringer. *J Physiol* 203:689-706.

Koblin DD, Lester HA (1979) Voltage-dependent and voltage-independent blockade of acetylcholine receptors by local anesthetics in *Electrophorus* electroplaques. *Mol Pharmacol* 15:559-80.

Koh DS, Burnashev N, Jonas P (1995) Block of native Ca^{2+} -permeable AMPA receptors in rat brain by intracellular polyamines generates double rectification. (Lond) *J Physiol* 486:305-312.

Konno T, Bush C, Von Kitzing E, Imoto K, Wang F, Nakai J, Mishina M, Numa S, Sakmann B (1991) Rings of anionic amino acids as structural determinants of ion selectivity in the acetylcholine receptor channel. *Proc R Soc Lond B* 244:69-79.

Krnjevic K (1974) Chemical nature of synaptic transmission in vertebrates. *Physiol Rev* 54:418-540.

Kubo Y, Baldwin TJ, Jan YN, Jan LY (1993) Primary structure and functional expression of a mouse inward rectifier potassium channel. *Nature* 362:127-133.

Kumpf RA, Dougherty DA (1993) A mechanism for ion selectivity in potassium channels: computational studies of cation- π interactions. *Science* 261:1708-1710.

Kuner T, Wollmuth LP, Karlin A, Seeburg PH, Sakmann B (1996) Structure of the NMDA receptor channel M2 segment inferred from the accessibility of substituted cysteines. *Neuron* 17:343-352.

Kurachi Y (1985) Voltage-dependent activation of the inward-rectifier potassium channel in the ventricular cell membrane of guinea-pig heart. *J Physiol* 366:365-85.

Kuryatov A, Gerzanich V, Nelson M, Olale F, Lindstrom J (1997) Mutation causing autosomal dominant nocturnal frontal lobe epilepsy alters Ca^{2+} permeability, conductance, and gating of human $5\alpha 4\beta 2$ nicotinic acetylcholine receptors. *J Neurosci* 17:9035-47.

Langley JN, Dickinson WL (1890) Action of various poisons upon nerve-fibres and peripheral nerve-cells. *J Physiol (Lond)* 11:509-527.

Leech CA, Stanfield PR (1981) Inward rectification in frog skeletal muscle fibres and its dependence on membrane potential and external potassium. *J Physiol* 319:295-309.

Léna C, Changeux JP (1993) Allosteric modulations of the nicotinic acetylcholine receptor. *TINS* 16:181-185.

Léna C, Changeux JP (1997) Role of Ca^{2+} ions in nicotinic facilitation of GABA release in mouse thalamus. *J Neurosci* 17:576-585.

Leonard RJ, Labarca CG, Charnet P, Davidson N, Lester HA (1988) Evidence that the M2 membrane-spanning region lines the ion channel pore of the nicotinic receptor. *Science* 242: 1578-1581.

Lewis CA (1979) Ion-concentration dependence of the reversal potential and the single channel conductance of ion channels at the frog neuromuscular junction. (*Lond*) *J Physiol* 286:417-445.

Liu M, Nakazawa K, Inoue K, Ohno Y (1997) Potent and voltage-dependent block by philanthotoxin-343 of neuronal nicotinic receptor/channels in PC12 cells. *Brit J Pharmacol* 122:379-385.

Lopatin AN, Makhina EN, Nichols CG (1994) Potassium channel block by cytoplasmic polyamines as the mechanism of intrinsic rectification. *Nature* 372:366-369.

Lorenz B, Francis F, Gempel K, Böddrich A, Josten M, Schmahl W, Achmidt J, Lehrach H, Meitinger T, Strom T (1998) Spermine deficiency in Gy mice caused by deletion of the spermine synthase gene. *Hum Molec Genet* 7:541-547.

Lukas RJ, Changeux JP, Le Novère N, Albuquerque EX, Balfour DJK, Berg DK, Bertrand D, Chiappinelli VA, Clarke PBS, Collins AC, Dani JA, Grady SR, Kellar KJ, Lindstrom JM, Marks MJ, Quik M, Taylor PW, Wonnacott S (1999) International union of pharmacology. XX. Current status of the nomenclature for nicotinic acetylcholine receptors and their subunits. *Pharmacol Rev* 51:397-401.

Lyon MF, Scriver CR, Baker LRI, Tenenhouse HS, Kronick J and Mandla S (1986) The Gy mutation: another cause of X-linked hypophosphatemia in mouse. *Proc Natl Acad Sci USA*. 83:4899-4903.

MacDermott AB, Role LW, Siegelbaum D (1999) Presynaptic ionotropic receptors and the control of transmitter release. *Annu Rev Neurosci* 22:443-485.

Mandelzys A, De Koninck P, Cooper E (1995) Agonist and toxin sensitivities of ACh-evoked currents on neurons expressing multiple nicotinic ACh receptor subunits. *J Neurophysiol* 74:1212-1221.

Mandelzys A, Pie B, Deneris ES, Cooper E (1994) The developmental increase in ACh current densities on rat sympathetic neurons correlates with changes in nicotinic ACh receptor α -subunit gene expression and occurs independent of innervation. *J Neurosci* 14:2357-2364.

Marton LJ, Pegg AE (1995) Polyamines as targets for therapeutic intervention. *Annu Rev Pharmacol Toxicol* 35:55-91.

Marubio LM, Del-Mar-Arroyo-Jimenez M, Cordero-Erausquin M, Léna C, LeNovèrre N, De Kerchove d'Exaerde A, Huchet M, Damaj I, Changeux JP (1999) Reduced antinociception in mice lacking neuronal nicotinic receptor subunits. *Nature* 398:805-810.

Mathie A, Cull-Candy SG, Colquhoun D (1987) Single-channel and whole-cell currents evoked by acetylcholine in dissociated sympathetic neurons of the rat. *Proc Roy Soc Lond B* 232:239-248.

Mathie A, Colquhoun D, Cull-Candy SG (1990) Rectification of currents activated by nicotinic acetylcholine receptors in rat sympathetic ganglion neurons. (*Lond*) *J Physiol* 427:625-655.

Mathie A, Cull-Candy SG, Colquhoun D (1991) Conductance and kinetic properties of single nicotinic acetylcholine receptor channels in rat sympathetic neurones. *J Physiol* 439:717-750.

Matsuda H, Saigusa A, Irisawa H (1987) Ohmic conductance through the inwardly rectifying K channel and blocking by internal Mg^{2+} . *Nature* 325:156-159.

Matsuda H (1991) Effects of external and internal K^+ ions on magnesium block of inwardly rectifying K^+ channels in guinea-pig heart cells. *J Physiol* 435:83-99.

McFarlane S, Cooper E (1992) Postnatal development of voltage-gated K currents on rat sympathetic neurons. *J Neurosci* 67:1291-1300.

McGehee DS, Heath MJS, Gelber S, Devay P, Role LW (1995) Nicotinic enhancement of fast excitatory synaptic transmission in CNS by presynaptic receptors. *Science* 269:1692-1696.

McGehee DS, Role LW (1995) Physiological diversity of nicotinic acetylcholine receptors expressed by vertebrate neurons. *Annu Rev Physiol* 57:521-546.

McGehee DS, Role LW (1996) Presynaptic ionotropic receptors. *Curr Opin Neurobiol* 6:342-349.

Meksuriyen D, Fukuchi-Shimogori T, Tomitori H, Kashiwagi K, Toida T, Imanari T, Kawai G, Igarashi K (1998) Formation of a complex containing ATP, Mg^{2+} , and spermine. *J Biol Chem* 273:30939-30944.

Methfessel C, Witzemann V, Takahashi T, Mishina M, Numa S, Sakmann B (1986) Patch clamp measurements on *Xenopus laevis* oocytes: currents through endogenous

channels and implanted acetylcholine receptor and sodium channels. *Eur J Physiol* 407:577-588.

Meyer RA, Henley CM, Meyer MH, Morgan PL, McDonald AG, Mills C, Price DK (1998) Partial deletion of both the spermine synthase gene and the *Pex* Gene in the X-linked hypophosphatemic, Gyro (*Gy*) mouse. *Genomics* 48:289-295.

Miledi R, Parker I (1984) Chloride currents induced by injection of Ca^{++} into *Xenopus* oocytes. (*Lond*) *J Physiol* 357:173-183.

Milone M, Wang H-L, Ohno K, Fukudome T, Pruitt JN, Bren N, Sine SM, Engel AG (1997) Slow-channel syndrome caused by enhanced activation, desensitization, and agonist binding affinity due to mutation in the M2 domain of the acetylcholine receptor alpha subunit. *J Neurosci* 17:5651-5665.

Mishina M, Kurosaki T, Tobimatsu T, Morimoto Y, Noda M, Yamamoto T, Terao M, Lindstrom J, Takahashi T, Kuno M, Numa S (1984) Expression of functional acetylcholine receptor from cloned cDNAs. *Nature* 307:604-608.

Mishina M, Takai T, Imoto K, Noda M, Takahashi T, Numa S, Methfessel C, Sakmann B (1986) Molecular distinction between fetal and adult forms of muscle acetylcholine receptor. *Nature* 321:406-411.

Mishina M, Tobimatsu T, Imoto K, Tanaka K, Fujita Y, Fukuda K, Kurasaki M, Takahashi H, Morimoto Y, Hirose T, Inayama S, Takahashi T, Kuno M, Numa S (1985) Location of the functional regions of acetylcholine receptor α -subunit by site-directed mutagenesis. *Nature* 313:364-369.

Morrison LD, Kish SJ (1995) Brain polyamine levels are altered in Alzheimer's disease. *Neurosci Lett* 197:5-8.

Mulle C, Choquet D, Korn H, Changeux JP (1992) Calcium influx through nicotinic receptor in rat central neurons: its relevance to cellular regulation. *Neuron* 8:135-143.

Mulle C, Lena C, Changeux, JP (1992a) Potentiation of nicotinic receptor response by external calcium in rat central neurons *Neuron*. 8:937-945.

Nakai C, Glimsmann W (1977) Interactions between polyamines and nucleotides. *Biochem* 16:5636-5641.

Neher E, Steinbach JH (1978) Local anaesthetics transiently block currents through single acetylcholine-receptor channels. *J Physiol* 277:153-176.

Neher E (1992). Correction for liquid junction potentials in patch-clamp experiments. *Meth Enzymol* 207. 123-131.

Neuhaus R, Cachelin AB (1990) Changes in the conductance of the neuronal nicotinic acetylcholine receptor channel induced by magnesium. *Proc R Soc Lond B* 241:78-84.

Nichols CG, Lopatin AN (1997) Inward rectifier potassium channels. *Annu Rev Physiol* 59:171-91.

Noda M, Takahashi H, Tanabe T, Toyosato M, Furutani Y, Hirose T, Asai M, Inayama S, Miyata T Numa S (1982) Primary structure of the α subunit precursor of *Torpedo californica* acetylcholine receptor deduced from cDNA sequences. *Nature* 299:793-797.

Noda M, Takahashi H, Tanabe T, Toyosato M, Kikuyotani S, Hirose T, Asai M, Takashima H, Inayama S, Miyata T Numa S (1983a) Primary structure of β and δ subunit precursors of *Torpedo californica* acetylcholine receptor deduced from cDNA sequences. *Nature* 301:251-255.

Nooney JM, Peters JA, Lambert JJ (1992) A patch-clamp study of the nicotinic acetylcholine receptor of bovine adrenomedullary chromaffin cells in culture. *J Physiol* 455:503-527.

Nutter TJ, Adams DJ (1995) Monovalent and divalent cation permeability and block of neuronal nicotinic receptor channels in rat parasympathetic ganglia. *J Gen Physiol* 105: 701-723.

Ohno K, Hutchinson DO, Milone M, Brengman JM, Bouzat C, Sine SM, Engel AG (1981) Congenital myasthenic syndrome caused by prolonged acetylcholine receptor channel openings due to a mutation in the M2 domain of the ϵ subunit. *Proc Natl Acad Sci USA* 92:758-762.

Oswald R, Changeux JP (1981) Ultraviolet light-induced labeling by noncompetitive blockers of the acetylcholine receptor from *Torpedo marmorata*. *Proc Natl Acad Sci USA* 78: 3925-3929.

Oswald RE, Changeux JP (1981) Selective labeling of the δ subunit of the acetylcholine receptor by a covalent local anesthetic. *Biochem* 20:7166-7174.

Papke RL (1993) The kinetic properties of neuronal nicotinic receptors: genetic basis of functional diversity. *Prog Neurobiol* 41:509-531.

Papke RL, Boulter J, Patrick J, Heinemann S (1989) Single-channel currents of rat neuronal nicotinic acetylcholine receptors expressed in *Xenopus* oocytes. *Neuron* 3:589-596.

Paton WD, Zaimis EJ (1951) Paralysis of autonomic ganglia by methonium salts. *Br J Pharmacol* 6:155-168.

Pascual JM, Karlin A (1998) State-dependent accessibility and electrostatic potential in the channel of the acetylcholine receptor. Inferences from rates of reaction of thiosulfonates with substituted cysteines in the M2 segment of the α subunit. *J Gen Physiol* 111:717-739.

Pegg AE (1986) Recent advances in the biochemistry of polyamines in eukaryotes. *Biochem J* 234:249-262.

Picciotto MR, Zoll M, Léna C, Bessis A, Lallemand Y, LeNovère N, Vincent P, Pich EM, Brulet P, Changeux JP (1995) Abnormal avoidance learning in mice lacking functional high-affinity nicotine receptor in the brain. *Nature* 374:65-67.

Raftery MA, Hunkapiller MW, Strader CD, Hood LE (1980). Acetylcholine receptor: Complex of homologous subunits. *Science* 208:1454-1457.

Ragozzino, D, Barabino, B, Fucile, S, Eusebi, F (1998). Ca^{2+} permeability of mouse and chick nicotinic acetylcholine receptors expressed in transiently transfected human cells. *J Physiol* 507:749-757.

Rang HP (1981) The characteristics of synaptic currents and responses to acetylcholine of rat submandibular ganglion cells. *J Physiol* 311:23-55.

Rang HP, Rylett RJ (1984) The interaction between hexamethonium and tubocurarine on the rat neuromuscular junction. *Brit J Pharmacol* 81:519-531.

Ravdin PM, Berg DK (1979) Inhibition of neuronal acetylcholine sensitivity by a-toxins from *Bungarus multicinctus* venom. *Proc Natl Acad Sci USA* 76:2072-2076.

Revah F, Bertrand D, Galzi JL, Devillers-Thiéry A, Mulle C, Hussy N, Bertrand S, Ballivet M, Changeux JP (1991) Mutations in the channel domain alter desensitization of a neuronal nicotinic receptor. *Nature* 353:846-849.

Revah F, Galzi JL, Giraudat J, Haumont PY, Lederer F, Changeux JP (1990) The noncompetitive blocker [³H]chlorpromazine labels three amino acids of the acetylcholine receptor γ subunit: implications for the α -helical organization of regions M2 and for the structure of the ion channel. *Proc Natl Acad Sci USA* 87:4675-4679.

Robichaud LJ, Boxer PA (1993) Polyamine modulation of excitatory amino acid responses in rat cortical wedge. *Neuropharmacol* 32:1025-1035.

Robinson RA, Stokes RH (1960) *Electrolyte Solutions*. Butterworths Scientific Publication, London.

Rock DM, MacDonald RL (1992) The polyamine spermine has multiple actions on N-methyl-D-aspartate receptor single channel currents in cultured cortical neurons. *Mol Pharmacol* 41:83-88

Role LW, Berg DK (1996) Nicotinic receptors in the development and modulation of CNS synapses. *Neuron* 16:1077-1085.

Sakmann B, Methfessel C, Mishina M, Takahashi T, Kurasaki M, Fukuda K, Numa S (1985) Role of the acetylcholine receptor subunits in gating of the channel. *Nature* 318:538-543.

Sands SB, Barish ME (1991) Calcium permeability of neuronal nicotinic acetylcholine receptor channels in PC12 cells. *Brain Res* 560:38-42.

Sands SB, Barish ME (1992) Neuronal nicotinic acetylcholine receptor currents in pheochromocytoma (PC12) cells: dual mechanisms of rectification. (*Lond*) *J Physiol* 447:467-487.

Sands SB, Barish ME (1991) Calcium permeability of neuronal nicotinic acetylcholine receptor channels in PC12 cells. *Brain Res* 560:38-42.

Sanes JR, Lichtman JW (1999) Development of the vertebrate neuromuscular junction. *Annu Rev Neurosci* 22:389-442.

Sargent PB (1993) The diversity of neuronal nicotinic acetylcholine receptors. *Annu Rev Neurosci* 16:403-443.

Scheffer IE, Bhatia KP, Lopes-Cendes I, Fish DR, Marsden CD, Andermann F, Andermann E, Desbiens R, Cendes F, Manson JI et al. (1994) Autosomal dominant frontal epilepsy misdiagnosed as sleep disorder. *Lancet* 343:515-517.

Schwartz RD, McGee R, Kellar KJ (1982) Nicotinic cholinergic receptors labeled by [³H]acetylcholine in rat brain. *Mol Pharmacol* 22:56-62.

Scott RH, Sutton KG, Dolphin AC (1993) Interactions of polyamines with neuronal ion channels. *TINS* 16:153-160.

Seguela P, Wadiche J, Dineley-Miller K, Dani JA, Patrick JW (1993) Molecular cloning, functional properties, and distribution of rat brain α_7 : A nicotinic cation channel highly permeable to calcium. *J Neurosci* 13:596-604.

Seiler N, Schmidt-Glenewinkel T (1975) Regional distribution of putrescine, spermidine and spermine in relation to the distribution of RNA and DNA in the rat nervous system. *J Neurochem* 24:791-795.

Selyanko AA, Derkach VA, Skok VI (1979) Fast excitatory postsynaptic currents in voltage-clamped mammalian sympathetic ganglion neurones. *Journal of the Autonomic Nervous System*. 1(2):127-37.

Shao Z, Mellor IR, Brierley MJ, Harris J, Usherwood PNR (1998) Potentiation and inhibition of nicotinic acetylcholine receptors by spermine in the TE671 human muscle cell line. *J Pharmacol Exp Ther* 286:1269-1276.

Shaw CG, Pateman AJ (1973) The regional distribution of the polyamines spermidine and spermine in brain. *J Neurosci* 20:1225-1230.

Shaw G (1979) The polyamines in the central nervous system. *Biochem Pharmacol* 28:1-6.

Steinbach AB (1968) A kinetic model for the action of Xylocaine on receptors for acetylcholine. *J Gen Physiol* 52:162-180.

Steinlein OK, Magnusson A, Stoodt J, Bertrand S, Weiland S, Berkovic SF, Nakken KO, Propping P, Bertrand D (1997) An insertion mutation of the CHRNA4 gene in a family with autosomal dominant nocturnal frontal lobe epilepsy. *Hum Molec Genet* 6:943-947.

Steinlein OK, Mulley JC, Propping P, Wallace RH, Philips HA, Sutherland GR, Scheffer IE, Berkovic SF (1995) A missense mutation in the neuronal nicotinic acetylcholine receptor alpha 4 subunit is associated with autosomal dominant nocturnal frontal lobe epilepsy. *Nature Genetics* 11(2):201-203.

Sumikawa K, Houghton M, Smith JC, Bell L, Richards BM, Barnard EA (1982) The molecular cloning and characterisation of cDNA coding for the alpha subunit of the acetylcholine receptor. *Nucleic Acids Research*. 10(19):5809-5822.

Swaerd K, Nilsson BO, Hellstrand P (1997) Inhibition of polyamine synthesis influences contractility of intestinal smooth muscle in culture. *Am J Physiol* 223:77-84.

Swanson GT, Feldmeyer D, Kaneda M, Cull-Candy SG (1996) Effect of RNA editing and subunit co-assembly single-channel properties of recombinant kainate receptors. *J Physiol* 492:129-42.

Szczawinska K, Ferchmin PA, Hann RM, Eterovic VA (1992) Electric organ polyamines and their effects on the acetylcholine receptor. *Cell Mol Neurobiol* 12:95-106.

Tagliatela M, Ficker E, Wible BA, Brown AM (1995) C-terminus determinants for Mg^{2+} and polyamine block of the inward rectifier K^+ channels IRK1. *EMBO J* 14:5532-5541.

Takeuchi A, Takeuchi N (1960) On the permeability of end-plate membrane during the action of transmitter. *J Physiol* 154:52-67.

Traynelis SF, Hartley M, Heinemann SF (1995) Control of proton sensitivity of the NMDA receptor by RNA splicing and polyamines. *Science* 268:873-876.

Trouslard J, Marsh SJ, Brown DA (1993) Calcium entry through nicotinic receptor channels and calcium channels in cultured rat superior cervical ganglion cells. (*Lond*) *J Physiol* 468:53-71.

Tsubokawa H, Oguro K, Masuzawa T, Nakaima T, Kawai N (1995) Effects of a spider toxin and its analogue on glutamate-activated currents in the hippocampal CA1 neuron after ischemia. *J Neurophysiol* 74:218-225.

Unwin N (1993) Nicotinic acetylcholine receptor at 9 Å resolution. *J Mol Biol* 229:1101-1124.

Unwin N (1995) Acetylcholine receptor channel imaged in the open state. *Nature* 373:37-43.

Vandenberg CA (1987) Inward rectification of a potassium channel in cardiac ventricular cells depends on internal magnesium ions. *Proc Natl Acad Sci USA* 84:2560-2564.

Verdoorn TA, Burnashev N, Monyer H, Seeburg PH, Sakmann B (1991) Structural determinants of ion flow through recombinant glutamate receptor channels. *Science* 252:1715-1718.

Vernino S, Amador M, Luetje CW, Patrick J, Dani JA (1992) Calcium modulation and high calcium permeability of neuronal nicotinic acetylcholine receptors. *Neuron* 8:127-134.

Vetter DE, Liberman MC, Mann J, Barhanin J, Boulter J, Brown MC, Saffioti-Kolman J, Heinemann SF, Elgohhen AB (1999) Role of alpha 9 nicotinic ACh receptor subunits in the development and function of cochlear efferent innervation. *Neuron* 23:93-103.

Villarroel A, Sakmann B (1996) Calcium permeability increase of endplate channels in rat muscle during postnatal development. (*Lond*) *J Physiol* 496:331-338.

Virginio C, North RA, Surprenant A (1998). Calcium permeability and block at homomeric and heteromeric P2X₂ and P2X₃ receptors, and P2X receptors in rat nodose neurones. *J Physiol* 510. 27-35.

Wada E, Wada K, Boulter J, Deneris E, Heinemann S, Patrick J, Swanson LW (1989) Distribution of α_2 , α_3 , α_4 , and β_2 neuronal nicotinic receptor subunit mRNA in the central nervous system: a hybridization histochemical study in the rat. *J Comp Neurol* 284:314-335.

Wang F, Gerzanich V, Wells GB, Anand R, Peng X, Keyser K, Lindstrom J (1996) Assembly of human neuronal nicotinic receptor $\alpha 5$ subunits with $\alpha 3$, $\beta 2$, and $\beta 4$ subunits. *J Bio Chem* 271:17656-17665.

Wang F, Imoto K (1992) Pore size and negative charge as structural determinants of permeability in the *Torpedo* nicotinic acetylcholine receptor channel. *Proc R Soc Lond B* 250:11-17.

Washburn M S, Numberger M, Zhang S, Dingledine R (1997) Differential dependence on GluR2 expression of three characteristic features on AMPA receptors. *J Neurosci* 17:9393-9406.

Washburn MS, Dingledine R (1996) Block of α -amino-3-hydroxy-5-methyl-4-isoxazolepropionic acid AMPA receptors by polyamines and polyamine toxins. *J Pharmacol Exp Ther* 278:669-678.

Watanabe S, Kusama-Eguchi K, Kobayashi H, Igarashi K (1991) Estimation of polyamine binding to macromolecules at ATP in bovine lymphocytes and rat liver. *J Biol Chem* 266:20803-20809.

Weiland S, Witzermann V, Villarroel A, Propping P, Steinlein O (1996) An amino acid exchange in the second transmembrane segment of a neuronal nicotinic receptor causes partial epilepsy by altering its desensitization kinetics. *FEBS Letters* 398:91-96

Weill CL, McNamee MG, Karlin A (1974) Affinity labelling of purified acetylcholine receptor from *Torpedo*. *Biochem Biophys Res Commun* 61:997-1003.

White BH, Cohen JB (1992) Agonist-induced changes in the structure of the acetylcholine receptor M2 regions revealed by photoincorporation of an uncharged

nicotinic noncompetitive antagonist. *J Biol Chem* 267(22):15770-83.

Wible BA, Tagliatela M, Ficker E, Brown AM (1994) Gating of inwardly rectifying K⁺ channels localized to a single negatively charged residue. *Nature* 371:246-469.

Williams K (1997) Interactions of polyamines with ion channels. *Biochem J* 325:289-297.

Williams K (1997) Modulation and block of ion channels: a new biology of polyamines. *Cell Signal* 9:1-13.

Williams K, Dawson VL, Romano C, Dichter MA, Molinoff B (1990) Characterization of polyamines having agonist, antagonist, and inverse agonist effects at the recognition site of the NMDA receptor. *Neuron* 5:199-208.

Wilson GG, Karlin A (1998) The location of the gate in the acetylcholine receptor. *Neuron* 20:1269-1281.

Winkler J, Suhr ST, Gage FH, Thal LJ, Fisher LJ (1995) Essential role of neocortical acetylcholine in spatial memory. *Nature* 375:484-487.

Wollmuth LP, Sakmann B (1998) Different mechanisms of Ca²⁺ transport in NMDA and Ca²⁺-permeable AMPA glutamate receptor channels. *J Gen Physiol* 112:623-636.

Wonnacott S (1997) Presynaptic nicotinic ACh receptors. *Trends Neurosci* 20:92-98.

Woodhull AM (1973) Ionic blockage of sodium channels in nerve. *J Gen Physiol* 61:687-708.

Xiang Z, Hunguenard JR, Prince DA (1998) Cholinergic switching within neocortical inhibitory networks. *Science* 281:985-988.

Yoneda Y, Ogita K, Enomoto R, Suzuki T, Kito S (1991) Identification and characterization of specific binding sites of [³H]spermidine in synaptic membranes of rat brain. *Brain Res* 563:17-27.

Yu CR, Role LW (1998) Functional contribution of the $\alpha 5$ subunit to neuronal nicotinic channels expressed by chick sympathetic ganglia neurones. *J Physiol* 509:667-681.

Zhang J, Xiao Y, Abdrakhmanova G, Wang W, Cleemann L, Kellar KJ, Morad M (1999) Activation and Ca^{2+} permeation of stably transfected $\alpha 3/\beta 4$ neuronal nicotinic acetylcholine receptor. *Mol Pharmacol* 55:970-981.